INFORMATION TO USERS

This manuscript has been reproduced from the microfilm master. UMI films the text directly from the original or copy submitted. Thus, some thesis and dissertation copies are in typewriter face, while others may be from any type of computer printer.

The quality of this reproduction is dependent upon the quality of the copy submitted. Broken or indistinct print, colored or poor quality illustrations and photographs, print bleedthrough, substandard margins, and improper alignment can adversely affect reproduction.

In the unlikely event that the author did not send UMI a complete manuscript and there are missing pages, these will be noted. Also, if unauthorized copyright material had to be removed, a note will indicate the deletion.

Oversize materials (e.g., maps, drawings, charts) are reproduced by sectioning the original, beginning at the upper left-hand corner and continuing from left to right in equal sections with small overlaps.

ProQuest Information and Learning
300 North Zeeb Road, Ann Arbor, MI 48106-1346 USA
800-521-0600

Links Between Pacific Basin Climatic Variability and Natural Systems of the Pacific Northwest

Ze'ev Gedalof

A dissertation submitted in partial fulfillment of the requirements for the degree of

Doctor of Philosophy

University of Washington
2002

Program Authorized to Offer Degree: Forest Resources, Ecosystem Analysis

ProQuest Information and Learning Company
300 North Zeeb Road
P.O. Box 1346
Ann Arbor, MI 48106-1346

In presenting this dissertation in partial fulfillment of the requirements for the Doctoral degree at the University of Washington, I agree that the Library shall make its copies freely available for inspection. I further agree that extensive copying of the dissertation is allowable only for scholarly purposes, consistent with "fair use" as prescribed in the U.S. Copyright Law. Requests for copying or reproduction of this dissertation may be referred to Proquest Information and Learning, 300 North Zeeb Road, Ann Arbor, MI 48106-1346, or to the author.

Signature 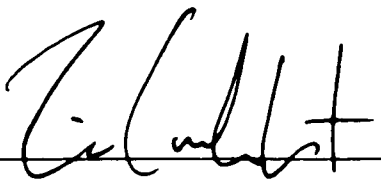

Date DECEMBER 11th 2002

University of Washington
Graduate School

This is to certify that I have examined this copy of a doctoral dissertation by

Ze'ev Gedalof

and have found that it is complete and satisfactory in all respects,
and that any and all revisions required by the final
examining committee have been made.

Chair of Supervisory Committee:

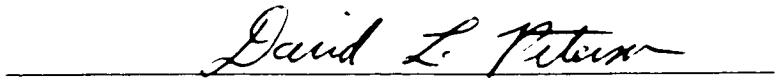

David L. Peterson

Reading Committee:

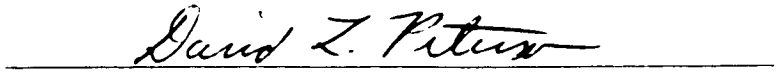

David L. Peterson

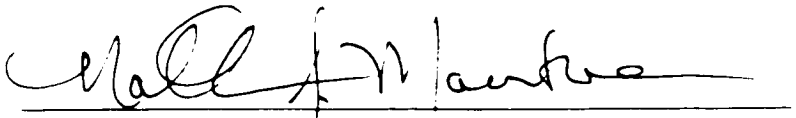

Nathan J. Mantua

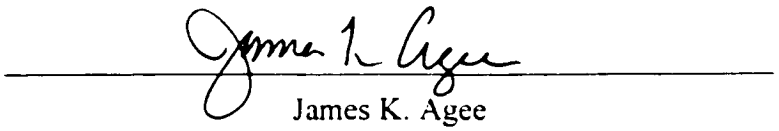

James K. Agee

Date: 11 December, 2002

University of Washington

Abstract

Links Between Pacific Basin Climatic Variability and
Natural Systems of the Pacific Northwest

Ze'ev Gedalof

Chair of the Supervisory Committee:
Professor David L. Peterson

This thesis is composed of three principal chapters, each describing a distinct line of inquiry:

1. Five paleoproxy reconstructions of Pacific Basin climatic variability are examined in order to identify the extent to which these records provide a coherent signal. A composite chronology of these records is well correlated with the Pacific Decadal Oscillation (PDO) index, and provides a better record of PDO variability than any of the constituent chronologies back to 1840. This record suggests that the PDO may not have been an important organizing structure in the North Pacific climate system over much of the 19th century.

2. Empirical Orthogonal Function (EOF) analysis is used to identify patterns in annual area burned by wildfire in the American Northwest. Extreme wildfire years are forced in part by antecedent drought and summertime blocking in the 500 hPa height field. However the response to these events is modulated by the ecology of the underlying forest. At more mesic forest types antecedent drought preconditions forests to burn, but is not a good predictor of area burned due to the rarity of subsequent ignition. At especially dry locations, blocking events alone can lead to increases in area burned even in the absence of antecedent drought. Summertime cyclones can also lead to increased area burned, probably due to dry lightning storms

that bring ignition and strong winds but little precipitation. Management paradigms that rely on fuel treatments alone to eliminate large, intense fires are consequently unlikely to succeed.

3. A network of drought sensitive tree-ring chronologies is used to reconstruct flow on the Columbia River at The Dalles, Oregon, since 1750. Residual statistics from this model exhibit a positive trend over time, indicating a change in the relationship between drought and streamflow caused by changes in land use over the twentieth century. The multiyear drought of the 1930s was the second most severe on record, with a more intense drought occurring during the 1840s. The period from 1950 to 1987 is unique in the last 250 years with respect to the relative absence of multiyear droughts.

Table of Contents

List of Figures

List of Tables

Acknowledgements

There are a great number of people to whom I owe sincere and heartfelt thanks. Indeed, my dissertation rightly ought to be authored by Gedalof *et al.*! My co-advisors, Dave and Nate, have given me ongoing guidance, support, freedom and encouragement throughout my graduate work. I could not have completed this work without them, nor would I have wanted to. They have acted far beyond the requirements of graduate advisors. My remaining committee members, Jim Agee and Dennis Hartmann, have always been generous with their time and experience, and also have contributed far beyond their roles on my committee.

Dan Vimont, Don McKenzie and Michela Biasutti were tireless in their efforts to teach me math (although of course any mistakes here remain my own). The Climate Impacts Group has provided me with financial support, encouragement and feedback at all stages of my research – in particular I would like to thank Ed Miles, Alan Hamlet, Bob Francis, Amy Snover and Philip Mote for their contributions.

My friends and colleagues in the former Cascadia Field Station were generous in their efforts to get me away from my computer, whether it be to go to the mountains or to Big Time. Thanks to Amy Hessl, Susan Prichard, Don McKenzie, Michael Case, Rob Norheim, Ella Elman, Megan Wilson, Jill Nakawatase, Melisa Holman, Hillary Cook, and Karen Kopper. My home-away-from-home, the University of Victoria Tree-Ring Laboratory, was similarly good to me. Thanks Dan Smith, Karen Brelsford and Alexis Johnson. Ian Walker brought me to the Queen Charlotte Islands and introduced me to the wonders of coastal dunes.

The Natural Sciences and Engineering Research Council of Canada (NSERC) funded me for the first two years of my Ph.D. work.

To my wife, Debbie, words fail to express my gratitude...

Chapter 1

Climate is conventionally defined as the statistics of weather; its mean state over a given space and time. However there is a growing recognition that the earth's climate is not static at any frequency of variability, and that mean conditions are inevitably a moving target. Natural systems are sensitive to these fluctuations, and the distributions of fish, trees, arable land and people can be interpreted to a large degree as responses to variations in climate across the surface of the planet. Past climatic surprises have dramatically altered the course of civilizations. Indeed, the history of natural resources management consists largely of attempts to predict, minimize and buffer against fluctuations in climate.

Scientific inquiries have led to many insights into the underlying causes and consequences of climatic variability, yet future climate remains as uncertain as ever. Human activities have altered the composition of the earth's atmosphere dramatically, giving rise to considerable debate over how the statistics of weather may change. Some insight into how natural systems may respond to these changes may be gained by analyzing the ways that they have responded to the rhythms of past fluctuations. These sorts of assessments address two principal questions: (1) which climatic factors influence the health of natural systems; and (2) are there thresholds in the response of natural systems to extreme events? Additionally, many biological organisms annually produce incremental growth, allowing these assessments to be undertaken retrospectively – that is, the organisms effectively monitor themselves. Those species that survive for long periods of time offer the further opportunity of hindcasting the climatic factors that limit their growth.

The overarching theme of this research program is to investigate links between past climatic variability and forest ecosystems of the Pacific Northwest. This theme emerges from relatively disparate lines of inquiry. Two perspectives are drawn from paleoproxy reconstructions of past climate, and a third from an assessment of the relationships

between area burned by wildfire and ocean-atmosphere processes. The results of these analyses are presented here as separate chapters, each standing relatively independently of each other.

This introduction represents chapter one. In chapter two I compare five paleoproxy reconstructions of North Pacific climatic variability, using the Pacific Decadal Oscillation (PDO) as an organizational touchstone. The combined record of these proxies provides a better index of PDO variability than any of the individual records, and suggests that the PDO has not been a constant organizing structure over time. In chapter three I examine the relationships between area burned by wildfire on national forestlands of the American Northwest and climatic processes – specifically 500 hPa circulation anomalies and drought. Climatic fluctuations play an important role in forcing extreme wildfire years at scales that range from synoptic to interannual and possibly longer. In some ecosystems, a specific sequence of events is necessary for extreme wildfire years to occur. In chapter four I use drought sensitive tree-rings to reconstruct discharge at The Dalles, Oregon since 1750. This record provides a long-term context for water resources planning, and suggests that the last 50 years have been anomalous in their relative absence of multiyear droughts.

Although this dissertation is composed of three distinct investigations, there are some recurring motifs that will emerge. In all three lines of inquiry I address climatic variability in the Pacific Northwest at annual to interdecadal time scales. I find that the underlying ecology of ecosystems modulates their response to climatic forcing. The natural records that these forests contain, in their ring width and fire history, are intrinsically nonlinear and must be interpreted cautiously. Lastly, disparate climatic forcings can give rise to similarly extreme events, and there may be as yet unidentified climatic surprises lurking in the wings.

Chapter 2

2.1 Abstract.

Annual growth increments from trees and coral heads provide an opportunity to develop proxy records of climatic variability that extend back in time well beyond the earliest instrumental records, and in regions where records have not been kept. Here I combine five published proxy records of North Pacific climatic variability in order to identify the extent to which these records provide a coherent picture of Pacific Basin variability. This composite chronology is well correlated with the Pacific Decadal Oscillation (PDO) index, and provides a better record of PDO variability than any of the constituent chronologies back to 1840. A comparison of these records suggests that the PDO may not have been an important organizing structure in the North Pacific climate system over much of the 19th century, possibly indicating changes in the spatial pattern of sea-level pressure and consequent surface climate patterns of variability over the Americas. Furthermore, the assumed stationarity between predictors and predictand in paleoclimatic studies may not be valid in the North Pacific sector.

2.2 Introduction

Instrumental climate records provide strong evidence that the North Pacific Basin experiences coherent modes of variability at interannual to interdecadal scales, generally termed the Pacific Decadal Oscillation (PDO) (Ware 1995; Mantua *et al.* 1997; Zhang *et al.* 1997). The spatial structure of this variability is very similar to that of El Niño / Southern Oscillation (ENSO), but with greater amplitude at high latitudes and a reduced tropical expression. During warm PDO regimes the western and central North Pacific Ocean typically exhibits cool surface temperature anomalies while the eastern Pacific exhibits above average temperatures. The opposite condition exists during cool regimes. The temporal variability of the PDO is characterized by much longer persistence than ENSO, on the order of 20 to 30 years. The PDO also appears to shift abruptly between warm and cool states, with observed shifts occurring in 1925, 1947 and 1977 (Hare 1996;

Minobe 1997) and some evidence that it may have exhibited many such shifts prior to instrumental observations (D'Arrigo *et al.* 2001; Gedalof and Smith 2001b). The cool-season Aleutian Low pressure system is generally more intense during warm PDO regimes and less intense during cool PDO regimes, with significant impacts on climate throughout North America (Wallace and Gutzler 1981; Latif and Barnett 1994).

In spite of the rapid developments in our understanding of the PDO, several key issues remain unresolved: (1) Is the PDO a robust feature of North Pacific climatic variability, or is it a 20th century phenomenon? (2) Does the PDO have a preferred time scale? (3) Are the observed regime shifts typical characteristics of the PDO? and (4) Does PDO forcing originate in the tropics or in the extratropics? Each of these issues has implications for the predictability of the North Pacific climate system and attendant resource management concerns. Given the long time scale of the PDO and the short length of the instrumental record there are some non-trivial limitations to analyses. Proxy records provide the opportunity to extend these records and gain some insight into the pre-instrumental (and pre-industrial) behavior of the North Pacific climate system. A number of proxy reconstructions have recently become available, incorporating tree rings (Minobe 1997; Kadonaga *et al.* 1999; Evans *et al.* 2000; Biondi *et al.* 2001; D'Arrigo *et al.* 2001; Gedalof and Smith 2001b) and coral skeletal chemistry (Linsley *et al.* 2000; Urban *et al.* 2000; Cobb *et al.* 2001). In this paper I compare five available, published, proxy reconstructions of North Pacific climatic variability in the context of the questions outlined above.

2.3 Data Description and Analytical Methods

I compiled five published climate reconstructions from around the Pacific Basin that all report a link to extratropical interdecadal variability (Table 2.1). Gedalof and Smith (2001b) used six high-elevation mountain hemlock (*Tsuga mertensiana*) chronologies from a transect extending from Oregon to Southeast Alaska to reconstruct the mean spring PDO index since 1600. This record has been extended from its original

termination date in 1983 to 1990 using several of the constituent chronologies as predictors in a simple linear regression. Biondi et al. (2001) used chronologies from Jeffrey pine (*Pinus jeffreyi*) and bigcone Douglas-fir (*Pseudotsuga macrocarpa*) from six sites in California and northwestern Mexico to construct the mean winter half-year PDO index back to 1661. Evans et al. (2000) used 15 tree-ring chronologies from various species located in Pacific influenced regions of extratropical North and South America to reconstruct one pattern in sea surface temperature (SST) that is structurally very similar to the PDO. Urban et al. (2000) used a δ18O chronology derived from a coral in Maiana to reconstruct regional SST variability back to 1840. This record exhibits good correspondence to drought in the American Southwest (Cole *et al.* 2002), and is well correlated to indices of North Pacific decadal variability. Linsley et al. (2000) developed a SST chronology based on Sr/Ca measurements from a coral in Rarotonga, located in the eastern subtropical South Pacific. This record extends back to 1726, and also exhibits interdecadal variability that is coherent with North Pacific records. Hereafter these studies and the chronologies they produced will be identified by their principal investigator.

Table 2.1. Summary of proxy chronologies used in the analysis.

Principal Author	**Data Type**	**Period of Record**	**Geographic Region**
Gedalof	Tree rings	1600 - 1990	Pacific Northwest, Gulf of Alaska
Biondi	Tree rings	1661 - 1991	American southwest, Mexico
Evans	Tree rings	1001 - 1990	Extratropical N. and S. America
Urban	Coral	1840 - 1994	Maiana, central tropical Pacific
Linsley	Coral	1726 - 1997	Rarotonga, eastern subtropical S. Pacific

There are several important differences between coral and trees that have implications for proxy climate reconstructions. In particular, tree rings represent a terrestrial, mid-latitude

response to climate, whereas coral records provide a marine, low-latitude response. Tree-ring time series typically provide an annually resolved record of growing season conditions, whereas coral continuously integrate their immediate environment, and the resolution is limited by sampling frequency and dating control. At present, tree-ring chronologies are well replicated and based on large sample sizes, whereas coral records are relatively sparse and reconstructions are often based on a single core. In order to directly compare these reconstructions the coral chronologies were resampled to a calendar-year timestep. While there may be more appropriate methods of resampling these time series, this approach is simple and objective, and suggests that the results presented here are a conservative estimate of the strength of the common signal between the tree-ring and coral chronologies.

In order to compare the five chronologies I used a principal components analysis (PCA) to extract common modes of variance from the chronologies. This analysis is restricted to the interval 1840 to 1990, the interval common to all of the proxy records. The resulting eigenvectors were scaled to have zero mean and unit variance, and were then projected onto the mean winter (Oct. to March) National Centers for Environmental Prediction / National Center for Atmospheric Research "reanalysis" SST field (Kalnay *et al.* 1996). The reanalysis data span the interval 1950 to the end of the proxy records in 1990. Pearson's product-moment correlation was used to assess the strength of the association between the eigenvectors and two indices of Pacific climatic variability: the Cold Tongue Index (CTI) is an ENSO index based on SST in the eastern equatorial Pacific (Zhang *et al.* 1997); and the PDO index is derived from the leading mode of variability in Pacific Ocean SST polewards of 20°N (Mantua *et al.* 1997).

2.4 Results and Discussion

Only the first eigenvector was well resolved (North *et al.* 1982), and was therefore retained from the PCA for further investigation. This leading mode of variability explains 41 percent of the total variance, and loads moderately strongly on all five proxy

records (Table 2.2). The principal component time series associated with this mode (PC1 hereafter) is well correlated with the PDO index ($r=0.64$, $p<0.001$; Figure 2.1). A partial correlation analysis indicates that this time series does not contain any information on the state of the CTI that is not intrinsically expressed in the PDO, suggesting that this record represents primarily a North Pacific climate signal, and not a tropical (i.e. ENSO) signal. It is worth noting that the observed correlation with the PDO index is higher than the correlation observed for any of the individual input series, indicating that the combined chronology is capturing more of the variability than any of its constituent components.

A distinct characteristic of the instrumental record of the PDO is the regime shifts that occurred in 1925, 1947 and 1977 (Hare 1996; Mantua *et al.* 1997). An intervention model (Box and Tiao 1975) applied to PC1 identified the 1947 and 1977 shifts as being significant, but failed to identify the 1925 shift. An intervention detection algorithm (see Gedalof and Smith 2001b) identified a significant shift from cool to warm states in 1905, consistent with the findings of Biondi, but no earlier shifts.

Table 2.2 The intercorrelations between the five proxy chronologies

	Gedalof	Biondi	Evans	Urban	Linsley	PC1
Gedalof	-	0.001	0.000	0.133	0.032	0.435
Biondi	**0.184**	-	0.000	0.365	0.033	0.406
Evans	**-0.461**	**-0.223**	-	0.000	0.000	-0.545
Urban	-0.126	-0.074	**0.370**	-	0.102	-0.342
Linsley	**-0.134**	**-0.131**	**0.349**	0.132	-	-0.483

The correlation coefficient is shown in the lower portion of the grid, and the p-values in the upper portion. Correlations that are significant at 95 percent confidence are indicated in bold script. The correlation between the proxy chronology and the leading PC is shown in the last column.

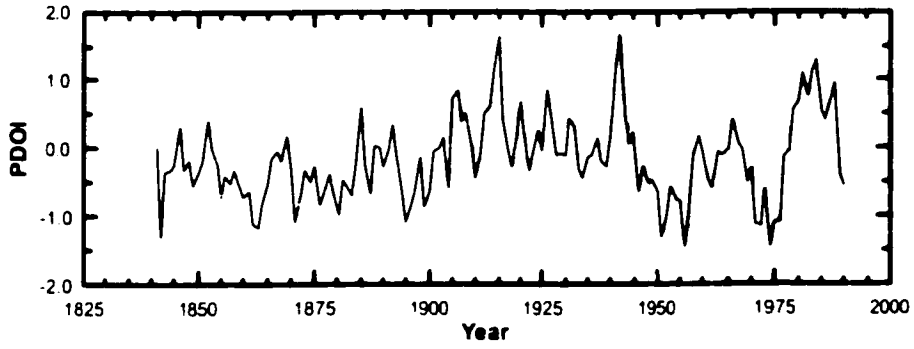

Figure 2.1 The time series of the leading principal component (PC1), scaled to match the mean October to March PDO index (shown in gray).

Regressing the SST field onto PC1 produces a spatial pattern that is similar in structure and magnitude to the PDO, with warm SST anomalies occurring in the eastern equatorial Pacific and along coastal western North America, and cool anomalies in the Aleutian Low region of the North Pacific (Figure 2.2). There is a similar cool anomaly in the South Pacific. This symmetrical structure in SST suggests a tropical forcing mechanism for the PDO (Garreaud and Battisti 1999; Evans *et al.* 2001; Folland *et al.* 2002).

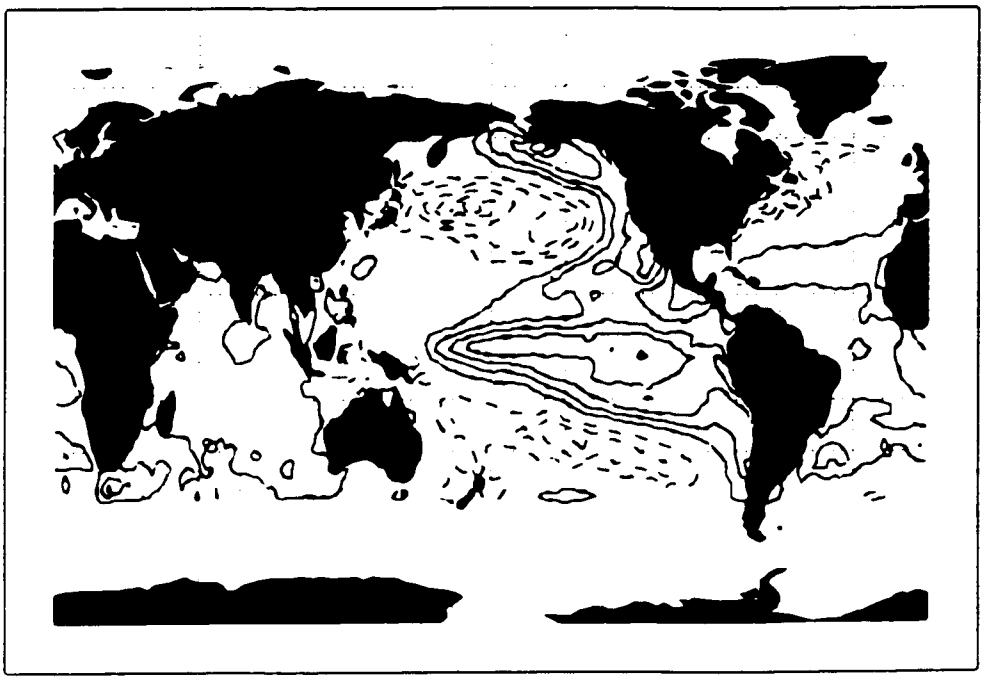

Figure 2.2 The NCEP SST data regressed onto PC1. Contour interval is 0.1°C per standard deviation of PC1. Positive anomalies are indicated by solid contours, negative anomalies by dashed contours, and the zero contour is not shown.

The fact that a PDO-like structure emerged as the leading eigenvector among these geographically dispersed proxies suggests that the PDO is a robust feature of Pacific climatic variability, because it represents the dominant mode of variability over the last 160 years. But an examination of the intercorrelation between the five proxy chronologies reveals a more complex situation (Figure 2.3). Eigenvector techniques are designed to find simple structure in data matrices and consequently will be biased towards regions or intervals with simple structure. Over the interval considered in this analysis there is a conspicuously stronger intercorrelation between the five proxies over the 20th century, and in particular since ca. 1975. This observation suggests that, while it may be the dominant mode of variability represented by these proxies, the PDO has not been a coherent structure over time. Also intriguing is the observation that the sign and strength of the correlations between the longest proxies prior to ca. 1825 suggest that a mode of variability with similar SST structure and downstream teleconnections to the

PDO was operating over this time. Interpreted together, these findings suggest that the PDO has probably been operating at least since 1600 but that it was not an important mode of variability over much of the 19th century. This interval is consistent with a period of poor correspondence between tree rings at high latitudes in North and South America (Villalba *et al.* 1999), and in proxy records of salmon abundance and SST in the Gulf of Alaska (Finney *et al.* 2000). Alternatively, this poor inter-correspondence could indicate non-stationarities in the climate-growth relationships developed for paleoproxy analyses.

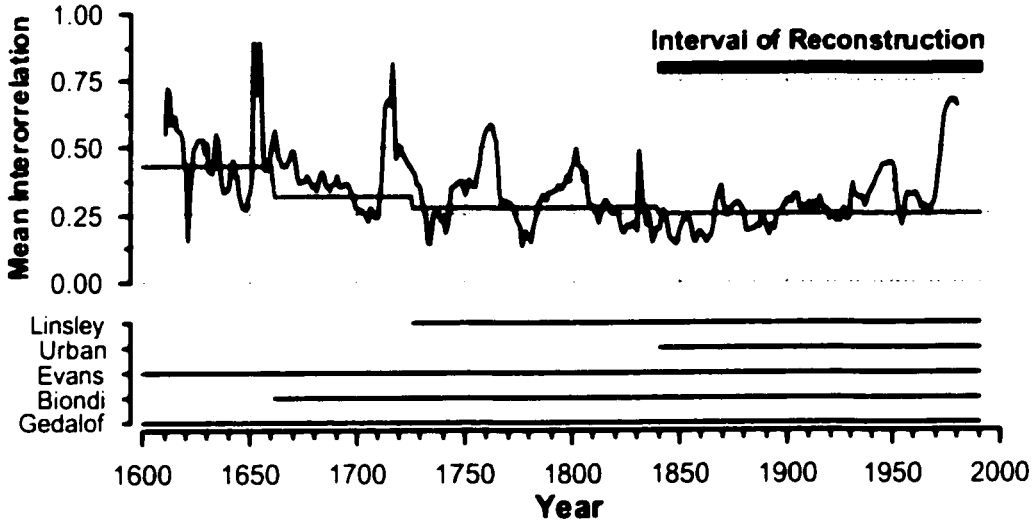

Figure 2.3 (upper panel) The mean intercorrelation between all proxies that have data, calculated over a 21-year moving window. The 95 percent confidence level for the appropriate number of intercorrelations is shown in gray. (lower panel) The interval for which each proxy record reports data. The shaded overbar indicates the interval used in the PCA, over which all proxies provide data.

These interpretations of PDO variability suggest that, over the interval considered in the PCA, there should not be a well-defined peak in variability at low frequencies. Indeed, a spectral analysis of PC1 reveals a predominantly red spectrum (results not shown). Any attempt to identify a preferred frequency of variability in the PDO will be intrinsically

complicated by the fact that the expected frequency is quite low (in the observed record there have probably been only two complete cycles since ca. 1890), and the possibility that the PDO has not exhibited a coherent structure over time.

Nonetheless, several studies have characterized the PDO as emerging from a phase-locked interaction between oscillations with ca. 20 and 50 to 70 year periods (Nakamura *et al.* 1997; Minobe 1999; Minobe 2000). The Aleutian Low is believed to be the keystone that connects these two processes. Regime shifts occur when the oscillations change phase simultaneously. Minobe (1999) noted that the synchrony of the oscillations was not strong in the early portion of the 20th century. I applied a singular spectrum analysis (SSA) (Vautard 1992) to the reconstructed PDO index in order to evaluate this characterization (Figure 4). Three dominant waveforms were identified in this analysis, with characteristic periods of approximately 85, 23 and 20 years. These three waveforms explain 53 percent of the variance in mean winter PDO index, and capture the observed regime shifts of the 20th century. An interesting feature of this analysis is the distinctly weak energy in the ~23 year mode prior to ca. 1875 – the interval when the proxies exhibit poor intercorrelation. SSA of the individual proxies supports this interpretation: the Gedalof, Evans and Linsley chronologies exhibit similar weak energy from ca. 1825 to 1875 in oscillatory modes with approximately bidecadal periods. These findings suggest that the poor correspondence between the proxy records over most of the 19th century may be a consequence of the small energy in this mode of variability. Interestingly, this mode appears to have been increasing in amplitude over the 20th century when the intercorrelation has been strongest. It is unclear from the current analysis whether the 20- and 23-year oscillatory modes are actually distinct, or if they are artifacts of differences in biological processes or the analytical approaches adopted by the original authors.

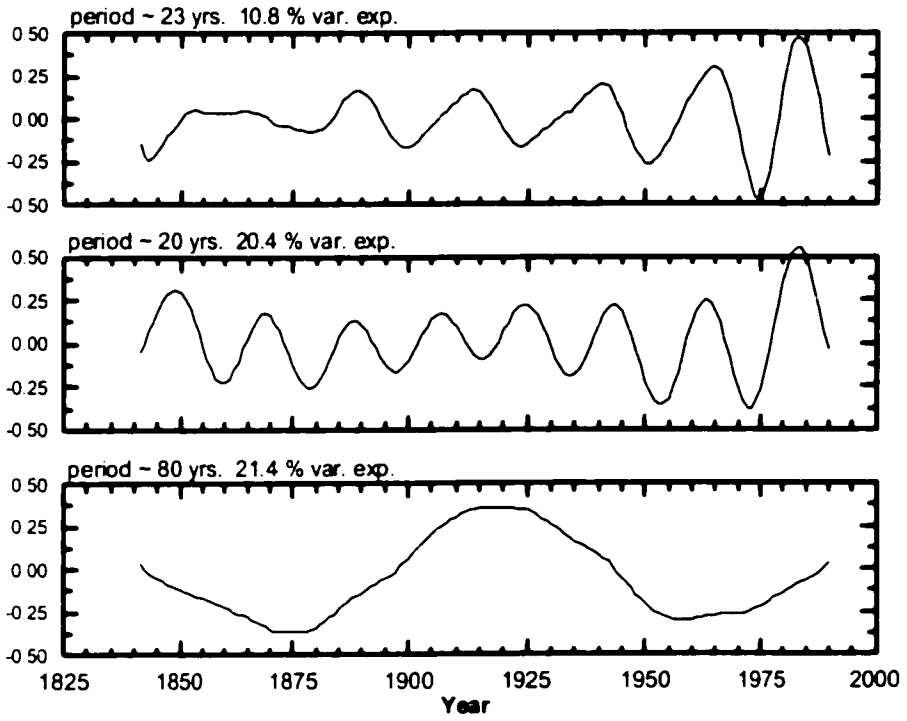

Figure 2.4 Weighted sums of the three leading pairs of eigenvectors extracted using singular spectrum analysis. The oscillatory modes have periods of (bottom panel) ca. 85 yrs., (middle panel) ca. 20 years, and (top panel) 23 years.

This analysis demonstrates that proxy chronologies from tree rings and coral may be directly incorporated into investigations of very large-scale ocean-atmosphere interactions. Reconstructions derived from these paleoproxy networks may capture these large-scale processes better than the spatially restricted networks necessitated by single-proxy analyses. In light of this observation further energy expended in extending the length of coral records will provide substantial and immediate returns in terms of an improved understanding of low-frequency variability in the ocean-atmosphere system.

2.5 Conclusions

These results provide insight into the long-term behavior of the PDO, and support the inference that North Pacific climatic variability at decadal and longer frequencies may be

a consequence of the complex interaction of several modes of variability. In the context of the four questions outlined in the introduction, this analysis supports the following interpretation: (1) The PDO does not appear to be a 20th century phenomenon only, but it also does not appear to have always been a robust feature of North Pacific climatic variability. Instead, it seems to have fluctuated in importance, with a notable interval of reduced influence over much of the 19th century. (2) Given this finding, and restricting the analysis to the period common to all five proxies, it was not possible to assess the extent to which the PDO exhibits a preferred time-scale in this analysis. However, there is some evidence to support the hypothesis of Minobe (1999) and others that the PDO is composed of phase-locked oscillations with periods of ca. 20 and 50 to 70 years. Consistent with Minobe I found poor synchrony between these modes in the early portion of the reconstructed PDO index. This interval is coeval with a period of poor intercorrelation between the individual paleoproxy records considered in the analysis. An examination of the longer proxy records suggests that this pattern of poor coherence occurred over much of the 19th century. (3) Given the uncertain nature of the PDO over the 19th century this analysis was unable to determine whether the observed regime shifts are characteristic features of the PDO. (4) The significant and consistent correlation structure between the tropical and extratropical proxies, including several from the Southern Hemisphere, all point to a tropical forcing mechanism for the PDO.

Chapter 3

3.1 Abstract

Wildland fire is an important ecological agent in forests of the American Northwest. Historical fire suppression efforts have contributed to an accumulation of fuels in many northwestern forests, and may result in more frequent and / or more severe wildfire events. Current management approaches therefore focus on fuel treatments as the primary method of avoiding extreme wildfire years. Here I investigate the extent to which atmospheric variability may force area burned on 20 national forests in Washington, Oregon and Idaho. Empirical Orthogonal Function (EOF) analysis was used to determine the coherence (or patterns) of area burned by wildfire in the Pacific Northwest. Anomaly fields of 500 hPa height were regressed onto the resulting principal component time series to determine the patterns in atmospheric circulation that are associated with variability in area burned by wildfire. Additionally, cross correlation functions were calculated for the Palmer drought severity index (PDSI) over the year preceding the wildfire season. A second analysis was undertaken using the same fire and climatic data sets, but based on superposed epoch analysis rather than linear regressions. This analysis focused only on the extreme fire years (both large and small), and does not require the association between fire and climate to be linear in nature. Four significant "modes" of burning were identified; each associated with distinct climatic processes:

1. Region-wide (with the exception of coastal temperate rainforest) increases in area burned are associated with the formation of a high-pressure blocking ridge over western North America throughout the fire season. This pattern is associated with drought in the spring and summer preceding the fire season maximum, but exhibits no association with either winter precipitation or snow accumulation.
2. Increases in area burned in eastern Washington and Idaho, coupled with reductions in area burned in southern and western Oregon are associated with reduced summertime 500 hPa heights in the region of the wintertime Aleutian Low, and increased heights over central and western North America. This pattern resembles the summer Pacific

North America (PNA) pattern, and contributes to increases in area burned independently of drought events.

3. Increases in area burned in the temperate rainforests of the Pacific Northwest occur when drought, beginning in summer of the previous year and persisting throughout the fire season, is coupled with particularly intense blocking.
4. Increased area burned in the forests of southern Oregon is also associated with summertime cyclonic circulation anomalies. In these particularly dry forests summer storms can deliver lightning and strong winds but often little rain, thereby providing an ignition source and a mechanism for rapid spread.

The results of these analyses support the hypothesis that climatic variability acts as an important control on the occurrence of extreme wildfire years. The extent of this control is modulated by the underlying ecology of the region, with coastal temperate rainforests responding to lower frequency variability than the drier steppe and savannah ecosystems of the interior. Stronger relationships were observed for the superposed epoch analysis than for the linear regressions, supporting the inference that climatic controls are more important in forcing extreme wildfire years than more moderate wildfire years. While forest management practices can alter fuel structures, they have no control over climatic variability. However fuels treatments should be undertaken in consideration of the relative roles of climate and fuels as limiting factors for large fires and in the specific ecological context of the management unit.

3.2. Introduction

There is a growing recognition that fire plays an integral role in developing the structure and composition of forest ecosystems in the Pacific Northwest (Agee and Huff 1987; Cwynar 1987; Huff 1995; Lertzman *et al.* 1998; Taylor and Skinner 1998; Everett *et al.* 2000). Historical fire exclusion practices are being revised to reflect these changes in attitude - forests are now subjected to "fire management" rather than the automatic suppression and exclusion policies of the past. Naturally occurring fires are occasionally allowed to burn, prescribed fires are intentionally set, and fuels are managed to encourage

natural fire regimes (Agee 1993). Fire exclusion continues at locations where cultural, economic, or ecological values require it. The exclusion of fire over the last century has changed its role in many ecosystems, however, and made many types of forest more prone to extreme fire events (Agee 1997; Agee 1998). Consequently, a better understanding of the factors that contribute to severe, extensive fires is critical for the integration of fire as an ecological process into managed landscapes.

Fire behaviour is determined largely by the nature of the fuels, topography, and weather occurring at the site of ignition (Johnson 1992). Of these factors weather is the most variable over time and the most poorly understood. Furthermore, a substantial proportion of total area burned is likely caused by relatively few fires that occur under extreme weather conditions (Schroeder 1969; Strauss *et al.* 1989; Johnson and Wowchuk 1993). The goal of this study is to determine if underlying patterns exist in annual area burned in the northwestern United States, and to associate these patterns with large-scale structures in the mid-troposphere and to variability in antecedent temperature, precipitation, and drought. This approach is distinct from most previous studies in two respects: (1) I do not treat the area west of the Rocky Mountains as a single coherent unit; and (2) I address large fire seasons, rather than individual large fires.

I divided the study area into multiple regions with coherent fire regimes for several reasons. First, the large contrast in forest types that occur throughout this region is almost certainly a response to different climatic and fire regimes that are in operation (Franklin and Dyrness 1973; Agee 1993). Given these differences it seems probable that there may be more than a single pattern in annual area burned, as well as distinct climatic controls on these patterns. Furthermore, by focusing on extreme wildfire years rather than individual large fires I am better able to assess the role of the atmosphere in forcing wildfires. By averaging over space and time I reduce the role that individual site characteristics play in contributing to fire extent. Lastly, by identifying elements of climate that contribute to extreme wildfire years in specific regions of the American

Northwest I provide fire managers with a tool that can be used with some skill to anticipate the severity of the upcoming fire season.

3.3 Regional Setting

Twenty national forests were considered in the analysis, located throughout Washington, Oregon and Idaho (Figure 3.1). This study region abuts the Canadian border to the North, the Pacific Ocean to the west, the Rocky Mountains to the east, and California and Nevada to the south. The Cascade Mountains unevenly bisect the study area along a north-south axis, and exert a strong orographic control on the region's climate. The Olympic and Coast Mountains, located in northwestern Washington and coastal Oregon respectively, exert additional climatic and ecological influences on the region. Southeastern Oregon is characterized by a complex mosaic of highlands, mountainous terrain, and basin and range topography that give rise to a spatially heterogeneous landscape.

This physiographic setting influences regional fire regimes in several ways: (1) orographic controls on temperature and moisture availability give rise to characteristic vegetation assemblages that in turn influence fuel accumulation and flammability of the landscape; (2) differences in parent material influence rates of soil development and soil chemistry, which can influence the relative abundance of forest types; (3) regional topography influences the location and intensity of summertime convection cells that affect the frequency of lightning ignitions; and (4) regional differences in elevation lead to dramatic adiabatic changes in temperature and relative humidity as air masses are translocated – in particular when circulation favors anomalous easterly winds, which can dry fuels quickly and lead to especially severe wildfire hazards.

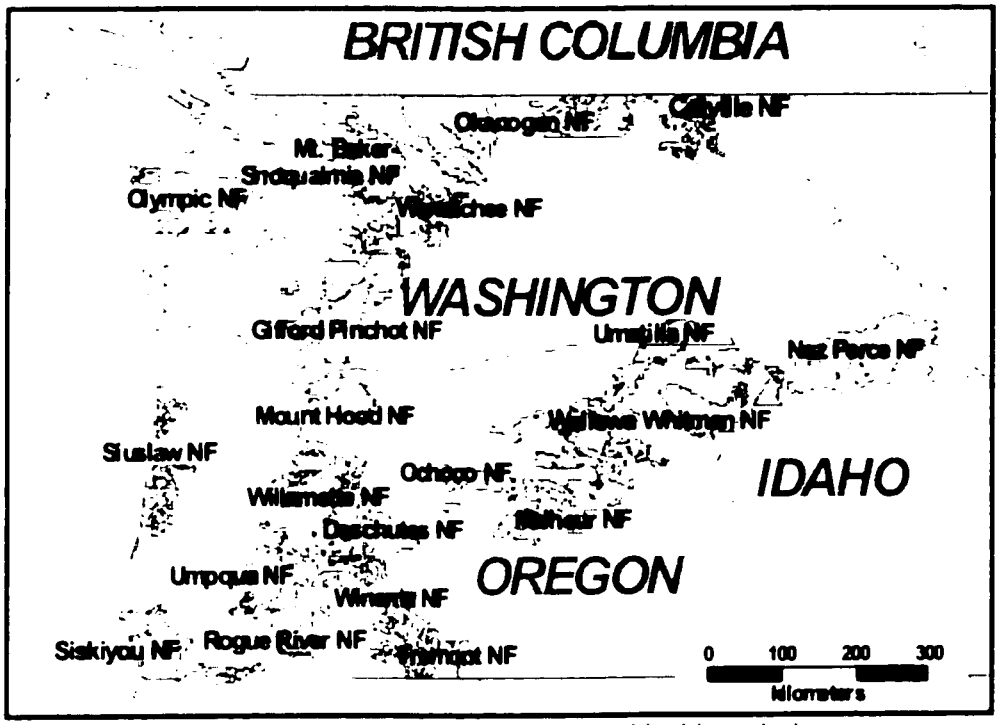

Figure 3.1 Locations of the 20 national forests considered in this analysis.

Orographic controls on precipitation lead to a considerable disparity in total annual precipitation across the study region. Mean annual precipitation ranges from over 250 cm on the Olympic Peninsula to less than 25 cm in the interior Columbia Basin. Average precipitation west of the Cascades is approximately 140 cm per year, about four times the 40 cm annual average east of the Cascades. The distribution of mean annual temperature is less affected by the mountains than is precipitation, although coastal regions are on average about 2°C warmer than interior regions. However the Cascade Mountains mark the approximate boundary between maritime and continental climates in the region, with summer-winter differences in temperature substantially greater east of the Cascades crest.

These differences in regional climate are reflected in the dominant vegetation types that occur throughout the Pacific Northwest (Franklin and Dyrness 1973) (Table 3.1). Along the northwest coastline of the study area coastal temperate rainforests dominate low

elevation stands. These dense, lush forests are characterized by Sitka spruce (*Picea sitchensis*), western hemlock (*Tsuga heterophylla*) and western redcedar (*Thuja plicata*). Douglas-fir (*Pseudotsuga menziesii*) and grand fir (*Abies grandis*) are less common associates. Although these forests are capable of burning, fire is infrequent due to very high annual precipitation and rapid decomposition of fine fuels. Fahnestock and Agee (1983) estimate a minimum fire return interval[1] of 1146 years for western Washington, and Gavin *et al.* (in press) found locations on western Vancouver Island that have not burned during the entire Holocene. When fire does occur the area burned appears to be large, and it usually results in total stand replacement (Agee 1993).

Just inland of the Sitka spruce zone is an extensive zone dominated by western hemlock, although Douglas-fir represents an important codominant at many sites. Important associates include western redcedar, grand fir and, less commonly, lodgepole pine (*Pinus contorta* var. *contorta*) and western white pine (*P. monticola*). These forests are generally drier than the Sitka spruce zone, and fire is a more common disturbance agent. Indeed, the presence of Douglas-fir in these forests is generally believed to be a response to episodic disturbance by fire, which exposes mineral substrate and creates openings in the canopy that allow the establishment of shade intolerant species (Agee 1991b; Edmonds *et al.* 1993; Huff 1995). The fire regime in western hemlock forests is quite variable in terms of frequency, intensity and severity (Agee 1993). Although most fires result in stand replacing events, mature Douglas-fir individuals may survive less severe fires. Fahnestock and Agee (1983) report a fire return interval of 230 years for these forests, although Agee (1993) cautions that this figure is probably highly variable across the landscape. Also, empirical models that are forced by climate predict a much longer fire return interval for these forests than are estimated from age distribution models (Agee

1. The mean fire return interval is defined here as the average number of years between two successive fire events in a given landscape. It is most commonly applied to regions with low to moderate severity fire regimes. The terms "fire rotation" and "fire cycle" are more commonly applied to forests with moderate to high severity fire regimes. These latter parameters are normally estimated from age-distribution models rather than from fire scars or other direct measurements, but otherwise indicate the same fire return properties (Baker and Ehle; 2001, Li, 2002).

1993).

Table 3.1 Biophysical characteristics of the 20 National Forests considered in this analysis

National Forest	Dominant Forest Types[1]	Mean Annual Precipitation (cm)	Typical Fire Regime[2]
Colville	**Douglas-fir, grand fir**, Engelmann spruce, subalpine fir	52	3-5
Deschutes	**Lodgepole pine, ponderosa pine**, Douglas-fir, grand fir	501	1-2
Fremont	**Ponderosa pine**, western juniper, lodgepole pine	67	2-3
Gifford Pinchot	**Western hemlock, Douglas-fir**, Pacific silver fir, mountain hemlock	157	4-5
Malheur	**Douglas-fir, grand fir**, ponderosa pine	34.5	3-5
Mount Baker-Snoqualmie	**Western hemlock, Douglas-fir, Pacific silver fir**, mountain hemlock	166	5-6
Mt. Hood	**Western hemlock, Douglas-fir, grand fir**, mountain hemlock, subalpine fir	153	4-5
Nez Perce	**Douglas-fir, grand fir, ponderosa pine**, Engelmann spruce, subalpine fir	59	4-6
Ochoco	**Douglas-fir, grand fir**, ponderosa pine	31	3-4
Okanogan	**Douglas-fir**, western hemlock, Engelmann spruce, subalpine fir	108	3-5
Olympic	**Sitka spruce, western hemlock, Pacific silver fir**, Douglas-fir, mountain hemlock	174	5-6
Rogue River	**Douglas-fir, white fir, red fir**, ponderosa pine,	70.7	3-5
Siskiyou	**Douglas-fir, western hemlock**, coast redwood, white fir, red fir	130	2-5
Siuslaw	**western hemlock, Sitka spruce, Douglas-fir, grand fir**, Pacific silver fir	168	4-6
Umatilla	**Douglas-fir, grand fir**, ponderosa pine, Engelmann spruce, subalpine fir	41	3-5
Umpqua	**Douglas-fir, ponderosa pine**, grand fir, incense cedar,	98	4-5
Wallowa Whitman	**Douglas-fir, ponderosa pine**, grand fir, Engelmann spruce, subalpine fir	47	2-4
Wenatchee	**Douglas-fir, grand fir, ponderosa pine**, subalpine fir	99	2-4
Willamette	**Douglas-fir, incense-cedar, ponderosa pine, Oregon white fir, red fir**, mountain hemlock	103	1-4
Winema	**Ponderosa pine, lodgepole pine**, Douglas-fir, grand fir	64	1-3

1. Species identified in bold are most commonly occurring

2. Fire regimes are based on Agee (1993): 1. Infrequent light surface fires (>25 year return interval); 2. Frequent light surface fires (1-25 year return interval); 3 Infrequent severe surface fire (>25 year return interval); 4. Short return interval crown - severe surface fire (25-100 year); 5. Long return interval crown - severe surface fire (100-300); 6. Very long return interval crown severe surface fire (300+ year).

Montane forests of the Cascade Mountains are characterized by Pacific silver fir (*Abies amabalis*) or red fir (*A. magnifica*). Important associates include Douglas-fir and western hemlock at lower elevations, and subalpine fir (*Abies lasiocarpa*), mountain hemlock (*Tsuga mertensiana*) and yellow cedar (*Chamaecyparis nootkatensis*) at higher elevations. At subalpine elevations mountain hemlock and subalpine fir usually dominate, although whitebark pine (*Pinus albicaulis*), yellow cedar and lodgepole pine may be locally important. Pacific silver fir is more common in the northern Cascades, where these forests are characterized by infrequent, high severity fires (Agee 1993). Agee *et al.* (1990) report a fire return interval of ca. 150 years for the northeastern Cascades. In contrast, Hemstrom and Franklin (1982) cautiously report a longer return interval (ca. 200 - 500 years) for forests at Mt. Rainier National Park, in the northwestern Cascades. In the southern Cascade and Klamath Mountains red fir replaces Pacific silver fir as the dominant montane species. This transition is probably a response to changes in precipitation and fire frequency (Franklin and Dyrness 1973). Typical fire regimes are variable in response to local topography, ecology and microclimatic features. Fire return intervals are difficult to assess due to "problematic characteristics of true firs" (Agee 1993), but are probably less than 50 years at most locations (Pitcher 1987; Taylor and Halpern 1991).

Middle elevation forests on the eastern slopes of the Cascade Mountains are characterized by stands of grand fir, Douglas-fir, or both. Western larch (*Larix occidentalis*), western hemlock, ponderosa pine (*Pinus ponderosa*), and occasionally Garry oak (*Quercus garryana*) are important associates depending on site conditions, with hemlock and larch more characteristic of locations where marine air masses spill over the Cascades crest, resulting in more mesic conditions. Ponderosa pine and Garry oak occur at cold-dry and hot-dry sites respectively. Because of the complex topography and associated microclimatic conditions, and the disparate fire adaptation strategies employed by different tree species, the fire regime in these forests is among the most complex of the entire region. Fires of all intensities and severities are common; low intensity fire return intervals are typically short – ca. 25 years for stands dominated by grand fir, and

probably less than a decade for Douglas-fir dominated stands (Agee 1993). Stand replacing events are more rare, occurring approximately once every 100 to 200 years (Antos and Habeck 1981; Barrett *et al.* 1991).

The forested lowlands east of the Cascade Mountains are dominated by ponderosa pine, with Douglas-fir, lodgepole pine and grand fir as important associates. In southern Oregon white fir (*Abies concolor*) is also a common associate. These forests are subjected to frequent, low-intensity fires that often result in little mortality of the overstory. Fire return intervals are difficult to assess in these forests because ponderosa pine is well adapted to survive fire and often there is little evidence preserved that a fire has occurred. Consequently, reconstructions based on fire-scarred individuals probably underestimate the frequency of fires. Even so, estimates based on fire scars alone range from as little as 3 years up to ca. 35 years, depending on site characteristics (Weaver 1959; Bork 1984; Agee 1993; Everett *et al.* 2000). Sites where ponderosa pine grows alongside more mesic species such as Douglas-fir and grand fir probably have longer fire return intervals (ca. 50 years, Agee *et al.* 1990). The typically low intensity of wildfires within ponderosa pine forests has allowed relatively effective fire suppression over the last several decades. Consequently there has been a trend towards increasing stand density, increased fuel loads, and often more shade-tolerant / fire intolerant species emerging from the understory (Weaver 1959; Agee 1993; Everett *et al.* 2000; Heyerdahl *et al.* 2001).

Stands dominated by lodgepole pine (*Pinus contorta* var. *latifolia)* are common throughout eastern Oregon and Washington. These stands are normally considered seral (Franklin and Dyrness 1973), and consequently are not considered in most forest cover schemes, which tend to identify climax or "potential" vegetation communities. Nonetheless, lodgepole pine stands may account for a significant proportion of the annual area burned in some national forests, and indeed may exist in a quasi-stable equilibrium at some sites (Gara *et al.* 1985; Stuart *et al.* 1989). Lodgepole pine stands often regenerate as dense, even-aged stands following stand replacing fires. As these stands

mature they self-thin and become highly flammable due to extensive down wood, ladder fuels and, often, reduced vigor following attack by mountain pine beetle (*Dendroctonus ponderosae*) (Gara *et al.* 1985). Because lodgepole pine is shade intolerant and can produce serotinous cones, it is well adapted to regenerate when this fire-prone stand burns (Gara *et al.* 1985; Stuart *et al.* 1989; Lotan and Critchfield 1990; Barrett *et al.* 1991). Lodgepole pine may also dominate at locations where poor soils inhibit the establishment of other species (Franklin and Dyrness 1973). Large portions of southern Oregon, for example, are characterized by serpentine soils derived from volcanic pumice, which are largely populated by pure stands of lodgepole pine. Typical fire return intervals in these forests are between 25 and 75 years, with stand replacing events occurring approximately once per 200 years (Barrett *et al.* 1991).

In addition to spatial variability in fuel production there is also variability in ignition frequency. Lightning strikes, the most important natural cause of fire ignitions in the Pacific Northwest, exhibit substantial spatial variability. West of the Cascade Mountains the annual density of lightning strikes is normally less than 0.05 strikes km^{-2}. In contrast, portions of Deschutes, Ochoco, Malheur and Umatilla National Forests typically experience 0.25 strikes km^{-2}, and Fremont, Wallowa-Whitman and Nez Perce more than 0.35 strikes km^{-2}. Rorig and Ferguson (1999; 2002) characterized the relationship between lightning strikes, atmospheric circulation, and fire ignitions in eastern Washington. They found that there are two distinct types of lightning, associated with "wet" and "dry" storms. Dry lightning occurs when the lower atmosphere is dry and unstable, contributing to intense convection but little or no precipitation reaching the ground. They also note that these same conditions contribute to dry, gusty winds that are conducive to the rapid spread of wildfire. In contrast, wet lightning is associated with a more conditionally unstable atmosphere and higher moisture levels in the lower atmosphere. They found that a simple index of low-level moisture and instability predicts dry lightning with good skill and exhibits a much stronger correlation with fire ignitions than does the total number of lightning strikes.

Regional differences in elevation contribute to the most severe types of fire weather in western North America. The continental interior is generally higher than the inter-mountain regions, which are in turn higher than coastal areas. Under normal conditions, air masses in the mid-troposphere move eastward from the coast to the interior, meandering through an alternating series of troughs and ridges. The Rocky Mountains promote the formation of a semi-permanent high-pressure ridge over western North America and a corresponding low-pressure trough over central and eastern North America. This circulation pattern can be interrupted by the development of a blocking ridge, characterized by an anomalous high-pressure system that remains quasi-stationary over the far eastern Pacific Ocean or western North America for prolonged intervals. These systems divert moisture away from the region immediately below and downstream, and in some circumstances can lead to anomalous easterly winds. These "foehn" or "chinook" winds warm and dry adiabatically as they move from the already warm and dry continental interior towards the coast. Under these conditions surface temperatures increase rapidly, relative humidity can plunge, and fuels can quickly become extremely dry (Flannigan and Harrington 1988; Johnson and Wowchuk 1993; Skinner *et al.* 1999). Blocking events may be interrupted by the rapid passage of one or more low-pressure systems that bring strong winds and potential ignition sources in the form of lightning (Schroeder 1969). When the blocking ridge has been especially strong and persistent, the extreme pressure gradient associated with cyclonic storms causes strong winds that result in rapidly spreading wildfires of unusual severity (Countryman *et al.* 1969; Sando and Haines 1972; Finklin 1973; Street and Birch 1986). Alternatively, at the edge of these high-pressure cells convective action alone can generate the winds (and ignition source) that contribute to high severity burning conditions and rapid rates of fire spread.

3.4 Data

Annual area burned by wildfire in the Pacific Northwest was determined in each of the 20 National Forests for the years 1948 to 1995, from USDA Forest Service Annual Fire Reports. Each year's observation was standardized relative to the area monitored for

wildfire to form a burned area index (BAI) for each of the national forests considered. This standardization was necessary because the area monitored for wildfire has not been consistent over time, and consequently there are spurious trends in area burned that result simply from the increase in area monitored. There are also differences in the relative areas of the national forests that make direct comparison otherwise difficult. The area burned data were available only as calendar-year totals, so no attempt to discriminate the timing of events within the fire season was possible. I also considered a region-wide composite BAI, defined as the area-weighted average of annual area burned in each of the 20 national forests. This regional chronology provides a basis for comparison for the regionalization strategy that I use, which must exhibit better coherence than this region-wide chronology in order to justify its additional complexity.

The upper-air observations consist of gridded measurements of 500 hPa geopotential height values, taken from the National Centers for Environmental Prediction / National Center for Atmospheric Research "reanalysis" project (Kalnay *et al.* 1996). Among the fields that were derived by the reanalysis, 500 hPa height is considered to be "well defined by the observations", and the reanalysis is not sensitive to model parameters (Kalnay *et al.* 1996). Monthly means were used for this analysis. The spatial domain considered included the region from 90° - 180° W, and from 30° - 75°N, with a resolu.ion of 2.5° latitude by 2.5° longitude.

The temperature, precipitation, and Palmer Drought Severity Index (PDSI) data were taken from the time bias corrected state climatic divisional data set (Guttman and Quayle 1996). The divisional data are derived from area-weighted averages of temperature and precipitation over regions of relatively homogeneous climate, and are reported as monthly means. These data probably represent conditions in the national forests better than single station data due to this spatial integration. All of the meteorological data had the annual cycle removed and were converted to anomaly values prior to analysis.

3.5 Methods

I considered several possible methods of subdividing the study area into regions of coherent fire patterns, including cluster analysis, classifications based on vegetation, climate and fire regime, and eigenvector techniques. I chose to use empirical orthogonal function (EOF) analysis because it incorporates most of the advantages of the other techniques considered, but has several key advantages. In particular, EOF analysis is able to identify patterns in area burned that might overlap in space (see Schroeder 1969). For example, one mode of atmospheric variability may lead to a north-south dipole in annual area burned, whereas another mode may cause an east-west dipole. Clustering and classification techniques would not be able to discriminate these modes as each national forest would be required to belong to a single group. Furthermore, even if the simplest structure in the data is a simple aggregation of individual forests based on geography or ecology, the EOF analysis should identify this structure.

EOF analysis has a rich tradition in climatological research (Preisendorfer 1988) but has rarely been applied to ecological data. Similar methods are commonly used in ecology, but with different terminology (McGarigal *et al.* 2000). EOF analysis is a type of eigenanalysis that identifies structures that explain the maximum amount of variance in a two-dimensional data set. In this application the structure dimension consists of 20 national forests, and the sampling dimension is time, with 48 years. Eigenanalysis of this matrix produces a set of spatial structures in the first dimension (EOFs), and a corresponding structure in the sampling dimension (principal component (PC)). Each PC describes the variability of the associated EOF over time. Each EOF is orthogonal to all other EOFs, and each PC is similarly orthogonal to all other PCs. Each EOF / PC pair has a corresponding eigenvalue that describes the variance explained by the pair. Alternatively, suppose that the input matrix, $\mathbf{A}$, consists of n rows (years) and m columns (national forests). The EOFs can be considered the eigenvectors of $\mathbf{A}^T\mathbf{A}$, and the PCs can be considered the eigenvectors of $\mathbf{A}\mathbf{A}^T$.

Each EOF consists of loadings for each national forest, which here represent the covariance between the BAI from that national forest and the PC. The EOFs can be interpreted as a pattern in area burned that is strongly expressed during years when the PC exhibits a large value, and is weakly expressed when the PC exhibits a small value. Positive loadings at a site therefore correspond to large fire years when the PC has a positive value. Because the patterns are linearly defined, the EOFs and PCs can arbitrarily be multiplied by -1 and the interpretation will not change. Thus, negative loadings also indicate large fire years when the PC exhibits a large negative value. In the case that a given national forest loads weakly on a particular EOF (i.e. has a loading near zero) then variability in the associated PC does not provide any information about area burned on that national forest.

I applied four types of EOF analysis to the BAI, using correlation and covariance matrices, and (Varimax) rotated and unrotated solutions (Preisendorfer 1988; Yarnal 1993). The Varimax rotation is intended to simplify the structure of the eigenvectors by concentrating the variability within each principal component (PC) on a small fraction of the input variables (Kaiser 1958; White *et al.* 1991). Ideally, the variance for a given variable is explained primarily by a single PC, and minimally by the remaining PCs. Rotation of the initial solution also avoids potential problems associated with the domain shape (Legates 1991; Richman 1993). The statistical significance of the solution was assessed by calculating a 95 percent confidence interval around the eigenvalues (North *et al.* 1982). This confidence interval can be used to assess whether the structures identified represent true "modes" in area burned. If there is a large overlap in the confidence intervals around the eigenvalues the spatial structures described by the EOFs are probably not stable, because any linear combination of the overlapping eigenvectors is equally significant. The confidence intervals can also be used to guide the decision on how many PCs to retain.

The atmospheric circulation anomalies associated with each EOF were determined by regressing the 500 hPa anomaly field onto the associated PC time series. Suppose **P** is a

$1 \times n$ vector of the PC time series, and **H** is an $n \times m$ matrix of 500 hPa height anomalies for a given month of the fire season. Here m indicates the number of gridpoints for which 500 hPa height anomalies were considered. Using matrix notation, the vector **K** can be calculated as:

$$\mathbf{K} = \mathbf{n}^{-1}\,\mathbf{PH} \qquad [3.1]$$

Where **K** is of length m, and can be mapped to show the anomaly field associated with a one-standard-deviation perturbation in **P**. These maps are commonly called spatial regressions, or projections, because a time-varying spatial field is being regressed (or projected) onto a time-varying vector. Maps of **K** were developed for each month of the fire season (May - September).

The variance in **P** that can be explained by **K** can be estimated by calculating the expansion coefficient time series of **K**:

$$\boldsymbol{k} = \mathbf{HK} \qquad [3.2]$$

which provides a vector describing the variability **K** over time. That is, when **K** is strongly expressed then ***k*** will be large; when conditions are opposite to **K** then ***k*** will be negative; when 500 hPa conditions are very different from **K** then ***k*** will be close to zero. The correlation between ***k*** and **P** provides an estimate of the variation in **P** that can be linearly explained by ***k***, but should be interpreted cautiously as **K** was initially defined using **P**. Similar time series can also be defined from the map composites generated in the superposed epoch analysis. Because these composites were generated from a subset of the data (from five years in most cases) the correlation between ***k*** and **P** is based largely on independent data and is therefore a more robust estimate of the strength of the linear association between atmospheric variability and area burned by wildfire.

The statistical significance of the association between **P** and each gridpoint of **H** was determined using Spearman's rank-order correlation coefficient. Spearman's coefficient is a non-parametric statistic comparable to Pearson's product-moment correlation, but it is suitable when the assumptions of Pearson's correlation are not met, or when there is uncertainty regarding the quality of the data measurements (Zar 1999). In this analysis

the BAI distribution is not normally distributed at many of the national forests. Also, variability in fire suppression policies and practices, differences in area monitored, and complexities in the relationship between fire extent, behavior and effects, suggest that the BAI is at best a first-order approximation of the severity of the fire season. Spearman's correlation coefficient is also more conservative than the Pearson correlation coefficient. Consequently, it is almost certainly a more robust measure of the strength of the association between circulation anomalies and annual area burned.

This analytical approach assumes that there is a linear association between atmospheric variability and wildfire activity. It is possible however that extreme wildfire years may occur under a much narrower set of climatic conditions than less extreme years. In this scenario the linear association could appear quite weak, and the underlying forcing pattern might be missed altogether. In order to assess this scenario I used superposed epoch analysis (SEA) to characterize the 500 hPa height anomalies during the smallest and largest fire years. A specific form of SEA has been employed extensively in fire ecology (e.g. Swetnam and Betancourt 1990; Swetnam and Betancourt 1998; Grissino-Mayer and Swetnam 2000); here I use a more general form. The five years with the largest area burned and the five years with the smallest area burned were identified based on the BAI (or the PC time series, depending on the analysis). The mean and standard deviation in the 500 hPa height field for the large and small wildfire years were calculated. A two-samples t-test was used to identify regions where 500 hPa height anomalies are significantly different between the epochs. For display purposes, the small-fire-years composite was subtracted from the large-fire-years composite to emphasize the difference in circulation between the two epochs. Additionally, the map composites were compared to the spatial regression maps for consistency.

The role of antecedent climate conditions in preconditioning forests for large wildfire years was explored using cross-correlation analysis. The correlation between the regional BAI (and PCs), and total precipitation, mean temperature, and PDSI, was calculated for each month of the fire season (May to September) as well as the 12 preceding months.

These results provide some insight into the relative roles of seasonal-scale climatic variability and shorter-term (presumably synoptic-scale) processes in driving large wildfire years. Similar to the analysis of 500 hPa described above this cross-correlation assumes a linear association between area burned and antecedent climate. For comparative purposes I also calculated composite maps showing the mean PDSI for the most extreme wildfire years.

3.6 Results and Discussion

3.6.1 Composite Burned Area Index

Projecting the 500 hPa height field onto the region-wide composite BAI reveals a significant association between increases in area burned and increases in 500 hPa height over western North America during June, July and August (Figure 3.2). This pattern is consistent with the development of a high-pressure blocking ridge upstream from the study area, which would divert storm tracks out of the region and reduce relative humidity. These events can also cause extremely warm and dry easterly winds that dramatically increase the fire hazard. Additionally, there is a significant correlation with lowered 500 hPa heights in the central and northern Pacific Ocean in August, which would enhance the east-to-west pressure gradient and cause air to flow from the continental interior down to the coast, warming and drying in the process. This pattern is most similar to the *Great Basin High* fire weather pattern described by Schroeder (1969), which he characterized as occurring when a portion of the Pacific High moves into the intermountain region and stagnates there.

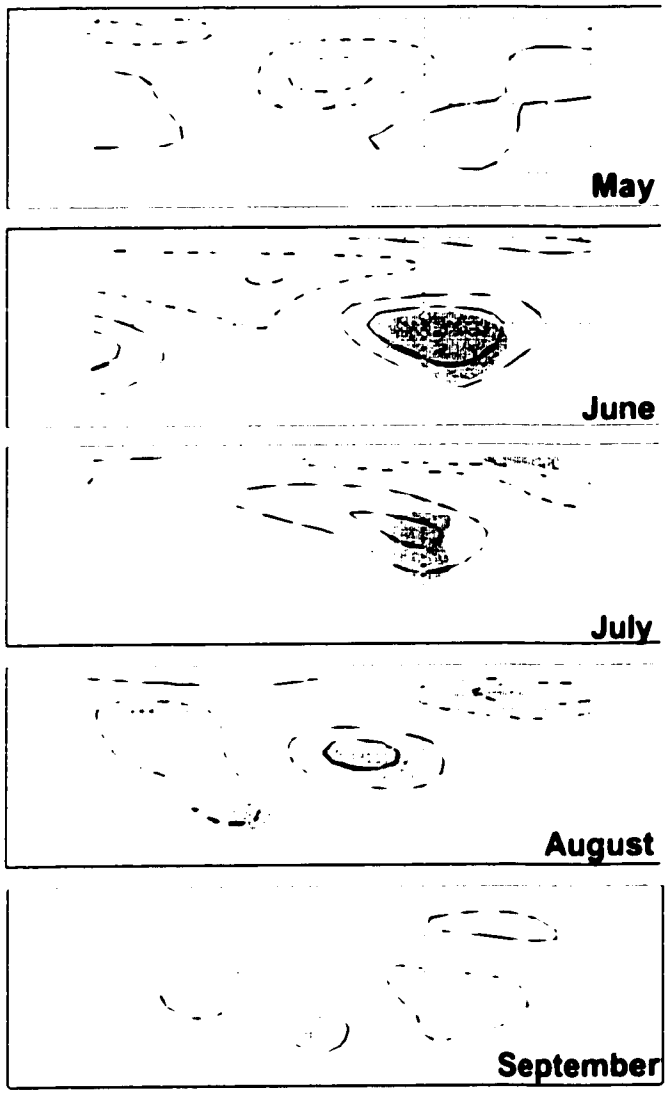

Figure 3.2 The 500 hPa height anomaly field projected onto the regional BAI. This pattern describes the atmospheric variability associated with a 1σ perturbation in BAI. The contour interval is 5 meters, with positive anomalies indicated by a solid contour, negative anomalies by a dashed contour, and the zero line not shown. Dark shaded regions indicate that the correlation is significant at 95 percent confidence.

The correlation between the expansion coefficient time-series of the projected patterns and the regional BAI ranges from 0.35 to 0.51 over the fire season (Figure 3.3, triangles). This correlation improves substantially when either the maximum or mean fire-season value is considered (r = 0.58 and 0.65 respectively). This finding is consistent with the hypothesis that several weeks of fire-conducive weather at any point in the fire season can lead to increases in area burned, but that the timing of fire weather is less important than the magnitude (i.e. maximum blocking index) or persistence (i.e. mean blocking index).

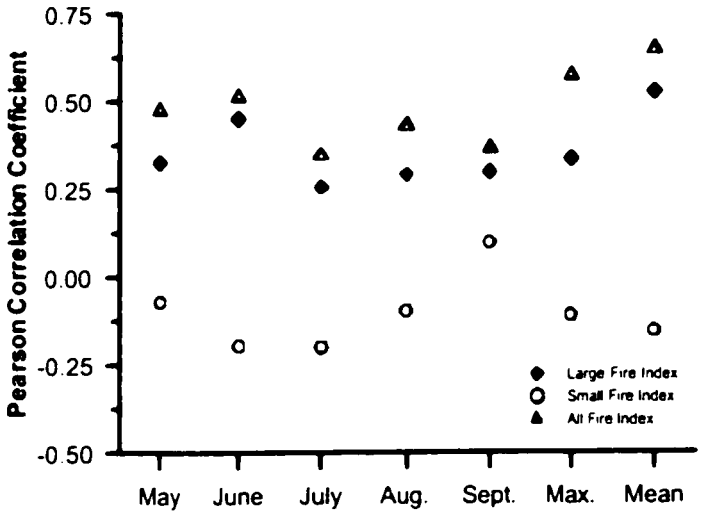

Figure 3.3 The correlation between the expansion coefficient time-series of the 500 hPa map pattern associated with: all years (triangles); the five largest fire years (diamonds); the five smallest fire years (circles), and the composite BAI. The correlation was calculated for all months of the fire season as well as the maximum and mean fire season indices.

The magnitude of the 500 hPa height anomalies shown in Figure 3.2 are relatively modest – only ca. 15 m (approximately 0.5 standard deviations). This result implies either that area burned is very sensitive to 500 hPa height anomalies, or that there is a lot of noise in the model. Some insight into the relationship can be gained by considering the results of the SEA (Figure 3.4). Composite maps of the five smallest and five largest

fire years indicate a strong association between increased (decreased) 500 hPa height and increased (decreased) area burned. The magnitude of these 500 hPa height anomalies is substantially larger than seen in the map projections, although the structure of the patterns is very similar. These results suggest that especially small and large fire years are more sensitive to atmospheric variability than are moderate fire years. Indeed, projecting the 500 hPa height field onto the BAI for the remaining years (not the five smallest or largest fire years) reveals virtually no association between atmospheric variability and fire extent (results not shown). Interpreted together these results suggest that extreme fire years (both large and small) are sensitive to variability in the mid-troposphere but more moderate fire years are not.

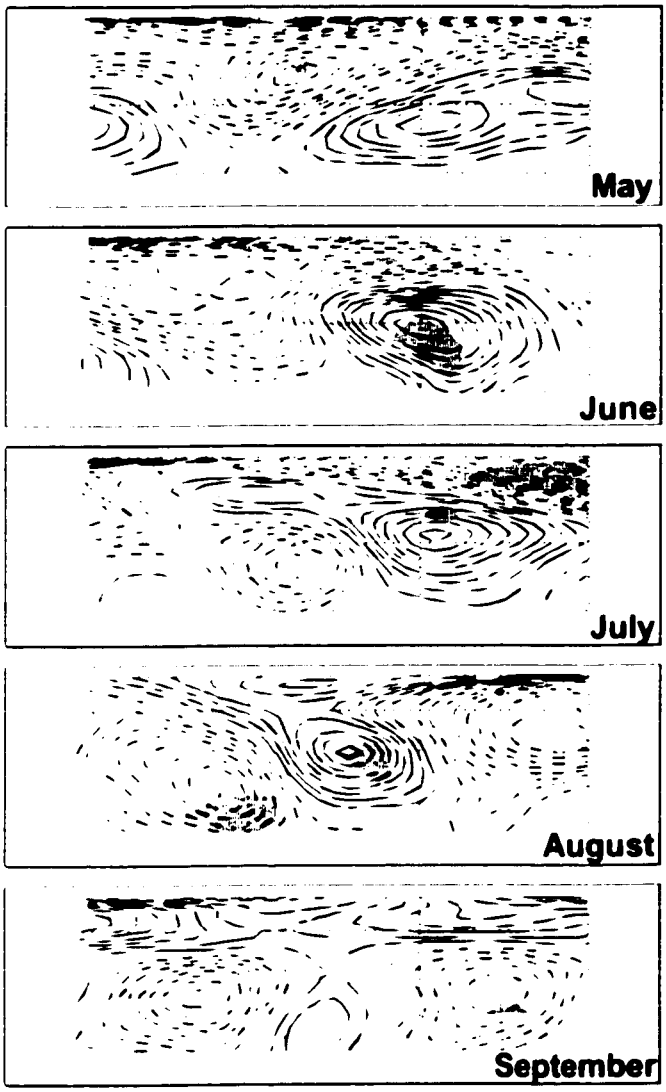

Figure 3.4 Difference in the 500 hPa height field between the five largest and smallest fire years in the regional BAI. Contour intervals are as in Figure 3.2. Regions where the difference between large and small fire years are significant at 95 percent confidence (two-samples t-test used) are indicated by dark shaded regions.

By deriving the expansion coefficient time series of the large and small fire year composite maps it is possible to calculate the correlation between the patterns identified

in the SEA and area burned. Unlike the analysis described above these time series are largely independent of the BAI data, and probably provide a more robust estimate of the strength of the linear association between atmospheric circulation and wildfire activity. The correlation between the index based on the large fire years composite and area burned is significant, and suggests at least a moderate linear association between the blocking structure and wildfire activity (diamonds in Figure 3.3). In contrast, the correlation between the index based on small fire years and area burned is very weak (circles in Figure 3.3), and provides little support for a linear relationship.

Scatter plots of these indices versus BAI provide some insight into the nature of the association between blocking (cyclonic) activity and large (small) wildfire years (Figure 3.5). The large fire year composite index suggests that the atmosphere imposes a strong constraint on fire activity. Eight of the 10 largest fire years occur during summers with positive mean blocking index values. Only 1977 stands out as a year with a high blocking index value but little wildfire activity. In contrast to this control on large wildfire years, only five out of the 10 smallest wildfire years occur under negative mean blocking index conditions. The scatter plot of the small fire composite index versus BAI presents a less obvious picture. While eight of the 10 smallest fire years occur under a positive index, a number of very small fire years also occur under a strongly negative index. There are several possible explanations for this scenario: (1) the conditions that contribute to very small fire years may be more spatially heterogeneous than was observed for large fire years. That is, a wide range of conditions may lead to small area burned in any given year. This interpretation is consistent with the observation that the larger fire years exhibit an inverse association to this index whereas the smaller years exhibit much greater scatter. (2) The time scale associated with the conditions that lead to particularly small wildfire years may be shorter than a month, and therefore are not evident in the monthly climatic variables considered in this analysis. For example, even a few days of heavy rain could suppress any active wildfires and reduce the probability of new ignitions even in the event of weather conditions that would otherwise be highly favorable for wildfire activity. (3) The fire data themselves may be spatially

heterogeneous. That is, there may be a narrow range of conditions that lead to region-wide reductions in area burned, but a more diverse set of conditions that lead to more localized reductions. This last possibility is explored in greater detail in the next section.

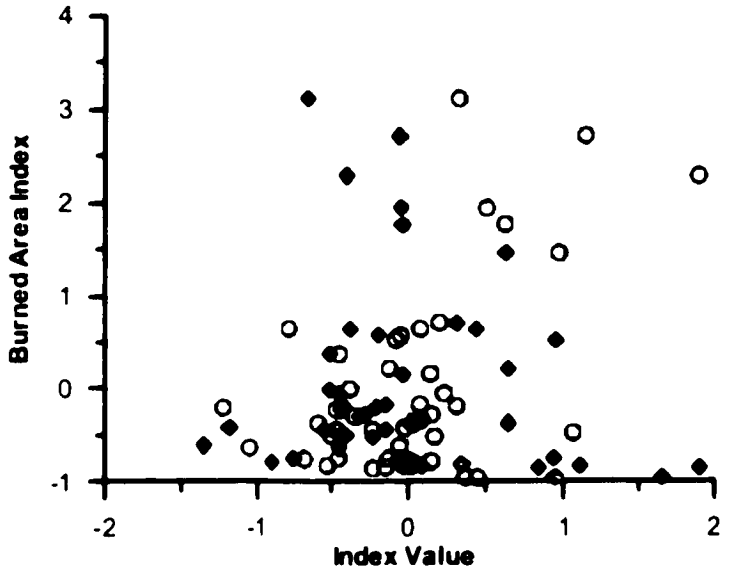

Figure 3.5 Scatter plots of the mean annual large-fire-composite index (circles) and small-fire-composite index (diamonds) versus regional BAI.

In order to assess the role of antecedent climate in preconditioning forests to burn I calculated lagged correlations between BAI and monthly PDSI, temperature and precipitation for the interval starting one year prior to the fire season. The correlation between BAI and PDSI exhibits a region-wide coherence, with increases in area burned associated with increased drought throughout spring and summer of the current year (Figure 3.6). The association with PDSI in the winter preceding the fire year is weak, and does not exhibit spatial coherence, suggesting that winter climatic variability does not exert an important control on wildfire activity.

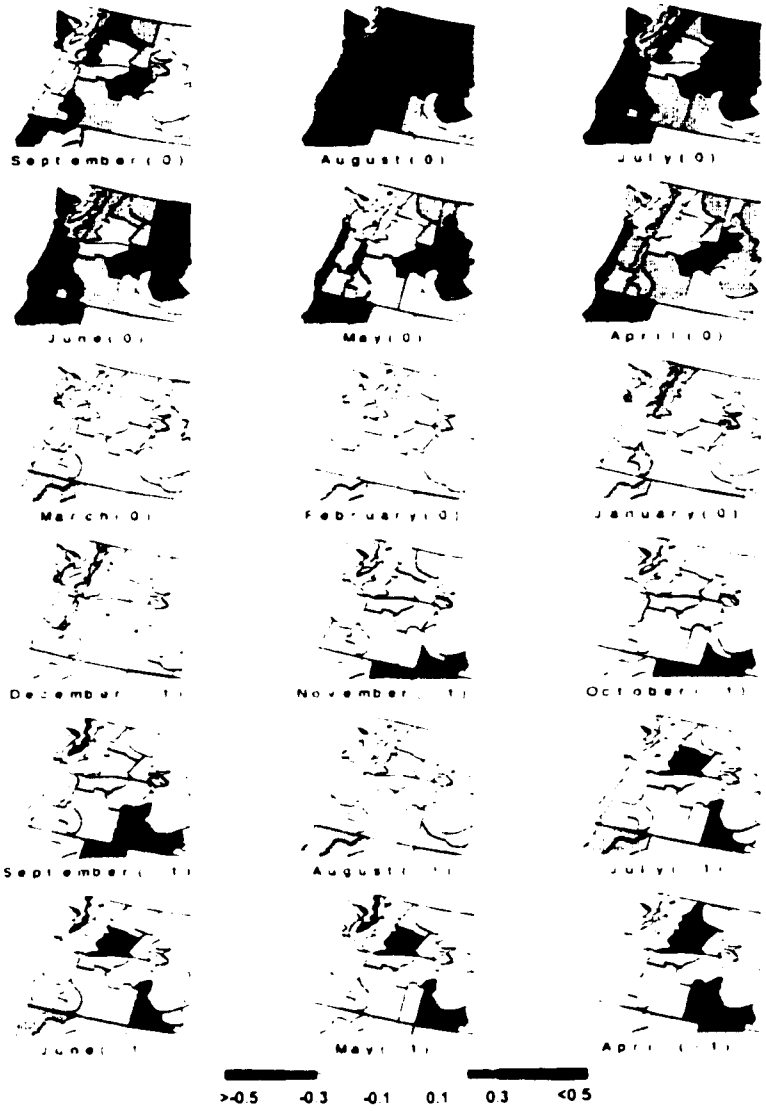

Figure 3.6 Lagged correlation between the regional BAI and PDSI. Inverse correlations are shown in red, and indicate a correspondence between increases in area burned and enhanced drought conditions.

The correlations with precipitation and temperature exhibit patterns consistent with the results for PDSI (not shown). Increases in area burned are associated with increased temperature in March through August. There is a weak association with cooler than average temperatures in the preceding autumn, and to above average temperatures in the preceding summer. The association with precipitation is more highly variable, with strong correlations exhibited only at the height of the fire season; increases in fire are

associated with reduced precipitation in June through August of the fire season. Prior to April of the fire year the correlations to precipitation are generally weak, exhibit both positive and negative signs, and show no obvious pattern. Interpreted together, these results suggest that the combination of temperature and precipitation is more important in preconditioning forests to burn than either of them individually.

In order to estimate the strength of the association between regional drought and area burned I calculated the average monthly PDSI value for all climate divisions in Washington and Oregon. The correlation between this regional PDSI record and area burned is -0.31, -0.30 and -0.37 for the months of June through August respectively. The magnitude of this correlation decreases rapidly both before and after the fire season, with non-significant correlations exhibited in April before the fire season ($r=-0.25$) and in October following the fire season ($r=-0.25$).

The results presented here suggest that climatic variability is an important cause of variation in area burned by wildfire in the American Northwest. Blocking ridges, evident in the 500 hPa height field, contribute to increased drought stress in spring and summer of the fire year. These soil moisture deficits presumably reduce fuel moisture contents, increasing the flammability of the landscape. The associations observed in this analysis were limited primarily to spring and summer months, implying that variability in winter conditions contributes little to wildfire activity in the following summer. This finding has important implications for the forecasting of seasonal wildfire severity, as wintertime climatic variability is much better understood than summer-time variability (Kumar and Hoerling 1998). Similarly, El Niño / Southern Oscillation (ENSO) and Pacific Decadal Oscillation (PDO) express themselves most strongly in winter months in the Pacific Northwest (Ropelewski and Halpert 1986; Yarnal and Diaz 1986; Mantua *et al.* 1997; Zhang *et al.* 1997; Gershunov and Barnett 1998), implying that skillful ENSO or PDO forecasts would contribute little information to a fire season forecast.

ENSO is a pattern of ocean-atmosphere variability that is characterized by episodic warming (cooling) in the western tropical Pacific and weakened (strengthened) trade winds. The North Pacific Ocean typically exhibits an enhanced (weakened) wintertime PNA pattern in response to warm (cool) ENSO events (Yarnal and Diaz 1986). Attendant teleconnections cause the Pacific Northwest normally to be warm and dry (cool and wet) (Ropelewski and Halpert 1986; Yarnal and Diaz 1986). The return interval for strong ENSO events is typically three to seven years. The PDO is an ENSO-like pattern of variability, with similar teleconnections, but is most strongly expressed in the extra-tropical North Pacific (Mantua *et al.* 1997). It is characterized by variability at interannual to interdecadal scales, but also appears to shift abruptly between warm and cool mean states every few decades (Mantua *et al.* 1997; Gedalof and Smith 2001b). Cool conditions persisted from ca. 1925 to 1947, and from 1977 to ca. 1989, and warm conditions persisted prior to ca. 1925 and from 1947 to 1977 (Mantua *et al.* 1997; Hare and Mantua 2000).

In order to test the hypothesis that these patterns are not important forcing mechanisms for extreme wildfire years I compared BAI during warm (i.e. El Niño) and cool (La Niña) ENSO years, and in the warm and cool phases of the PDO using a two-samples t-test. These tests confirmed that there is no significant difference in area burned between warm and cool ENSO events ($p = 0.255$) and between warm and cool PDO regimes ($p = 0.178$). As an additional measure I calculated the Pearson correlation coefficient between the Cold Tongue Index (CTI), an index of ENSO activity (Zhang *et al.* 1997), the PDO index (Mantua *et al.* 1997), and the regional BAI. This analysis supported the finding that there is no association with ENSO activity ($r = -0.01$, $p = 0.953$), but suggests that there is at least a modest association between the PDO and area burned ($r = 0.40$, $p = 0.005$). This latter disparity can be explained by the fact that interannual variability in the PDO often exceeds the inter-regime variability (Figure 3.7). Although only six out of the 10 largest fire years occurred during the warm phase of the PDO, seven of the 10 largest years followed winters when the PDO index was positive, and eight of the 10 smallest fire years occurred following winters when the PDO index was negative. Presumably

wildfire extent is more closely related to this higher-frequency variability than to the lower-frequency regime-scale variability. Nonetheless, this finding does imply that in the long run there will be increases in area burned during the warm phase of the PDO, because the PDO index will be, on average, higher during these regimes. It is likely that the short time series considered in this analysis (less than one complete cycle of the PDO) does not provide a sufficiently large sample to detect this difference. Alternatively, there may be a signal related to fire management practices that obscures the underlying nature of the relationship.

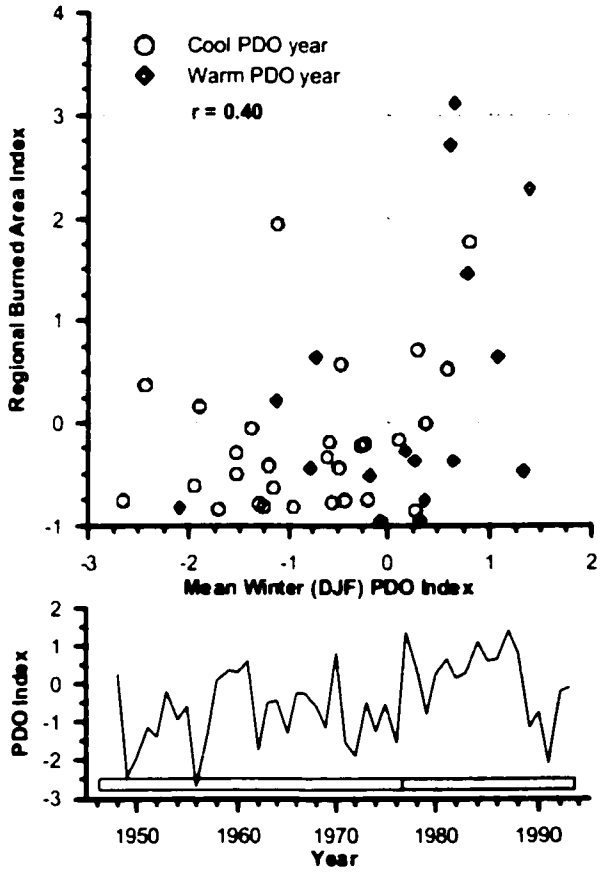

Figure 3.7 (Upper panel) scatterplot of mean winter (Oct. to March) PDO index versus regional BAI. Warm PDO regime years (1978 - 1994) are indicated by a diamond, and cool years (1949 to 1976) are indicated by a circle. (Lower panel) the time evolution of the PDO index, showing the transition from cool to warm conditions between 1976 and 1977.

3.6.2 Regionalized Burned Area Indices

The four applications of EOF analysis all identified similar dominant patterns of variability, although there were subtle differences in structure and variance explained depending on the EOF parameters. The results I present here are based on the correlation matrix and an unrotated solution. The use of a correlation matrix minimizes biases that could be introduced by the relative sizes and spatial arrangement of the national forests (Karl *et al.* 1982), and differences in the fire regimes of the different locations and forest types (Franklin and Dyrness 1973; Agee 1993). While the application of the Varimax rotation did not change the dominant patterns of variability substantially, it did increase the number of eigenvalues that were statistically greater than 1.0, thereby unnecessarily complicating interpretation.

The leading four eigenvectors were retained from the EOF solution, collectively explaining 52 percent of the variance in area burned in the 20 national forests (Figure 3.8). Although eigenvalues 5 and 6 were also greater than 1.0 at 95 percent confidence I found that the structure of the EOFs was unstable, depending on the dispersion matrix used and whether or not the solution was rotated, and so they were excluded from further examination.

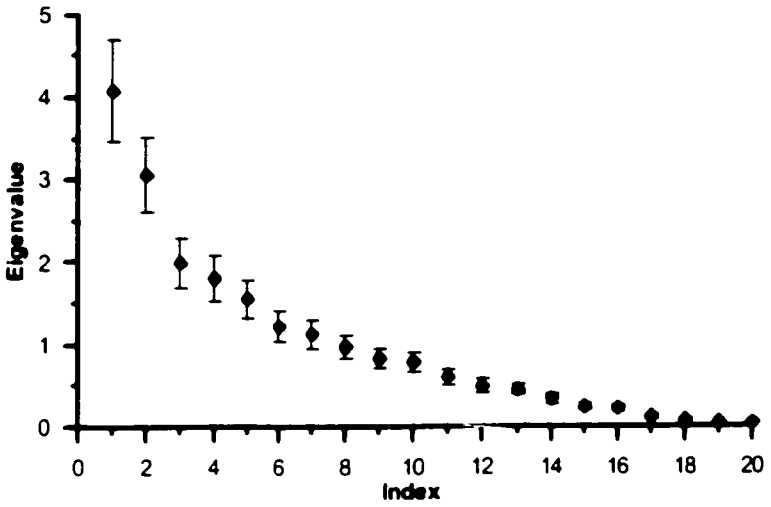

Figure 3.8 Eigenvalue spectrum for the EOF analysis of BAI at the 20 national forests. Confidence intervals are calculated after North *et al.* (1982).

The leading mode of variability (EOF-1) is characterized by increases in area burned throughout most of the region, although the national forests in northwestern Washington and central Oregon load weakly on this EOF (Figure 3.9a). The national forests that load strongly on EOF-1 comprise a wide range of forest types, however all of them contain substantial tracts of Douglas-fir dominated or co-dominated stands. Ponderosa pine is also well represented among the forests that load strongly on EOF-1; only Ochoco and Winema National Forests contain a large ponderosa pine component but load weakly on EOF-1. None of the more mesic forest types load strongly on this EOF.

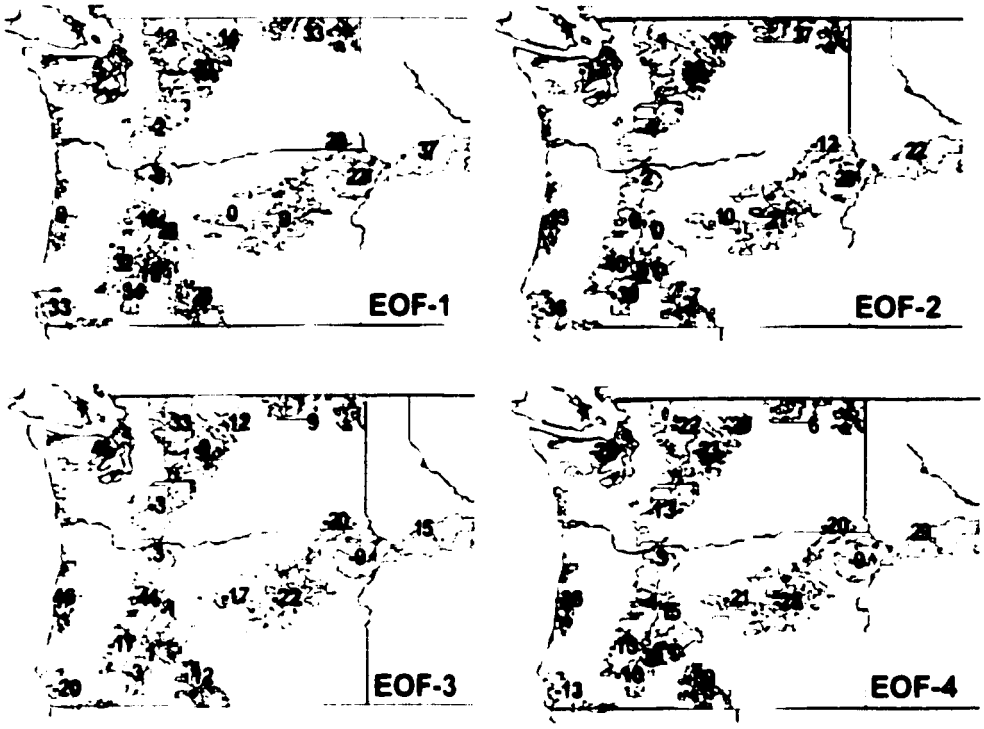

Figure 3.9 Loading values (×100) for the leading four EOFs of area burned. EOFs 1 through 4 explain 17, 13, 12 and 10 percent of the variance in BAI respectively.

Projecting the 500 hPa height field onto PC-1 reveals a significant association between this pattern in burning and positive height anomalies over western North America (Figure 3.10). This feature appears to migrate southwestward over the course of the fire season, starting out in central Canada in May and ending up over the central North Pacific in September. While the feature is absent in July the mean circulation conditions in this month do not normally inhibit fire ignition or spread. One possible interpretation of this result is that the differences between small and large fire years are driven by events that occur outside of the fire season maximum. That is, because mid-summer climatological conditions are naturally conducive to wildfire activity, variability in area burned is most sensitive to conditions in the early or late fire season. Although the apparent migration of this blocking feature is consistent with the *Great Basin High* pattern described by Schroeder (1969), the time evolution seen here is clearly much longer than he intended.

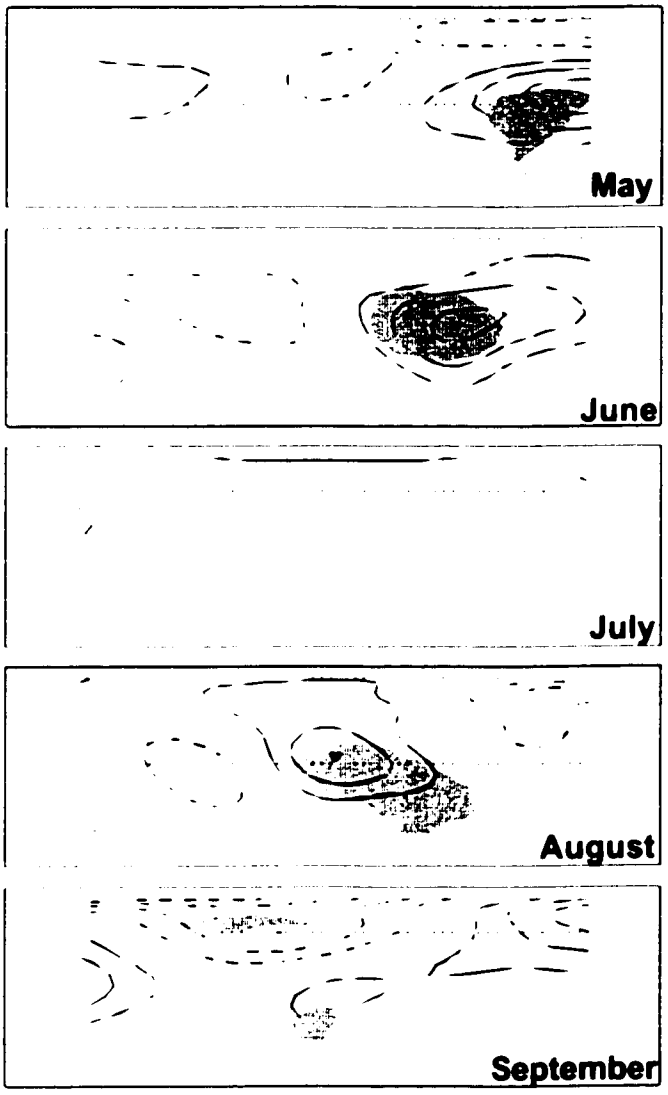

Figure 3.10 The 500 hPa height anomaly field projected onto the PC-1 (contours and significance shown as in Figure 3.2).

Map composites of 500 hPa height anomalies for the five smallest and largest fire years captured by PC-1 are consistent with the relationships seen in the spatial regressions (Figure 3.11). The five largest fire years are characterized by pronounced positive height anomalies over western North America in May, June, July and August, and, except for July, negative height anomalies over the central Pacific. In spite of the few degrees of

freedom in this analysis the difference between small and large fire years is statistically significant in May, June and July ($p<0.05$). The map projection for September reveals a significant association to anomalous high 500 hPa heights over the central Pacific and reduced heights over western North America. These patterns are nearly identical to those identified in the analysis of the regional BAI (see Figure 3.2), but in every month considered the magnitude of the 500 hPa height anomalies observed is greater for PC-1 than for the regional BAI. This finding implies that the EOF analysis is effectively capturing the coherent signal in the area burned record, and that atmospheric forcing is responsible for at least some of the coherence in this signal. This result could be due to the efficiency of eigenvector techniques at extracting meaningful patterns from noisy data (Gauch 1980), or it could be that the regional BAI is in fact composed of multiple signals – only one of which is forced by this pattern of atmospheric variability.

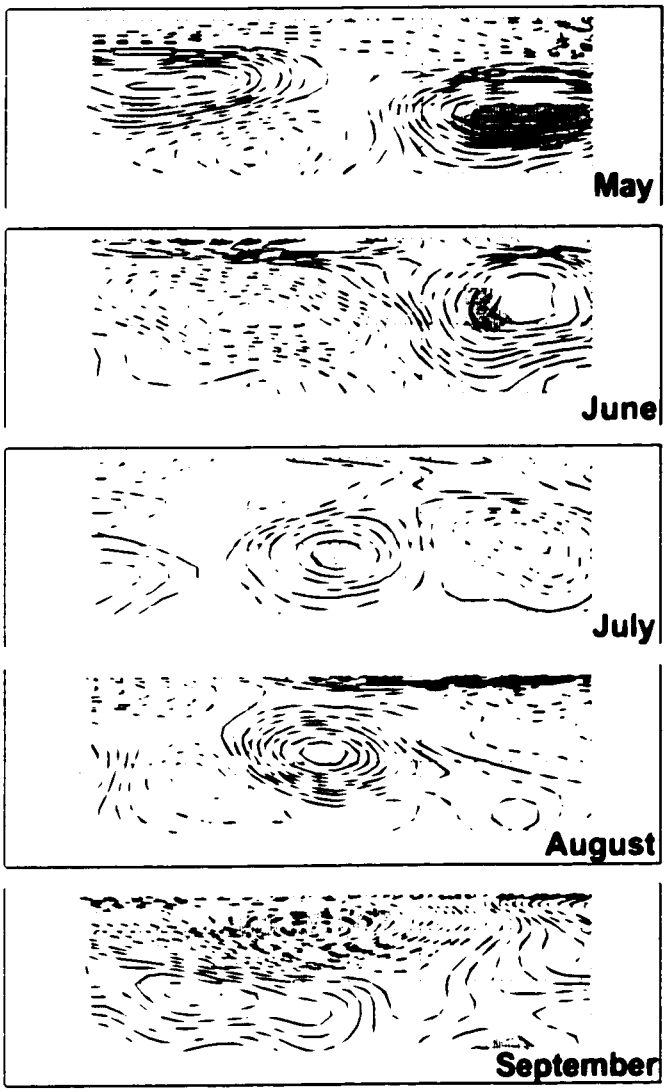

Figure 3. 11 Difference in the 500 hPa height field between the five largest and smallest fire years represented by PC-1. Contours and statistical significance shown as in Figure 3.4.

Lagged correlations between PC-1 and PDSI suggest that increases in area burned are associated with enhanced region-wide drought in the winter, spring and summer leading up to the fire season (Figure 3.12). Consistent with the results from the 500 hPa height field the magnitude of the correlation coefficients is greater for the EOF results than for

the regional BAI. For comparison, the correlation between PC-1 and the mean Washington and Oregon PDSI is -0.59, -0.55 and -0.61 for June, July and August, respectively, of the fire season. This correlation remains significant at increasing lags, back to October of the preceding year.

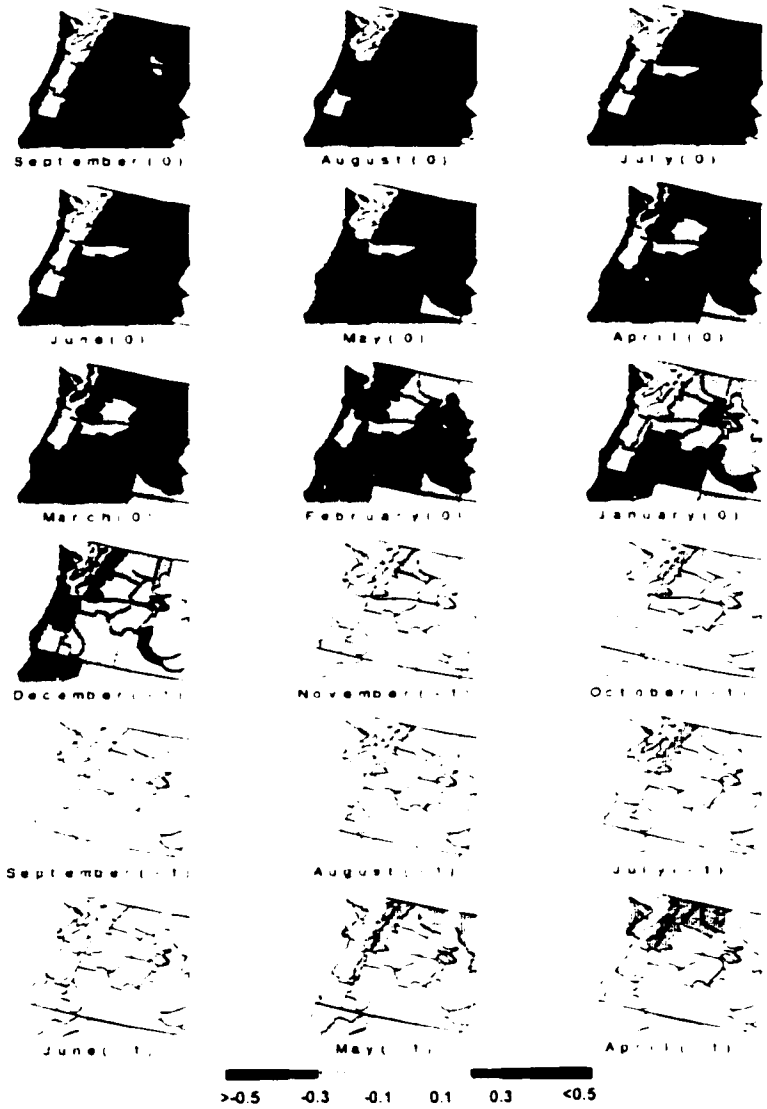

Figure 3.12 Lagged correlation between PC-1 and PDSI. Inverse correlations are shown in red and indicate a correspondence between drought and increases in area burned.

Interpreted together these results suggest that this pattern of wildfire variability is associated with drought conditions that initiate in the preceding winter and persist through the wildfire season, accompanied by summertime blocking events. This pattern is consistent with the climatic conditions associated with increased area burned in the American Southwest where increased wildfire is associated with anomalous dry weather preceding the fire season (Swetnam 1990; Swetnam and Betancourt 1998). Unlike Swetnam and Betancourt, (1998), however, I did not find a correlation to increased PDSI in the year prior to wildfire activity. This disparity may be attributable to differences in the relative abundance of fine fuels between the two environments. In some Southwest forests the abundance of fine fuels is attributed to herbacious production. In contrast, in the Pacific Northwest perennial shrubs, woody debris, and fallen needles typically dominate. This latter fuel type is rarely patchy enough to limit the spread of wildfire (Agee 1993).

The second EOF of area burned is characterized by a northeast-southwest dipole (Figure 3.9b), with increases in area burned at Colville, Okanogan, Wenatchee and (to a lesser extent) Nez Perce and Wallowa-Whitman National Forests, corresponding to reductions at Siskiyou, Umpqua and Rogue River National Forests. There are important differences between the two regions in terms of their ecology: Colville, Okanogan and Wenatchee contain extensive stands of pure Douglas-fir. Siskiyou, Umpqua and Rogue River represent a transitional zone between the temperate forests of the Pacific Northwest and the drier, more Mediterranean forests of the Pacific Southwest. These latter forests also contain a large portion of red fir that is distinct within the study region. However these two centers of action also exhibit strong similarities to other forests of the region, in terms of their composition and fire regime, that do not load particularly strongly on this EOF. This observation, along with the strong spatial arrangement of the EOF loadings, suggests that the pattern is driven largely by top-down (i.e. atmospheric / climatic) rather than bottom-up (i.e. ecological) controls.

Projecting the 500 hPa height field onto PC-2 reveals generally weak associations with atmospheric circulation. The only significant association that seems relevant occurs during July, and is characterized by increased 500 hPa heights over western North America and decreased heights over the Gulf of Alaska (Figure 3.13). This pattern resembles the summertime Pacific North America (PNA) pattern (Knox and Lawford 1990), and is virtually identical to patterns associated with severe wildfire years in western Canada (Johnson and Wowchuk 1993; Skinner *et al.* 1999). The PNA-like structure is also present in the map composites of the five largest fire years (results not shown). These results can not be directly compared to the regional BAI map composites because large positive values indicate increases in area burned in the northeastern portion of the region but reductions in area burned in the southwest; the five minimum values indicate the opposite scenario. Therefore the five smallest values do not indicate small fire years, but rather years when there were increases in area burned in the southwest and reductions in the northeast. Additionally, the PC-2 time series indicates only one extreme negative anomaly, implying that a composite of the five minimum values is not likely to represent a coherent signal. Nonetheless, the composite maps do indicate the presence of reduced 500 hPa heights over the North Pacific / Gulf of Alaska during high PC-2 index years in the months of May, June and July. It is unclear from the inferred circulation why this pattern would lead to enhanced area burned in the northeast but reduced area burned in the southwest. The PNA has been shown in winter months to divert precipitation away from the Pacific Northwest northwards into British Columbia and Alaska, with a second storm track often directed into the southwestern United States (Trenberth and Hurrell 1994). In summer months this pattern could deliver precipitation to southern Oregon, reducing the fire hazard there, while diverting precipitation away from northern Washington and thereby increasing the fire hazard there.

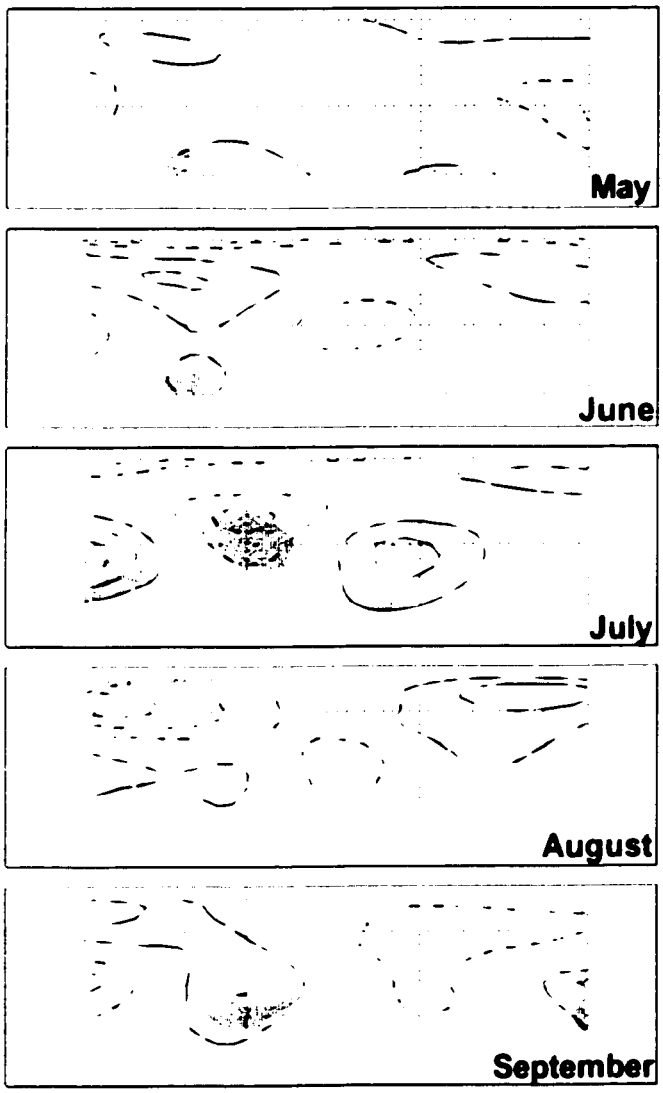

Figure 3.13 The 500 hPa height anomaly field projected onto PC-2 (contours and significance shown as in Figure 3.2).

Lagged correlations between PC-2 and PDSI reveal very weak correspondence between area burned and antecedent drought conditions (results not shown): there is a small inverse correlation between PC-2 and PDSI for climate divisions along the western flanks of the Cascade Mountains, and in Idaho, over winter, spring and summer of the fire season. Given the overall weak correlation to PDSI, and that the correlation is primarily to drought west of the Cascade Mountains, it is unlikely that there would be a strong

association to the regional drought signal. Indeed, the correlation to mean Washington and Oregon PDSI is not significantly different from zero at any point of the fire season or the preceding months. (r = -0.06, -0.09 and -0.11for June, July and August respectively).

These findings suggest that a summer PNA pattern can contribute to a northeast-southwest dipole in area burned. This pattern may be weakly modulated by local drought, but is not controlled to any significant extent by regional drought severity. This pattern appears to be related to the arrangement of the national forests in space rather than their underlying ecology or fire regime. The EOF / PC pair that was identified in this analysis is clearly not a simple linear pattern, though, and is probably not well defined by the analysis. Additionally, the record of area burned is probably too short to capture enough "extreme" fire years to develop good map composites of this mode in annual area burned.

EOF-3 is characterized by increases in area burned in Olympic, Mount Baker-Snoqualmie, Siuslaw, and Willamette national forests, and reductions at Siskiyou, Umpqua, Ochoco, Malheur and Umatilla national forests (Figure 3.9c). This pattern is consistent with increased fire activity at the wettest forests of the region – in particular at the two national forests with temperate rainforest components – but also at Mount Baker-Snoqualmie and Willamette, which have extensive western hemlock and Pacific silver fir components. Although Siskiyou National Forest also contains these mesic forest types they are generally restricted to a narrow coastal band that is defined by the landward extent of fog occurrence. Beyond this fog belt the forests are characterized by much drier vegetation types than occur at more northern coastal forests (Franklin and Dyrness 1973), and historical fire occurrence is generally more frequent and less severe (Agee 1991a).

Projecting the 500 hPa height anomaly field onto PC-3 reveals virtually no linear correspondence between atmospheric circulation and annual area burned (results not shown). In contrast, however, the map composites indicate an association between persistent blocking features over western North America and the five most extreme fire

years represented by PC-3 (Figure 3.14, left panel). This relationship is more readily apparent if the (only) three very large events contained in the record are considered (Figure 3.14, right panel). This 500 hPa height surface is similar to the blocking structures identified for the regional analysis (see Figure 3.4) and for PC-1 (see Figure 3.10), however the system appears to be located further west throughout most of the fire season. This pattern would be especially conducive to anomalous easterly winds in the coastal region, as air circulates clockwise around the high.

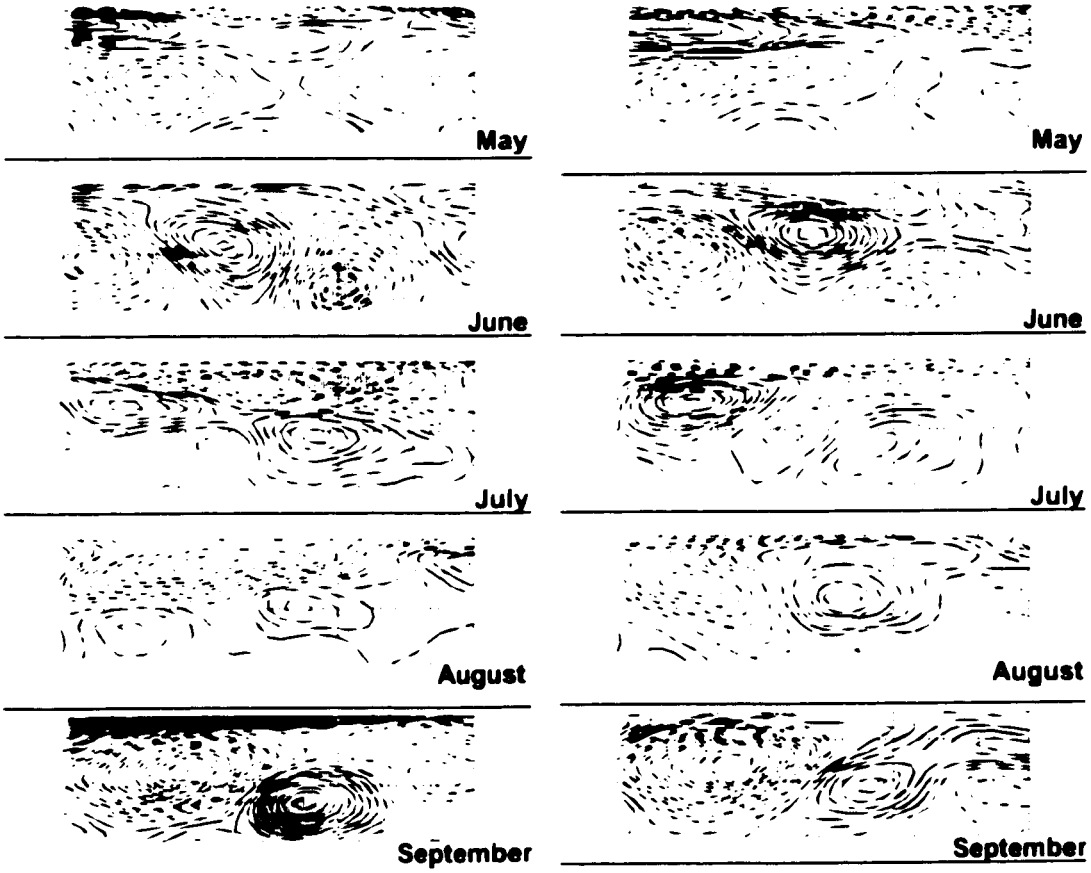

Figure 3.14 (left) Difference in the 500 hPa height field between the five maximum and the five minimum values of PC-3 (contours and significance shown as in Figure 3.4). (right) Composite map of the three large fire years (1951, 1967 and 1988) represented by PC-3 (contours shown as in Figure 3.2).

Lagged correlations to the PDSI reveal a weak association between area burned and drought in western Washington during the fire season. There is a weak positive correlation to PDSI in the winter and spring preceding the fire season. This result seems counter-intuitive, because these forests are typically too moist to carry fire in most years. One possible explanation for this result is that these forests are strongly ignition limited. That is, drought conditions alone may not lead to increases in area burned unless there is also a source of ignition. Additionally, because there have been very few large fire years in Olympic and Siuslaw National Forests (and therefore in PC-3) linear analyses will almost certainly fail to identify the causes of these extreme fire years. In order to investigate this possibility I developed composite maps of the (only) three large fire years represented by PC-3 (Figure 3.15). This analysis reveals good correspondence between drought west of the Cascade Mountains and large area burned for the interval beginning in the preceding fall and continuing through the fire season.

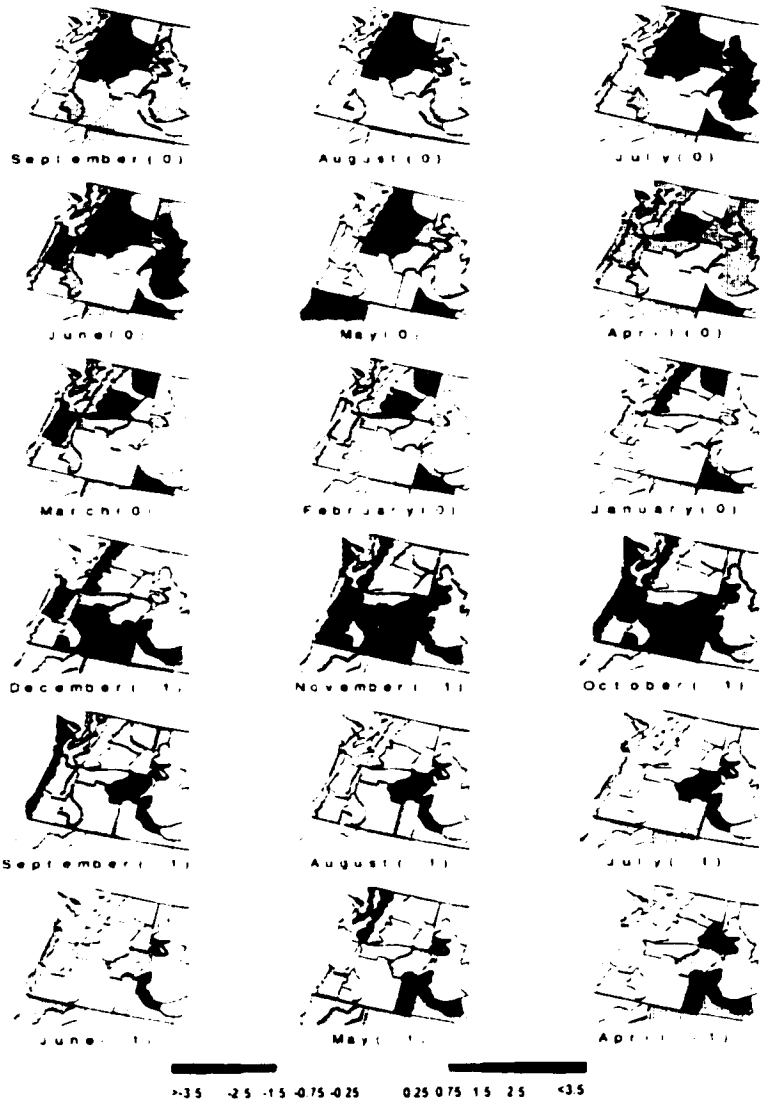

Figure 3.15 Composite PDSI values for the three largest fire years (1951, 1967 and1988) represented by PC-3.

These results imply that in the northwestern coastal forests large fire years occur only when drought persists through several seasons leading up to the fire season, followed by summertime circulation anomalies that favor hot, dry easterly winds. This pattern is consistent with the ecology of these forests, which tend to be characterized by complex age structures and abundant woody debris, but a microclimate that favors high relative humidity and rapid decomposition of organic material (Chen *et al.* 1999). This environment contains substantial potential fuel, but requires exceptional circumstances to

dry out the landscape sufficiently that it will burn readily (Agee 1993). These forests may also be ignition limited, so that even when fuels are dry increases in area burned by wildfire may not necessarily follow.

EOF-4 is characterized by increases in area burned at a few national forests in southern Oregon (Fremont, Winema and Deschutes) as well as at Nez Perce National Forest, and reductions at most other forests. These forests are among the driest of the region, and are all characterized by extensive stands of lodgepole and ponderosa pine. Summertime precipitation often totals less than 2 cm, and temperatures are the highest of the study area (Jackson and Kimerling 1993). The 500 hPa height field associated with this pattern in burning is significantly lower than normal over western North America in June, July and September, although the magnitude of these departures is generally quite small (results not shown).

The SEA again shows a stronger and more consistent relationship (Figure 3.16) than the map regression. Large values of PC-4 occur when very low 500 hPa heights persist over the study region throughout much of the summer. At these particularly dry forests this circulation pattern would bring summer cyclones with lightning and strong winds, but potentially very little precipitation, thereby providing a source of ignition and a cause for rapid wildfire spread. In contrast, these same storms could deliver significant rainfall to regions west of the Cascade Mountains and to more northerly interior regions, thereby reducing the fire hazard at those forests. The five minimum values of PC-4 are associated with approximately opposite conditions – that is, anomalous high pressure over western North America. This pattern is comparable to the blocking ridges described above, and would lead to increases in area burned (at those forests which load negatively on EOF-4) for the reasons already discussed. Most of the forests that load strongly negatively on EOF-4 load weakly on EOF-1, the other pattern in burning that shows a good relationship to persistent blocking features. These results imply that most of the forests of the region do show increases in area burned in response to blocking events, but

that there are differences in either the atmospheric forcing or the ecological response to these events.

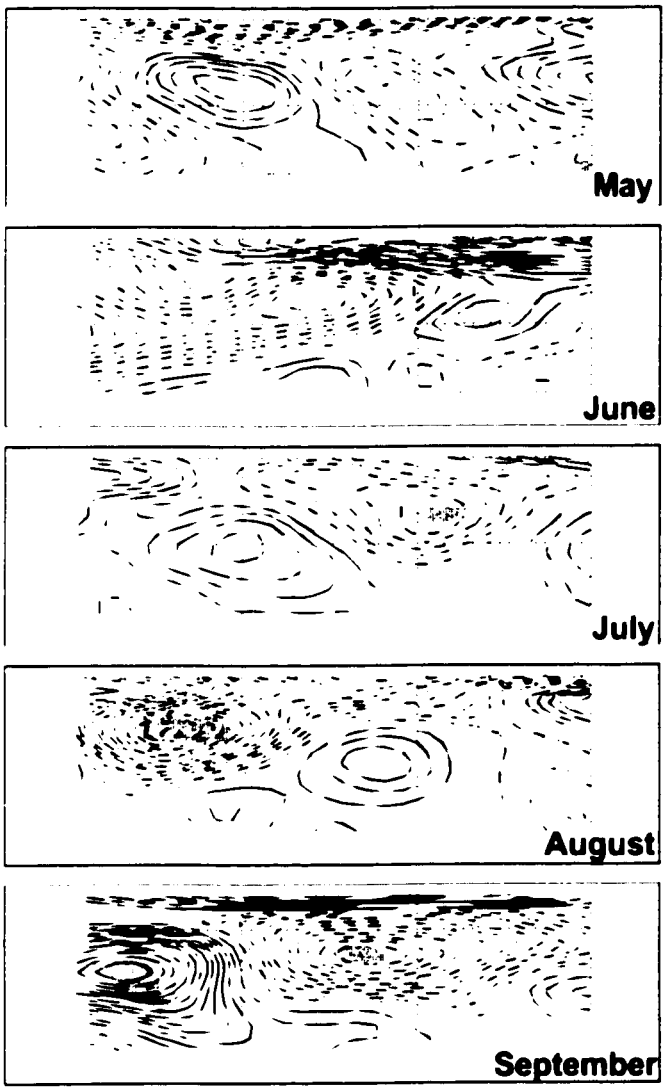

Figure 3.16 Difference in the 500 hPa height field between the five maximum and the five minimum values of PC-4 (contours and significance shown as in Figure 3.4).

Some insight into the cause for these differences can be gained by examining the lagged correlation to PDSI: there is a modest correlation between PC-4 and drought occurrence east of the Cascades crest for the entire year preceding the fire season, and between PC-4 and reduced drought stress west of the Cascades during the fire season (Figure 3.17). This result suggests that summertime cyclones lead to increases in area burned east of the Cascades most commonly when the region is experiencing long-term soil moisture deficits. The increased moisture west of the Cascades is consistent with the hypothesis that summertime cyclones are delivering precipitation only to the coastal region. The forests that load negatively on EOF-4 therefore tend to exhibit increases in area burned when the PDSI is negative - a response that is distinct from the relationships seen for PC-1. The exception to this finding is Olympic National Forest, which is located in the region characterized by a positive correlations to summertime PDSI; increases in area burned therefore correspond to enhanced fire-season drought. This response is similar to the relationship identified for PC-3, but the persistence of the antecedent drought is much shorter. One possible explanation, that cannot be verified by the current analysis, is that this eigenvector is capturing variability at stands within Olympic National Forest that are located in the rainshadow of the Olympic Mountains, and therefore do not require long preceding drought in order to burn.

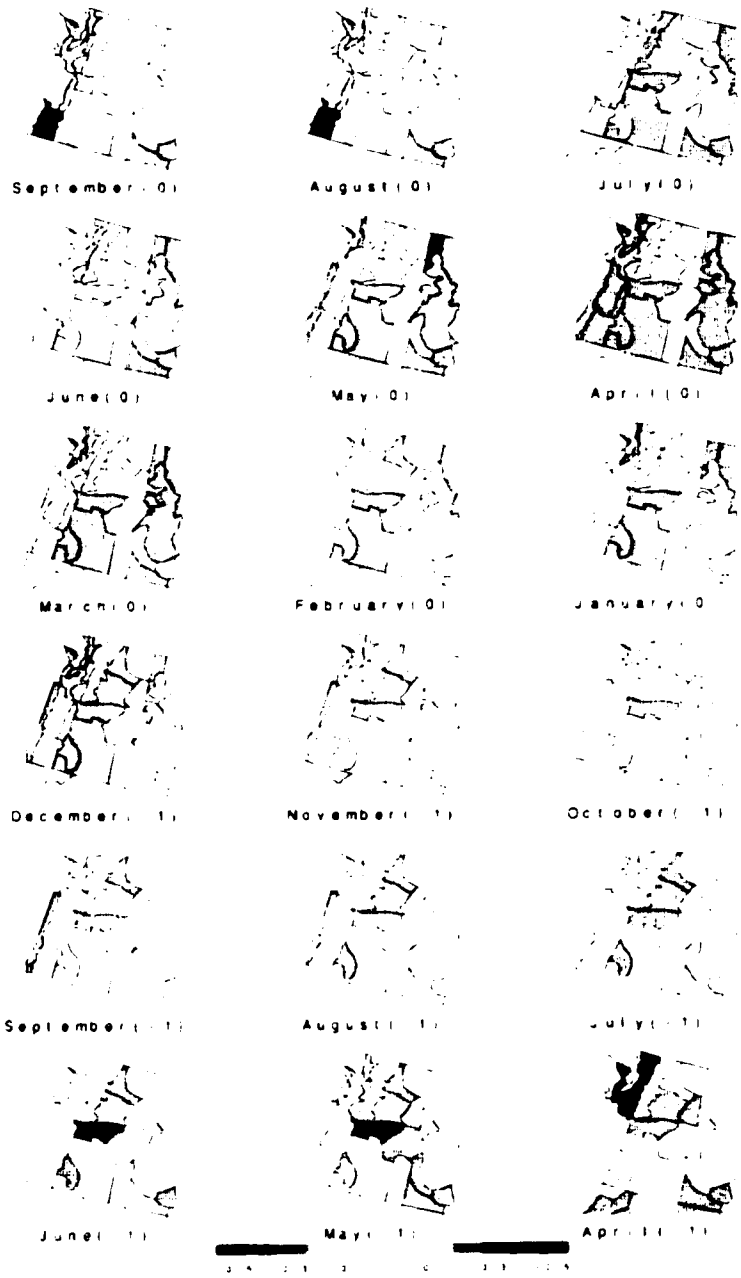

Figure 3.17 Lagged correlation between PC-4 and PDSI. Inverse correlations are shown in red and indicate a correspondence between drought and increases in area burned.

Correlations between the four PC time series and the CTI and PDO index reveal significant associations only between PC-1 and the PDO (Table 3.2). Furthermore, a difference of means test identified a significant difference in area burned (as represented

by PC-1) between the warm and cool PDO regimes (Figure 3.18). No statistically significant association with ENSO was found for any of the PC time series. These results are consistent with the climatic impacts of the PDO, which are expressed most strongly as reduced wintertime precipitation (Mantua *et al.* 1997; Gershunov and Barnett 1998; Barlow *et al.* 2001). PC-1 exhibits the strongest and most consistent relationship to drought of the patterns identified here. While PC-3 also exhibited good correspondence to drought, the lack of a linear relationship suggests that drought alone is not sufficient to trigger large wildfires.

Table 3.2 Pearson correlation coefficients for indices of area burned and ENSO and the PDO

	BAI	**PC-1**	**PC-2**	**PC-3**	**PC-4**
R-ENSO[1]	-0.009	0.272	-0.052	-0.056	0.227
R-PDO[1]	**0.403**	**0.422**	0.018	-0.173	0.125
t-test ENSO[2]	0.255	0.275	0.646	0.923	0.740
t-test PDO[2]	0.178	**0.047**	0.652	0.204	0.179

1. Pearson product moment correlation; $r \geq 0.25$ is significant at 95 percent confidence level. Mean October to March index used for both the CTI and the PDO index.
2. P-value from t-test shown.

Statistically significant results (α=0.05) indicated by bold script.

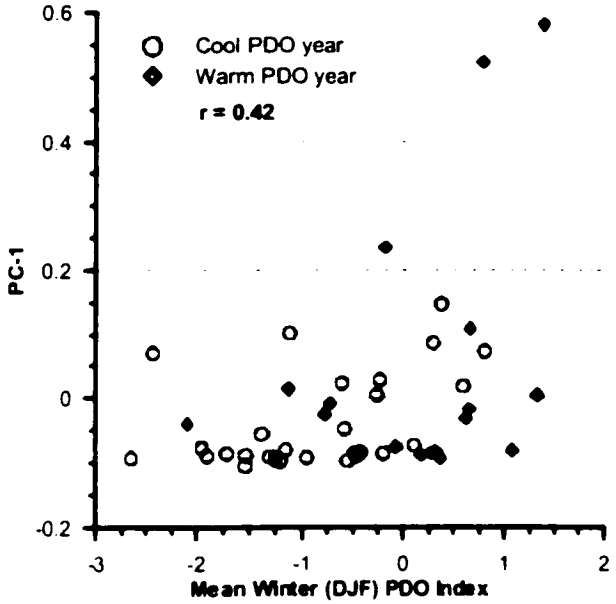

Figure 3.18 Scatterplot of mean winter (Oct. to March) PDO index versus regional BAI. Warm PDO phase years (1978 - 1994) are indicated by a diamond, and cool phase years (1949 to 1976) are indicated by a circle.

3.6 Conclusions

The results presented here provide evidence for a climatic component in forcing extreme wildfire years. The application of EOF analysis to the area burned record revealed four distinct patterns in area burned; each in turn was related to underlying geographic and ecological factors. Throughout the region, increases in annual area burned are associated with increased 500 hPa heights over western North America and the adjacent North Pacific Ocean. These blocking ridges divert moisture away from the region, raising air temperatures and reducing relative humidity. In extreme cases, this circulation pattern can lead to anomalous easterly "foehn" winds that warm and dry as they descend adiabatically from the continental interior. Extended antecedent drought preconditions many of the forests of the region to burn; in particular mesic to wet highly productive forests dominated by Sitka spruce and western hemlock. These forests typically have substantial fuel loads, but require remarkable circumstances to become flammable. The

relationship between circulation anomalies and area burned is weakly linear in nature, with particularly large fire years exhibiting a stronger association to circulation anomalies than either modest or small fire years.

The finding that many of the national forests respond to similar patterns in atmospheric circulation and drought has implications for the suitability of eigenvector techniques in discriminating true "modes" in area burned, because the patterns in area burned are unlikely to be entirely independent of each other. Furthermore, the linearity assumption of PCA does not appear to be appropriate either, as small fire years are not simply the inverse of large fire years in their underlying forcing agents or spatial arrangement. Nonorthogonal rotations could potentially overcome some of these limitations, and their suitability for analyses of this type merits further investigation.

The principal findings of this analysis are:

- Region-wide increases in area burned are characterized by enhanced drought in the seasons preceding the fire season, followed by increases in 500 hPa height over western North America and the eastern Pacific Ocean throughout the fire season.
- Distinct ecological characteristics modulate the response to atmospheric forcing, with wetter forests requiring more severe drought and prolonged blocking to burn than drier forests, which may respond to blocking events without antecedent drought.
- The PDO appears to influence wildfire activity, although area burned appears to respond to annual to interannual fluctuations in the PDO more strongly than to interdecadal regimes. It is unclear from this analysis whether the PDO influences wildfire activity through its influence on drought severity (i.e. largely a wintertime connection) or by altering the statistics of summertime circulation. No significant association to ENSO was found for any of the records of area burned.
- Eigenvector techniques are able to discriminate distinct patterns in area burned, however they do not appear to be the most appropriate method of analyzing wildfire data in the American Northwest. There are at least three possible explanations for this situation: (1) the record of area burned is too short and too noisy to resolve

meaningful "modes" in forests with long fire return intervals; (2) the patterns in area burned may not be statistically independent from each other; (3) the patterns in area burned are not linear in nature, and small fire years are not simply the inverse of large fire years.

In the context of these findings, fire management needs to consider that there are both top-down and bottom-up controls on extreme wildfire years. Although fuel treatments are undoubtedly a necessary component of effective fire management, they cannot realistically be expected to eliminate large area burned in severe fire weather years. Additionally, the potential consequences of impending climate change on fire severity needs greater consideration. The most recent Intergovernmental Panel on Climate Change assessment (IPCC 2001) predicts increased drought stress for the American Northwest, which could lead to more frequent and/or more severe wildfire years in spite of ongoing fuel treatments.

Chapter 4

4.1 Abstract

A network of drought sensitive tree-ring chronologies is used to reconstruct flow on the Columbia River at The Dalles, Oregon, since 1750. The reconstruction accounts for 25 to 30 percent of the variability in mean water-year flow, with a large portion of unexplained variance caused by underestimates of the most severe low-flow events. Residual statistics from the tree-ring reconstruction, as well as an identically specified instrumental reconstruction, exhibit positive trends over time. This finding suggests that the relationship between drought and streamflow has changed over time, supporting results from hydrologic models, which suggest that changes in land cover over the 20th century have had measurable impacts on runoff and evapotranspiration. Lowpass filtering the flow record suggests that persistent low flows during the 1840s were probably the most severe of the past 250 years, but that flows during the 1930s were nearly as extreme. The period from 1950 to 1987 is anomalous in the context of this record for having no notable multiyear drought events. A comparison of the flow reconstruction to paleoproxy records of the Pacific Decadal Oscillation (PDO) and El Niño / Southern Oscillation (ENSO) support a strong 20th century link between large-scale circulation and streamflow, but suggests that this link is very weak prior to 1900.

4.2 Introduction

The Columbia River Basin is the second largest drainage basin in the United States, and supports a diverse range of human and natural interests, including hydroelectric production, agricultural irrigation, navigation, fish stocks (including endangered salmon runs), fisheries, recreation, and habitation (Bonneville Power Administration *et al.* 2001). Imposed on these interests is the need to minimize the risk of floods. In many years the demands imposed on the Columbia River system account for more water flows through the system, leaving managers especially vulnerable to low-flow years (Cohen *et al.* 2000; Miles *et al.* 2000). The storage potential of the Columbia is currently exploited to its

limits, so adaptations to variability or changes in the supply of water need to be driven by reductions in demand rather than through infrastructure developments (Bonneville Power Administration *et al.* 2001). A longer record of streamflow variability in the Columbia River system would help water planners to develop contingency plans for extreme events by providing a longer context for drought assessment (Stockton 1990). In particular, the gauged record on the Columbia probably does not contain all the relevant low-frequency fluctuations, abrupt shifts in flow that might be caused by changing climatic regimes, or multiyear drought events that are relevant to water-resource planners.

Climate-sensitive tree-ring chronologies provide the opportunity to extend instrumental records of streamflow by exploiting the strong links between climate and runoff (Cayan 1989; Cayan 1996; Moore 1996; Nigam *et al.* 1999). In particular, the Columbia River system is sensitive to climatic forcing associated with the Pacific Decadal Oscillation (PDO) and El Niño / Southern Oscillation (ENSO) (Hamlet and Lettenmaier 1999a). Well verified tree-ring based reconstructions have been undertaken for the Sacramento River Basin (Earle 1991; Meko *et al.* 2001), the Gila River (Meko and Graybill 1995), Crater Lake (Peterson *et al.* 1999), and many smaller basins (see reviews in Jones *et al.* 1984; and Stockton 1990). Trees of the Pacific Northwest are very long-lived, often reaching ages that exceed 1000 years (Brubaker 1986; Peterson and Peterson 1994; Laroque and Smith 1999; Gedalof and Smith 2001a). Many of these species are sensitive to climatic variability, including Douglas-fir (*Pseudotsuga menziesii*) (Wiles *et al.* 1996; Zhang 1996; Biondi *et al.* 2001), yellow-cedar (*Chamaecyparis nootkatensis*) (Laroque and Smith 1999), mountain hemlock (*Pseudotsuga menziesii*) (Heikkinen 1985; Graumlich and Brubaker 1986; Wiles *et al.* 1996; Gedalof and Smith 2001a; Peterson and Peterson 2001), subalpine fir (*Abies lasiocarpa*) (Peterson and Peterson 1994; Ettl and Peterson 1995), ponderosa pine (*Pinus ponderosa*) (Graumlich 1987), subalpine larch and western larch (*Larix lyallii, L. occidentalis*) (Colenutt and Luckman 1991; Peterson and Peterson 1994; Colenutt and Luckman 1995), Engelmann spruce (*Picea engelmannii*), (Luckman and Colenutt 1992; Peterson and Peterson 1994), and others (Fritts 1991;

Schweingruber 1993). The primary objective of this research is to reconstruct streamflow in the Columbia River Basin using dendrohydrological techniques, and to use this reconstruction to contextualize the instrumental record.

4.3 Data

Recent efforts to compile tree-ring chronologies into centralized data banks (e.g. Grissino-Mayer and Fritts 1997) provide the opportunity to compile networks of climate sensitive tree-ring chronologies for the analysis of large-scale climatic processes (Minobe 1997; Kadonaga *et al.* 1999; Gedalof and Smith 2001b; McKenzie *et al.* 2001). Two such data banks were used in this analysis: the International Tree-Ring Data Bank (ITRDB) (Grissino-Mayer and Fritts 1997), and the "Past PDO working group" collective data set (https://pastpdo.ltrr.arizona.edu). From these data banks all tree-ring chronologies lying within (or near to) the Columbia River Basin were compiled into a regional data set. Because the analysis of these data relies on eigenvector techniques, which are limited to the temporal interval common to all sites, I excluded from further analysis all chronologies that were collected prior to 1985. This screen resulted in a pool of 66 potential chronologies. The choice of a starting year for the analysis involved a tradeoff between increased sample depth and reduced temporal coverage. That is, I had to choose between a relatively short but data rich reconstruction and a much longer but data sparse reconstruction. A plot of the initial year of chronology against number of sites reporting data revealed several natural breaks that provide logical cutoffs: ca. AD 1450, 1600 and 1750. I chose to focus on the post-1750 interval because it allowed me to work with the widest range of tree species and locations – thereby providing the best insight into the underlying dynamics. As it turned out this subset produced the only robust reconstruction, for reasons that will be addressed later. Of the 66 potential chronologies 57 extend back to 1750 and were retained for further investigation.

Individual ring-width series were transformed into stationary, dimensionless, indices in order to remove trends in growth related to tree-age and stand dynamics (Cook 1987).

This transformation was undertaken in two steps using the computer program ARSTAN (Cook and Holmes 1986). First, a negative exponential curve or linear trend was fit to each series, and each observed ring width in the series was divided by this "expected" value. Next, each series was detrended a second time by fitting a cubic smoothing spline of a specified rigidity to the residual series (Cook *et al.* 1990). In order to preserve low-frequency information related to the PDO, I specified a 50 percent frequency cutoff of 128 years. This filter is sufficiently flexible to effectively remove most of the stand dynamics effects I encountered, but still preserves 90 percent of the variance at periods shorter than 75 years (Cook and Peters 1981; Cook *et al.* 1990). Each ring-width-index series was prewhitened using autoregressive moving average (ARMA) models, to remove any autocorrelation effects (Biondi and Swetnam 1987; Cook 1987), before being combined into a single representative site chronology using a robust mean (Mosteller and Tukey 1977).

Streamflow data for the Columbia River were provided by the Bonneville Power Authority. These data have been "naturalized" to remove the influences of water diversion and storage and changes in evaporation (A.G. Crook Company 1993; Hamlet *et al. in review*). This procedure uses an empirical flow model to incorporate records of reservoir volume, water withdrawal, and theoretical evaporative losses from reservoir surfaces, and derive a record of what flow at The Dalles would have been in the absence of regulatory structures. I focused on reconstructing mean water-year flow at The Dalles, Oregon, for three principal reasons: (1) the flow record at The Dalles integrates variability over a large portion of the Columbia River drainage basin, and is therefore representative of the large-scale processes occurring within the system; (2) water resources managers use flow at The Dalles to develop a number of operational applications, so statistics for this location are likely to be of practical utility; and (3) flow at The Dalles has been the focus of other investigations, so the results of this study will provide a direct basis for comparison. Flow at The Dalles has been routinely gauged since 1878, but "naturalized" records extend back only to 1931 due to quality assurance

concerns in the early portion of the record. A log-10 transformation was applied to induce normality in the flow data.

The U.S. "Time Bias Corrected" state climatic divisionial data set (Guttman and Quayle 1996) was used to investigate relationships between radial growth and climate, and between streamflow and climate. Because the divisional data are developed from area-weighted averages of temperature and precipitation over regions of relatively homogeneous climate they are often considered preferable for dendroclimatic analyses (Brubaker 1980; Blasing *et al.* 1981; Heikkinen 1985; Ettl and Peterson 1995). Monthly values of temperature, precipitation and Palmer drought severity index (PDSI) data are available for the interval 1895 to present.

4.4 Methods

The pool of available chronologies was screened for sensitivity to drought in order to restrict the pool of predictors to candidates exhibiting a physically consistent relationship to streamflow. Pearson correlation coefficients were calculated between annual radial growth index and monthly PDSI values within the pertinent climate division over the interval from December of the year preceding growth to August of the year of growth. Sites that did not exhibit a significant correlation to drought during at least one month were removed from the analysis. Because PDSI is not calculated in Canada an alternative screening process was required. For sites close to the United States border I identified representative climate divisions and used these records. For more distant sites I identified individual meteorological stations and used the correlation to precipitation as a guide.

Principal components analysis (PCA) was applied to the subset of screened chronologies to derive a reduced set of independent predictors. From this analysis, only the eigenvectors that exhibited physically meaningful loadings and had eigenvalues that were statistically greater than 1.0 were retained for further investigation (North *et al.* 1982).

This approach is distinct from most other dendrohydrological reconstructions that typically include non-zero lags of radial growth increment and retain a large number of principal components as regressors (but see Hidalgo *et al.* 2001). By limiting the number of statistical predictors considered I minimize the probability of identifying spurious relationships, and of overfitting the regression model. Each principal component (PC) time series was prewhitened using ARMA models to remove any autocorrelation that may have been introduced by site chronology calculation or PCA. In all cases an AR(1) model was sufficient to describe the autocorrelative structure of the series. Prewhitening is necessary because tree-ring records often exhibit year-to-year persistence due to nutrient storage, foliage production, recovery from disturbance, and other biological processes (Fritts 1976). The streamflow record, in contrast, exhibits no serial autocorrelation.

Myriad regression models are possible given the large number of potential predictors. In order to identify the most appropriate model I used a bootstrapping technique to assess the stability of regression coefficients. Pseudodata sets of the same length as the full calibration interval (56 years) were generated by sampling-with-replacement from the data set. Regression models were estimated from this pseudodata set, with PCs entered in descending order of eigenvalue (i.e. PC1 then PC2, etc.). This process was replicated 1000 times in order to derive summary statistics. Regression coefficients whose mean value was more than twice its standard deviation were considered robust and were used to develop the full model (Guiot 1991).

Cross-validation statistics were generated by excluding every third year from the analysis and using the remaining two-thirds of the years to predict these years. This process was repeated three times to develop an independent reconstruction for the full calibration interval (1931 - 1987). The Pearson correlation coefficient and the reduction of error (RE) statistic were generated from this cross-validated record as indicators of model performance. A second regression model, using the entire calibration interval to estimate the regression coefficients, was developed in order to reconstruct flow since 1750. For

comparative purposes the performance statistics for this model were also calculated. Additional verification was undertaken by comparing the reconstructed flow record to the extended USGS flow record (1879 - 1987), and to other paleoproxy reconstructions.

4.5 Results

4.5.1 Reconstruction Model Development

Of the 57 potential tree-ring chronologies 32 exhibited a significant correlation to at least one month's PDSI (Figure 4.1, Table 4.1). Two general trends were evident in the calculation of the drought correlations. First, species that are characteristic of subalpine environments generally exhibited a positive correlation to PDSI (i.e. higher drought severity is associated with higher radial growth), and low-elevation species generally exhibited an inverse correlation. (2) Second, subalpine sites normally exhibited the strongest association to PDSI during winter and spring months, and low elevation sites exhibited the strongest correlation during summer months. These results corroborate previous studies that found that radial growth at subalpine locations is often limited by the length of the growing season, which is in turn largely a function of the snow-free interval (Peterson and Peterson 1994; Ettl and Peterson 1995; Gedalof and Smith 2001a; Peterson and Peterson 2001; Peterson *et al.* 2002). In contrast, growth at low elevation sites is often limited by moisture availability during the growing season (Graumlich 1987; Cook *et al.* 1999; Stahle *et al.* 2000).

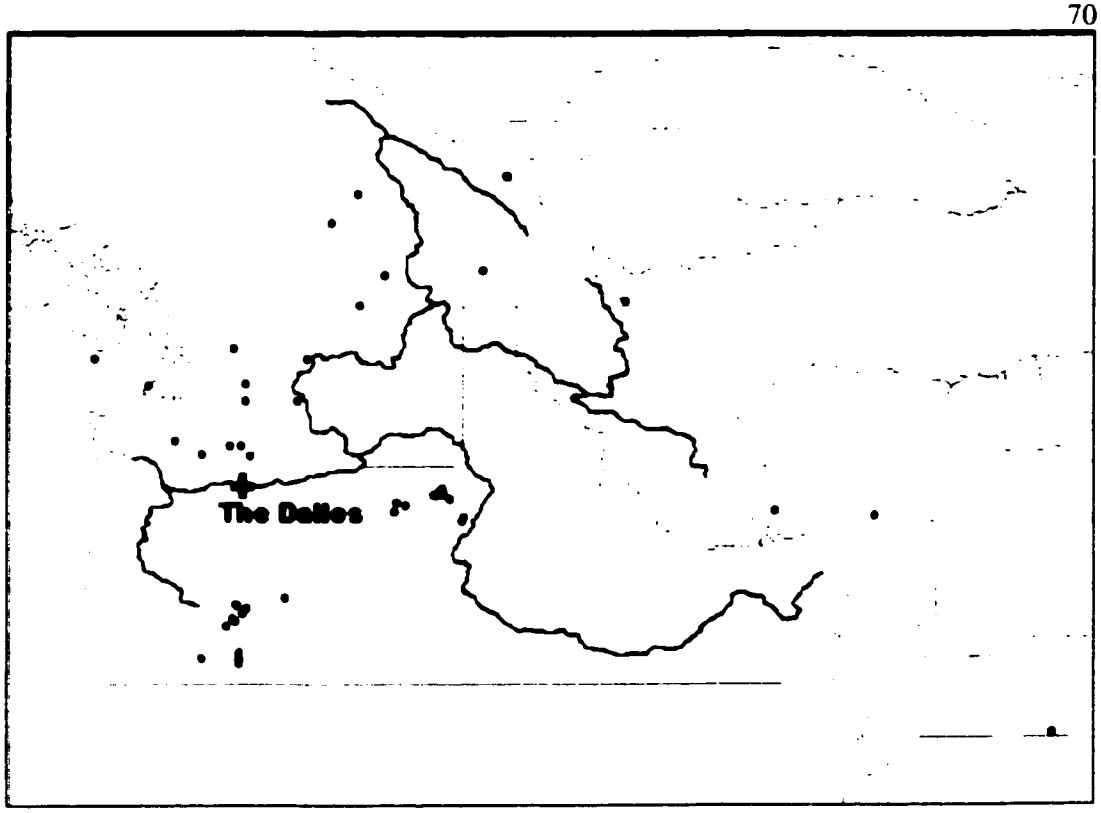

Figure 4.1 Map of the Columbia River basin showing the location of The Dalles, Oregon, and tree-ring sites used in the analysis.

Table 4.1 Descriptions of the sites used in this analysis.

File Name	Site Name	Species	Lat (N)	Long (W)	Elevation (m)	Start Year	End Year	R(PDSI)
CANA147.RWL	Sicamous Creek	PCEN	50.49	-119.54	1550	1665	1994	N A
CANA150.RWL	Big White	PCEN	49.52	-118.51	1700	1669	1998	-0.248
CANA152.RWL	Big White	ABLA	49.52	-118.51	1700	1712	1998	-0.256
CANA161.RWL	Adams Lake	PCEN	51.02	-119.03	1900	1710	1996	N A
CANA162.RWL	Adams Lake	ABLA	51.02	-119.03	1900	1710	1996	N A
FRED	Fredrick Butte, OR	JUOC	43.58	-120.45	1494	936	1996	0.683
GPStdInd.txt	Gray Creek Pass	LALY	49.62	-116.67	2275	1216	1993	-0.323
LVF_S	Larch Valley	LALY	51.35	-116.22	2250	1347	1994	-0.256
MT110.RWL	North Fork Ridge	PSME	45.18	-111.20	2500	819	2000	0.416
MT111.RWL	North Fork Ridge	PIFL	45.18	-111.20	2500	500	2000	0.211
OR029.RWL	Cross Canyon	PIPO	45.58	-117.41	1317	1485	1991	0.399
OR030.RWL	Grizzly Bear	PIPO	45.58	-117.43	1231	1502	1991	0.458
OR031.RWL	Drumhill Ridge	PIPO	45.28	-118.12	N A	1672	1990	0.202
OR032.RWL	Indian Crossing	PIPO	45.07	-117.01	N A	1550	1990	0.316
OR033.RWL	Bally Mountain	PIPO	45.17	-118.34	N A	1469	1990	0.436
OR038.RWL	Big Sink	PIPO	45.47	-117.55	1203	1665	1990	0.377
OR039.RWL	Fish Lake	PIPO	45.00	-117.04	1600	1585	1991	0.238
OR040.RWL	Lugar Springs	PIPO	45.46	-117.58	1200	1675	1991	0.251
OR048.RWL	Pringle Falls RNA	PIPO	43.42	-121.37	1460	1476	1993	0.350
OR049.RWL	Experimental Forest	PIPO	43.43	-121.36	1530	1334	1993	0.243
OR051.RWL	Deschutes	PIPO	43.28	-121.24	1420	1574	1995	0.377
OR052.RWL	Jctn. HWYS 51 & 97	PIPO	43.19	-121.45	1420	1419	1995	-0.229
OR054.RWL	Diamond Lake	PIPO	43.05	-121.57	1510	1513	1995	-0.263
OR055.RWL	Blue Jay Spring	PIPO	42.55	-121.32	1490	1423	1995	0.259
OR057.RWL	Telephone Draw South	PIPO	42.45	-121.31	1550	1442	1995	0.335
OR058.RWL	Crater Lake	PIPO	42.47	-122.04	1370	1572	1990	0.224
WA069.RWL	Hart's Pass N1	LALY	48.00	-120.00	N A	1685	1991	-0.203
WA085.RWL	Annette Lake Trail	PSME	47.22	-121.20	798	1515	1987	0.421
WA086.RWL	Big Quilcene	PSME	47.50	-123.02	867	1288	1987	0.265
WA088.RWL	Olympic Road 3116	PSME	48.00	-124.00	267	1394	1987	0.203
WA089.RWL	Silver Creek	PSME	46.38	-121.50	900	1539	1987	0.244
wy019.crn	Sheep Mountain, Wyoming	PSME	41.08	-106.03	2375	1412	1990	0.526

PCA of the 32 site chronologies resulted in 8 PCs with eigenvalues greater than 1.0. Of these 8, only the first 7 were statistically greater than 1.0 and only the first 5 were readily interpretable in the context of geographic or ecological characteristics. Bootstrapping of the regression coefficients suggested that PCs 1, 2 and 4 are stable predictors of mean flow at The Dalles. The cross-validated correlation between observed and reconstructed flow is 0.50, and the reduction of error statistic is 0.24. The statistics from the full calibration model, using all available years, are only marginally stronger: the Pearson

correlation is 0.59 and the reduction of error is 0.29. These results suggest that the model is not being overfit, and that the reconstruction contains useful information (Figure 4.2).

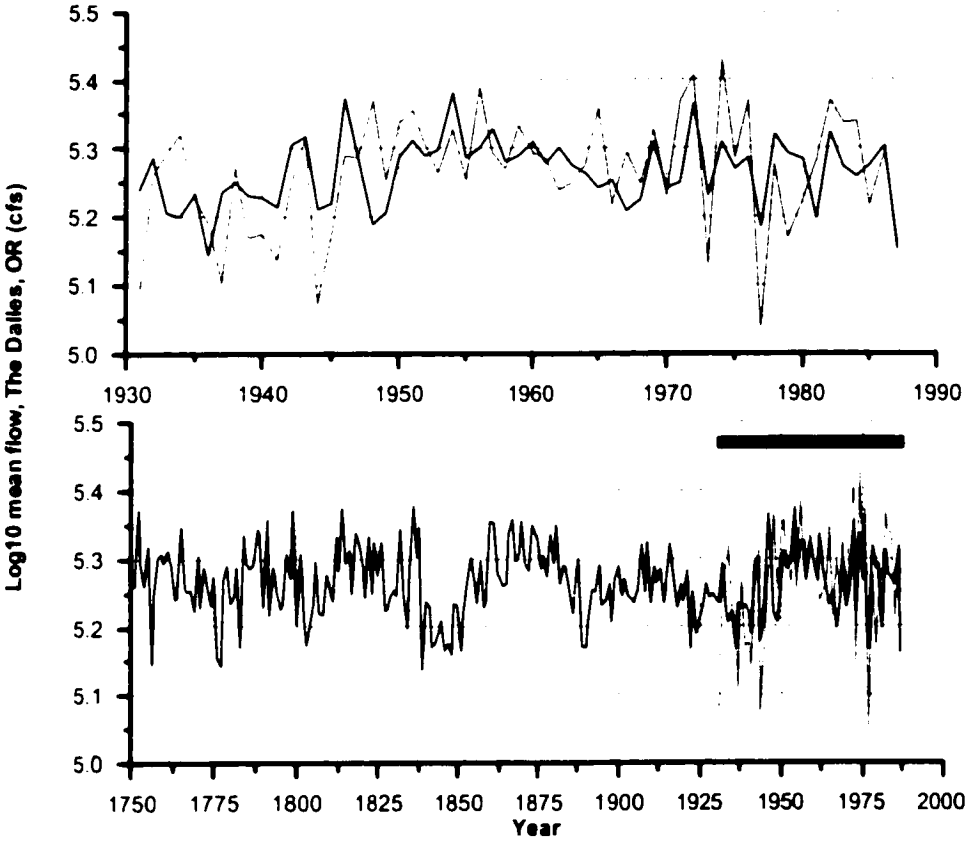

Figure 4.2 (top panel) Observed (gray) and cross-validated reconstructed (black) flow at The Dalles, Oregon, for the calibration interval 1931 to 1987. (bottom panel) Flow at The Dalles, Oregon, since 1750 reconstructed using tree rings (black line). The gray overbar indicates the calibration interval.

4.5.2 Residuals Analysis

An examination of the regression residuals revealed two factors that complicate interpretation of the results. First, the model underestimates the magnitude of extreme events; in particular, the severity of low-flow years is poorly captured by the

reconstruction. This bias is evident in a cumulative probability plot of the gauged, cross-validated and reconstructed flow records (Figure 4.3). This result is typical of regression analyses in general (Meko and Graybill 1995), and tree-ring based reconstructions in particular (Fritts 1976; Fritts *et al.* 1990; Peterson *et al.* 1999). Indeed, a scatter plot of the regression residuals against the gauged flow record suggests that underestimates of severe low-flow events account for a substantial fraction of the error in the regression model (Figure 4.4). One interpretation of this finding is that the reconstructed record is probably performing better than the verification statistics suggest – at least with respect to the simple occurrence of low-flow events if not the absolute magnitude of those events.

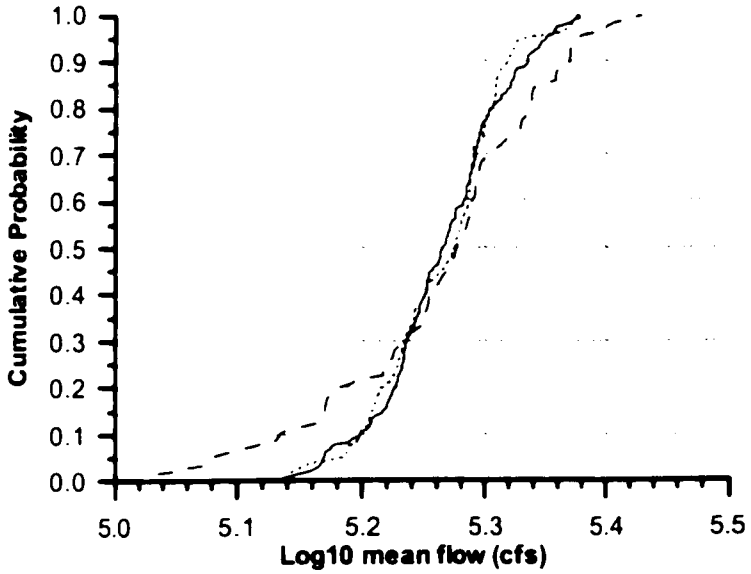

Figure 4.3 The cumulative probability density of log10 mean flow at The Dalles, Oregon. The gauged record (1931-1987) is indicated by the dashed line; the cross-validated reconstructed record (1931-1987) by the dotted line; and the reconstructed record (1750-1987) by the solid line.

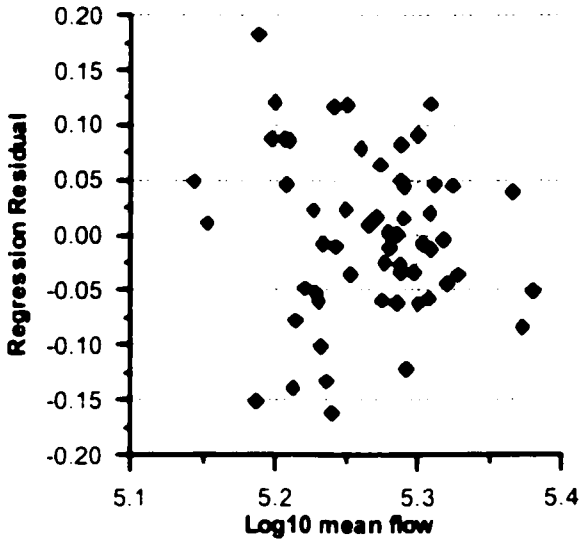

Figure 4.4 Scatter plot of the regression residuals against the cross-validated reconstructed flow record.

Secondly, the residuals exhibit an increasing trend over time. This trend is evident in a plot of the residuals as a function of time (Figure 4.5), and is significant at the 90 percent confidence level ($p = 0.08$). This finding can be explained as a consequence of increases in the gauged flow at The Dalles that are not matched by increases in radial growth at the sites considered in this study. The most likely explanation for this trend is that changes in land cover within the Columbia River basin are contributing to increased runoff relative to total precipitation or drought severity. Hessburg *et al.* (2000) document large changes in forest composition and structure within the Columbia River basin over the 20th century, which they attribute to forest management practices including timber harvest, fire exclusion, cropland expansion and introduced species. These changes have almost certainly had a measurable impact on the hydrology of the basin. Using the variable infiltration capacity (VIC) model Matheussen *et al.* (2000) estimated changes in runoff production that could be attributed to land cover changes between 1900 and 1990. They determined that runoff has increased within all but one of the sub-basins of the Columbia River system, typically by 2 to 7 percent. Because they used the same climatic parameters to force the model under both land cover scenarios this change in runoff can

be attributed to changes in surface characteristics. Losses of mature forest stands to logging and agriculture have resulted in increased snow accumulation and reduced evapotranspiration, which in turn have increased runoff. This trend has been partially offset by fire suppression efforts, which have increased the area of mature forest types in some regions, thereby increasing evapotranspirative losses. Although they do not report the total change in naturalized flow at The Dalles, summer high flows are ca. 10 percent higher and winter low flows are 2-3 percent lower under modern land cover than under 1900 conditions (see Figure 5 in Matheussen *et al.* 2000).

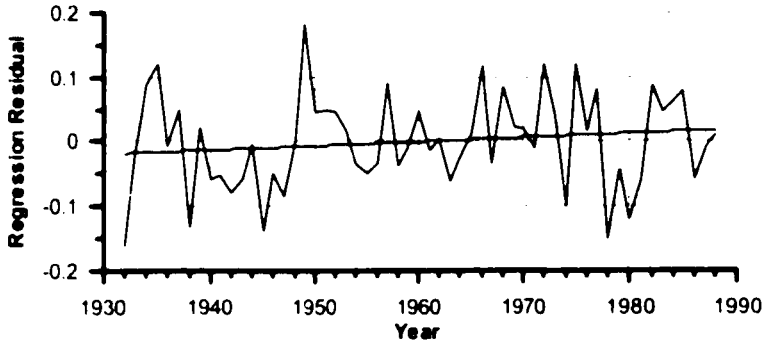

Figure 4.5 Regression residuals plotted as a function of time. The trend line exhibits an increase in transformed flow of ca. 1.2 percent per century.

Because the tree-ring sites considered in this study have not been subjected to land-use changes I do not expect them to exhibit this trend. As a consequence of this disparity, the trend in the regression residuals can be interpreted as physical supporting evidence of the modelled results. The magnitude of the trend is relatively small – only 1.2 percent per century – although given that the reconstruction underestimates the magnitude of low-flow events relative to high-flow events this estimate probably represents a lower limit to the actual disparity between the two records.

4.5.3 Multiyear Drought Events

In order to assess the persistence of drought over the period of the record I filtered the reconstruction using a range of multiyear center-moving averages. Window lengths of 5,

11 and 25 years were chosen to characterize interannual, decadal and interdecadal flow regimes. Years that fell into the lowest 15 percent (i.e. the 35 lowest flow years) were then ranked and plotted as a function of time (see Woodhouse 2001) (Figure 4.6). Using this criterion the distribution of single-year low-flow events is fairly constant over time, although there is a conspicuous cluster of low-flow years during the 1840s. Intervals of persistent drought become more evident as longer window lengths are considered. In particular, the interval from ca. 1840 to 1855 appears to be the most severe and most persistent drought on record. The 1930s also emerge as a period of sustained low flows. Notable shorter intervals of low flow occurred at ca. 1775, 1805 and 1890. The period from 1950 to 1987 is notable for having no multiyear droughts in the bottom 15th percentile.

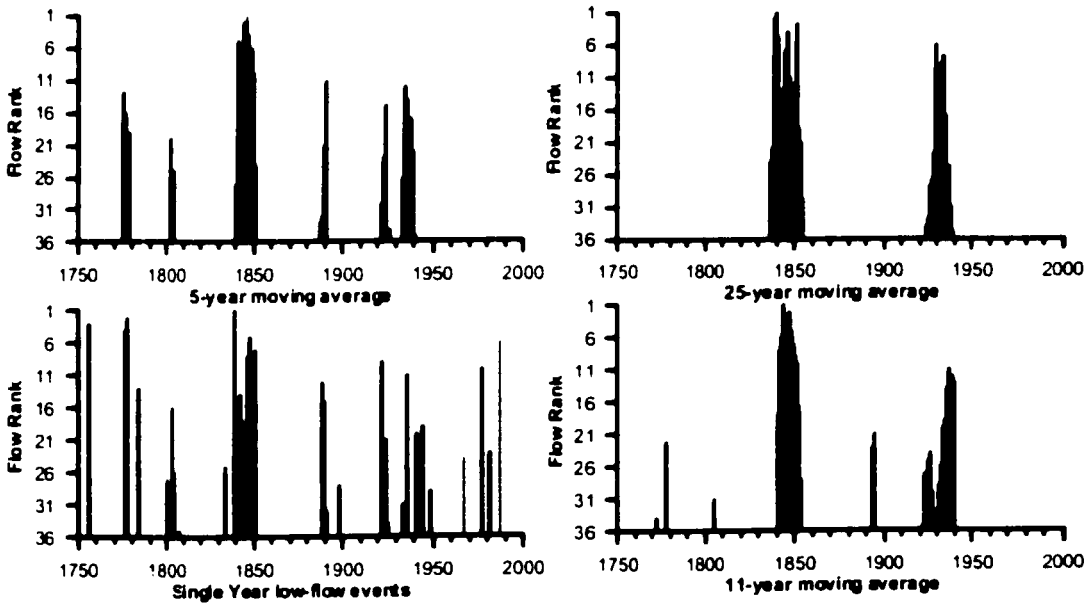

Figure 4.6 The distribution of n-year moving average mean flow for the lowest 15th percentile over the period of reconstruction. Low rankings are indicated by longer bars, and represent lower flow events.

The period of low flows during the 1840s coincides with drought on the Great Plains as reconstructed from tree rings and historical reports of sand dune activity (Muhs and

Holliday 1995; Woodhouse and Overpeck 1998; Woodhouse 2001). Similarly, streamflow in California as reconstructed by tree rings was also substantially below normal (Earle 1991; Meko *et al.* 2001). In contrast, lake levels at Crater Lake were likely among the highest they have been in the last 200 years (Peterson *et al.* 1999), and streamflow in the US Southwest was close to normal (Meko and Graybill 1995). Cook et al. (1999) describe a pattern in drought that is fairly persistent throughout the 1940s east of the Cascade Mountains, but sporadic in coastal areas, possibly accounting for these discrepancies in the paleorecords. In contrast to these findings, the drought of the 1890s is absent from the records of California streamflow (Earle 1991; Meko *et al.* 2001) and Crater Lake level (Peterson *et al.* 1999), but is present in the Colorado Front Range (Woodhouse 2001), the Great Plains, and the US Southwest (see Figure 3 in Woodhouse and Overpeck 1998).

The drought of the 1930s is well recognized, and corresponds to a period of widespread crop failures and mass migrations out of the Great Plains region. Analyses of tree-ring reconstructions suggest that in some regions this drought may have been the most severe of the last 300 years (Earle 1991; Cook *et al.* 1999; Meko *et al.* 2001). In northwestern New Mexico and parts of the Great Plains however, the 1930s drought is relatively minor in the longer context (D'Arrigo and Jacoby 1991; Woodhouse and Overpeck 1998). The results presented here suggest that in the interior Columbia River Basin the 1930s drought was probably matched only once for length in the last 250 years; although the drought of the 1840s was probably more severe in terms of sustained low flows.

4.5.4 Comparison to the Instrumental Record

The strength of this reconstruction, as measured by the correlation coefficient and RE, is comparable to other dendrohydrologic reconstructions from temperate regions (e.g. Cook and Jacoby 1983; Jones *et al.* 1984), but is weaker than reconstructions from arid and semi-arid regions (e.g. Meko and Graybill 1995; Meko *et al.* 2001; Woodhouse 2001). In order to assess whether this difference can be attributed to limitations in the tree-ring record or to a low signal-to-noise ratio in the streamflow data I attempted an identically

specified reconstruction of streamflow using the divisional PDSI data in lieu of the tree-ring record. I considered four scenarios: (1) mean water-year PDSI at all climate divisions within the Columbia River basin; (2) mean winter and mean summer PDSI at all climate divisions; (3) mean water-year PDSI for only those climate divisions represented by tree-ring chronologies; and (4) mean winter and mean summer PDSI for the same climate divisions. These data were treated in the same manner as the ring-width chronologies – that is, they were combined using PCA, autoregressive modelled, bootstrapped, and independently cross-validated (Table 4.2).

Table 4.2 Cross-validated summary statistics for the instrumental PDSI based reconstruction of streamflow at The Dalles, Oregon.

Subset[1]	PCs in model	Reduction of Error	Pearson R	R^2
1	1,2	0.650	0.81	0.65
2	1,2,5	0.719	0.85	0.72
3	1,2	0.716	0.85	0.72
4	1,2,5	0.779	0.88	0.78
Cross-validated reconstruction	1,2,4	0.241	0.50	0.25
Full model reconstruction	1,2,4	0.290	0.59	0.35

1. See preceding text for subset descriptions.

The instrumental record captures between 65 and 78 percent of the variability in the flow record. Additionally, the quality of the reconstruction increases when only those climate divisions from which this study uses tree-ring data are used. This result suggests that the tree-ring chronologies used in this study are capturing between one-third and half of the recoverable signal in streamflow variability. Most likely, the sites considered are not adequately representing drought variability within their locale, and the relationships

presented here are not limited by the relatively sparse network of tree-ring sites. While it is possible that a more restrictive screening process could produce a stronger reconstruction, I found that even modest increases in the minimum correlation to PDSI resulted in very small data matrices. For example, increasing the correlation threshold to $r > 0.35$ excluded all but 8 of the potential chronologies, including all of the sites in Canada and Washington. Bootstrapping the resulting PC regression coefficients did not yield any significant predictors of streamflow. An alternative interpretation of this result is that whereas the climate division records represent composites of dozens of measuring stations throughout the region, each tree-ring site represents a single point. The spatial heterogeneity of precipitation (in particular) may contribute to local noise being incorporated into the streamflow reconstruction because of the sparseness of the sampling network compared to the instrumental record. Similar to the analysis of the tree-ring data, the regression residuals from the instrumental record showed an increasing trend of between 1.3 and 1.5 percent per century.

4.5.5 Comparison to the Extended Gauged Record

The USGS gauged flow record at the Dalles extends back to 1879, although the early portion of this record has not been corrected for possible biases due to water diversions or evaporative losses. Three consistency checks were undertaken using this record: (1) the choice of PCs to include in the regression model as well as their sign and approximate magnitude was determined using this longer calibration interval; (2) verification statistics were calculated for the extended (1879 - 1987) and independent (pre-1931) portions of the gauged record; and (3) the regression residuals were examined for the presence of any systematic bias in either record. These analyses were undertaken using both the tree-ring and instrumental PDSI records.

Bootstrapping the regression coefficients by sampling from the USGS gauged flow record resulted in the same choice of predictors (i.e. PCs 1, 2 and 4), and similar regression coefficients. Additionally, the cross-validated flow record developed using this longer calibration interval is very highly correlated to the record developed using the

naturalized flow record (r=0.96). The performance statistics are not as strong for this reconstruction, though, suggesting some sensitivity to the calibration interval (r=0.40, RE=0.156; Figure 4.7). When the independent portion of this reconstruction is considered separately, though, a different perspective emerges. The correlation between the gauged and reconstructed flow record over the interval 1879 - 1930 is r=0.42, and for the interval 1931 - 1987 r=0.48. There are two implications of these results. First, the correlation for each of these intervals is stronger than the correlation for the two intervals combined. This observation suggests that there is a shift in the mean of the gauged record relative to the reconstructed record between the two segments considered. Second, the overall quality of the reconstruction appears to decrease when the longer calibration interval is used.

Some insight into the possible cause of these disparities can be gained from the analysis of the instrumental PDSI record. For the purposes of this exercise I used data subset 1 above: mean water-year PDSI for all climate divisions within the Basin. Like the results for the tree-ring records, the same predictors were chosen with similar regression coefficients. Also like the results for the tree-ring records, the overall quality of the reconstruction decreased (r=0.79, RE=0.618), although by a smaller amount. As with the tree-ring results, the bias between the gauged and reconstructed records is apparent in the earliest portion of the calibration interval: the correlation between the gauged and reconstructed flow record over the interval 1896 - 1930 is r=0.82, and for the interval 1931 - 1987 r=0.83. Interpreted together, the results of these analyses suggest that most of the loss in skill of the tree-ring reconstruction can be attributed to bias in the early portion of the USGS gauged record. The cause of this disparity is not clear from this analysis, and the limited metadata that describe the gauged data do not provide any clues. Possible sources of bias include the naturalization scheme applied to the post-1931 portion of the record, changes in the gauging techniques used at The Dalles, and changes in the relationship between climate and runoff. It is important to determine which of these explanations is relevant, because if this extended record is reliable then there has

been a *decreasing* trend in the regression residuals for both the tree ring and instrumental analyses.

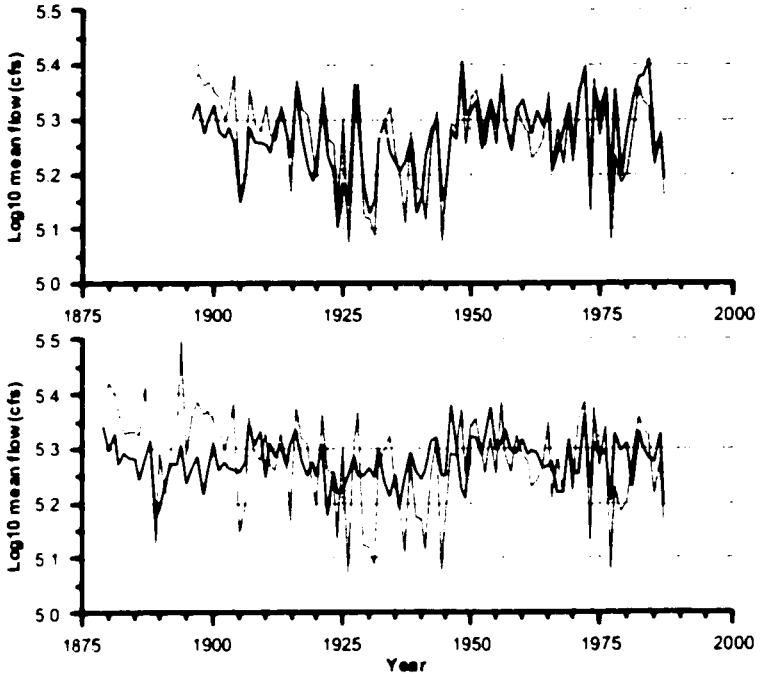

Figure 4.7 (upper panel) The cross-validated PDSI reconstructed (black) and USGS gauged flow. (lower panel) The cross-validated tree-ring reconstructed (black) and USGS gauged (grey) flow records at The Dalles, Oregon (1879 - 1987).

4.5.6 Comparison to Proxy Records of Large-Scale Climatic Variability

Streamflow on the Columbia River responds strongly to climatic forcing from El Niño / Southern Oscillation (ENSO), the Pacific Decadal Oscillation (PDO), and interactions between the two (Hamlet and Lettenmaier 1999a). Warm ENSO events (i.e. El Niños) are characterized by positive sea-surface temperature (SST) anomalies in the far eastern tropical Pacific, coupled with weakened or reversed trade winds (Enfield 1989). The typical response in the North Pacific sector to ENSO forcing is a deepened wintertime Aleutian Low, cold SST anomalies in the Gulf of Alaska, warm SST anomalies in coastal regions, and associated downstream teleconnections (Ropelewski and Halpert 1986; Yarnal and Diaz 1986). ENSO events typically recur every three to seven years, although strong events are more rare (Enfield 1989). The PDO is similar to ENSO in its effects on

the North Pacific ocean-atmosphere system, except that it is expressed primarily in the extratropics, and individual events typically persist for two or more decades (Mantua *et al.* 1997; Zhang *et al.* 1997). Interannual variability within individual phases of the PDO is substantial, and shifts between states may be abrupt (Mantua *et al.* 1997; Gedalof and Smith 2001b), making it difficult to identify the state of the system except in hindsight. Constructive (destructive) interference typically causes the effects of ENSO and the PDO to be additive (confounded) when the modes are acting in (out of) phase (Gershunov and Barnett 1998).

Hamlet and Lettenmaier (1999a) developed composite hydrographs for various combinations of warm, cool and neutral PDO and ENSO events, and showed that forecasting skill could be improved significantly by incorporating information on the state of these systems. Streamflow during El Niño events is on average 12 percent below normal, and during La Niña events it is on average 8 percent higher. The response to PDO is comparable, with flow typically 9 percent below normal during warm regimes and about 6 percent above normal during cool regimes. When ENSO and the PDO are in phase flow is on average 17 percent below normal (El Niño coeval with warm phase PDO) and 14 percent above normal (La Niña coeval with cool phase PDO). When the two systems are in opposing states their effect on flow may be diminished due to interference in the teleconnections.

Several long records of PDO / ENSO activity offer the possibility of evaluating these relationships prior to the initiation of instrumental records (e.g. Quinn *et al.* 1987; Stahle *et al.* 2000; Biondi *et al.* 2001; D'Arrigo *et al.* 2001; Gedalof and Smith 2001b). Here I use three reconstructed indices of ocean-atmosphere variability to interpret the reconstructed flow record. First, Gedalof and Smith (2001b) developed a proxy record of the PDO index since 1600 using chronologies of mountain hemlock (*Tsuga mertensiana*) from the Pacific Northwest. Second, Biondi et al. (2001) used chronologies form Jeffrey pine (*Pinus jeffreyi*) and bigcone Douglas-fir (*Pseudotsuga macrocarpa*) from six sites in California and northwestern Mexico to construct the mean winter half-year PDO index

back to 1661. These two records of PDO variability were chosen because they are derived from separate centers of action of the PDO and are respectively proximal and distal to the Columbia River basin. They were chosen in lieu of the reconstruction developed in Chapter 2 because they cover the full time period of the flow reconstruction. Third, Stahle *et al.* (1998) developed a record of the Southern Oscillation Index (SOI) from ENSO-sensitive regions of subtropical North America and Indonesia. In order to characterize the relationship between flow at The Dalles and these records I calculated the correlation over selected intervals (Table 4.3). This analysis shows that over the 20th century the correspondence between streamflow and ENSO, and streamflow and the PDO, is significant, whether instrumental or proxy records are considered. In contrast when the pre-instrumental interval is considered separately the correlations are nearly zero for all proxies. The correlation to the Stahle *et al.* (1998) SOI is significant prior to 1900, but is substantially weaker than over the 20th century.

Table 4.3 Cross correlations for the gauged and reconstructed flow at The Dalles, Oregon, with proxy records of PDO and ENSO variability for selected time intervals.

Proxy Record	**Gauged Flow Record**	**Reconstructed Flow Record**		
	1931 - 1987	1750 - 1987	1900 - 1987	1750 - 1899
Instrumental PDO index	**-0.435**	-	**-0.334**	-
Instrumental SOI	**0.346**	-	**0.254**	-
Gedalof and Smith (PDO)	**-0.246**	-0.101	**-0.241**	-0.044
Biondi *et al.* (PDO)	**-0.279**	-0.003	-0.095	0.054
Stahle *et al.* (SOI)	**0.518**	**0.195**	**0.240**	**0.177**

Correlations that are significant at 90 percent confidence are indicated by bold script.

These results imply that the relationship between PDO, ENSO and flow on the Columbia River has not been consistent over time. Gedalof et al. (*in press*; see also Chapter 2) found evidence that a number of proxy records of Pacific Basin variability (including the PDO reconstructions of Gedalof and Smith and Biondi *et al.* used here) exhibited poor intercorrelations over much of the 19th century. Prior to ca. 1825, however, the intercorrelations are comparable to those seen in the 20th century. They concluded that the PDO might have been a less important organizing structure of the North Pacific ocean-atmosphere system over this interval. The tree-ring chronologies used to develop this reconstruction are independent of those reconstructions and support these inferences regarding the North Pacific ocean-atmosphere system during the 19th century.

One other relevant paleoproxy reconstruction is the gridded PDSI reconstruction of Cook *et al.* (1999). This reconstruction was developed using tree-ring chronologies not used in this analysis, and therefore represents an independent verification of the reconstruction presented here. From the network of reconstructed PDSI gridpoints I chose the points needed to represent variability within the Columbia River drainage basin (GPs 1-4, 8-11 and 16-18). Because these grid points are highly spatially autocorrelated I applied a PCA to reduce the dimensionality of the data set and derive orthogonal predictors. Two PCs were retained, explaining 65 and 16 percent of the variance respectively. The leading PC is well correlated with the reconstructed flow record ($r = 0.502$), as well as the gauged flow records ($r=0.479$, naturalized record; $r=0.483$, USGS extended record). The intervals of persistent low flows identified in the streamflow reconstruction generally correspond to periods of prolonged drought (Figure 4.8). In particular, low flows during the 1770s, 1840s, 1890s, and 1930s all correspond to periods of reconstructed drought.

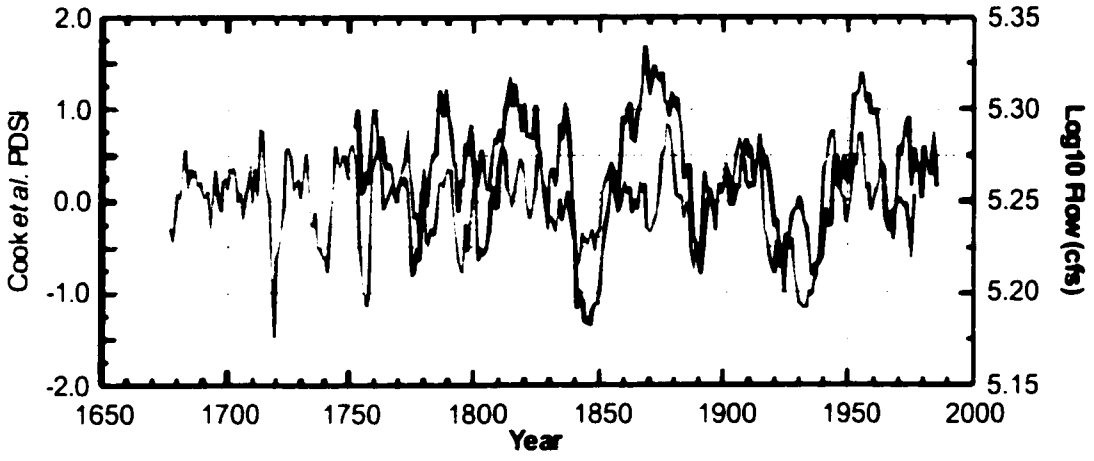

Figure 4.8 The leading principal component of reconstructed PDSI for gridpoints representing the Columbia River Basin (gray), and the reconstructed Columbia River flow for The Dalles, Oregon (black). The low frequency variability has been emphasized in both records using a 5-year running average filter.

4.6 Concluding Remarks

Tree-ring chronologies offer the opportunity to extend instrumental records into the past for the purpose of assessing the representativeness of recent observations, especially with respect to low frequency changes and extreme events. This reconstruction of flow on the Columbia River has revealed four key findings:

1. Severe droughts have occurred in the past, probably more severe than what has been seen in the 20th century. An interval of persistently lower flows than has been seen during the gauged record occurred around the 1840s. However, the drought of the 1930s is probably the second most severe of the last 250 years. This drought should not be regarded as an anomalous event, but rather a normal component of the Columbia River system.

2. Land-use changes in the Columbia River Basin have contributed to increases in runoff relative to drought severity or precipitation. This trend is evident in the residual

statistics of both instrumental and tree-ring based regressions of flow, and is on the order of 1.2 percent per century.

3. The tree-ring chronologies used in this study do not adequately capture the magnitude of severe low-flow events. This limitation is probably not caused by the sparse distribution of tree-ring sample sites within the basin, because a comparable network of climate divisions was able to reconstruct flow records much more accurately. The moderate model performance may be due to the imperfect correspondence between PDSI and radial growth increment, or it may be due to the sparse within-division distribution of tree-ring sample sites relative to instrumental stations.

4. The relationship between reconstructed flow and long records of ocean-atmosphere variability has not been constant over time. In particular, the correlation between the PDO and reconstructed flow is conspicuously stronger during the 20th century than during earlier centuries. This result is coeval with a period of poor correspondence between independent proxy records distributed throughout the Pacific Basin.

The Columbia River Basin supports diverse natural resources, economic investment and social values. With a rapidly growing population this region is increasingly vulnerable to drought events (Miles *et al.* 2000). Recent droughts have led to conflicts among uses (e.g. hydroelcetric production versus protecting salmon runs), increased costs to end users (notably municipal power users), and in some cases the total loss of access to water (in particular junior water rights holders in the agricultural sector). These recent droughts were not exceptional in the context of the last 250 years and were of shorter duration. Furthermore, water management strategies have been developed over the last half-century, a period characterized by a unique lack of multiyear droughts. Additionally, impending climate change could cause the frequency of severe low flow years in the Columbia River system to at least double by 2045, and possibly quadruple (Hamlet and Lettenmaier 1999b). Interpreted together these findings pose substantial challenges to water managers in the Pacific Northwest: the Basin has been fully exploited in terms of

storage capacity, the demands posed on the system continue to increase, availability is likely to diminish, and the potential for multiyear droughts has probably been underestimated.

Final Thoughts

Although this research program consisted of three largely unrelated investigations, some insights can be gained by considering the results collectively. In chapter two I compared five long, well verified, paleoproxy reconstructions of interdecadal climatic variability in the Pacific Basin. These records suggest that the climate system of the North Pacific sector was organized differently prior to the twentieth century than it has been over most of the instrumental record. In chapter three I examined the factors that contribute to large increases in area burned by wildfire in the American Northwest. Within mesic forest types a particular sequence of events contributes to increases in area burned: drought in the preceding winter and spring followed by summertime blocking ridges. At more xeric forest types the role of antecedent drought is smaller, with intense blocking events alone sufficient to cause significant increases in area burned. At the driest locations considered in this analysis summertime cyclones were also associated with increases in area burned – probably due to dry lightning and strong winds. In chapter four I used extant tree-ring chronologies to reconstruct Columbia River flow at The Dalles, Oregon, since 1750. This record revealed three interesting features of the Columbia River system: (1) the relationship between climatic forcing and resulting flow has changed due to changes in land cover over the twentieth century; (2) the drought of the 1930s was probably exceeded in terms of intensity and length around the 1840s; and (3) the last 50 years of this record is anomalous with respect to the relative absence of multiyear droughts. Two main challenges to research emerge from the sum of these results:

- The most severe drought of the past 250 years in the Pacific Northwest occurred under a climate system that may have been organized substantially differently from what has been seen over the instrumental record. In contrast, the drought of the 1930s occurred under a recognized warm phase of the PDO. This observation implies that disparate forcing mechanisms may contribute to persistent drought events. This finding is similar to results from Chapter 3, which showed that apparently opposite

circulation anomalies could lead to comparable increases in area burned – in that case due to the underlying ecosystem modulating the response to forcing.

- The assessment of fire-climate relations described here was undertaken during a period characterized by the relative absence of multiyear droughts. Consequently the observational record is probably not sufficient to assess the role of multiyear droughts in contributing to wildfire variability. In particular, if climate change leads to more frequent (and therefore a greater probability of more persistent) droughts, the consequences for fire management may be unexpected.

These challenges underpin the need to develop long, spatially explicit, paleoproxy records for the purpose of better understanding the relationships between ecological processes and climate. Specifically: (1) long fire histories are needed to evaluate the relationships between low-frequency climatic variability, wildfire, and ecology, in the American Northwest; and (2) dense, extensive, networks of proxy climate records are needed to reconstruct patterns of elements of the North Pacific ocean-atmosphere system. Additionally, these investigations need to be conscious of the ecological context from which the records are taken.

Works Cited

A.G. Crook Company (1993). Adjusted Streamflow and Storage: Columbia River and Coastal Basins, 1928 - 1989, Prepared for Bonneville Power Administration, Contract No. DE-AC79-92BP21958.

Agee, J.K. (1991a). Fire history along an elevational gradient in the Siskiyou Mountains, Oregon. *Northwest Science* **65**: 188 - 199.

Agee, J.K. (1991b). Fire history of Douglas-fir forests in the Pacific Northwest. *Wildlife and Vegetation of Unmanaged Douglas-Fir Forests.* Eds. L.F. Ruggiero, K.B. Aubry, A.B. Carey and M.H. Huff, USDA Forest Service General Technical Report PNW-GTR-285: 25 - 33.

Agee, J.K. (1993). *Fire Ecology of Pacific Northwest Forests.* Washington, DC, Island Press.

Agee, J.K. (1997). The severe weather wildfire: Too hot to handle? *Northwest Science* **71**: 153 - 157.

Agee, J.K. (1998). The landscape ecology of western forest fire regimes. *Northwest Science* **72**: 24 - 34.

Agee, J.K., M. Finney and R. De Gouvenain (1990). Forest fire history of Desolation Peak, Washington. *Canadian Journal of Forest Research* **20**: 350 - 356.

Agee, J.K. and M.H. Huff (1987). Fuel succession in a western hemlock / Douglas-fir forest. *Canadian Journal of Forest Research* **17**: 697 - 704.

Antos, J.A. and J.R. Habeck (1981). Successional development in *Abies grandis* (Dougl.) Forbes forests in the Swan Valley, western Montana. *Northwest Science* **55**: 26 - 39.

Barlow, M., S. Nigam and E.H. Berbery (2001). ENSO, Pacific Decadal Variability, and U.S. Summertime precipitation, drought, and stream flow. *Journal of Climate* **14**: 2105 - 2128.

Barrett, S.W., S.F. Arno and C.H. Key (1991). Fire regimes of western larch-lodgepole pine forests in Glacier National Park, Montana. *Canadian Journal of Forest Research* **21**: 1711 - 1720.

Biondi, F., A. Gershunov and D.R. Cayan (2001). North Pacific decadal climate variability since 1661. *Journal of Climate* **14**: 5 - 10.

Biondi, F. and T.W. Swetnam (1987). Box-Jenkins models of forest interior tree-ring chronologies. *Tree-Ring Bulletin* **47**: 71 - 96.

Blasing, T.J., D.N. Duvick and D.C. West (1981). Dendroclimatic calibration and verification using regionally averaged and single station precipitation data. *Tree-Ring Bulletin* **41**: 37 - 43.

Bonneville Power Administration, U.S. Army Corps of Engineers and U.S. Bureau of Reclamation (2001). The Columbia River System Inside Story, Report DOE/BP-3372.

Bork, J.L. (1984). *Fire history in three vegetation types on the eastern side of the Oregon cascades*. Unpublished PhD dissertation, Oregon State University, Corvalis, OR.

Box, G.E.P. and G.C. Tiao (1975). Intervention analysis with applications to economic and environmental problems. *Journal of the American Statistical Association* **70**: 70 - 79.

Brubaker, L.B. (1980). Spatial patterns of tree growth anomalies in the Pacific Northwest. *Ecology* **61**: 798 - 807.

Brubaker, L.B. (1986). Responses of tree populations to climatic change. *Vegetatio* **67**: 119 - 130.

Cayan, D.R. (1989). The influence of North Pacific atmospheric circulation on streamflow in the west. *Aspects of Climate Variability in the Pacific and the Western Americas*. Ed. D.H. Peterson. Washington, D.C., American Geophysical Union: 375 - 397.

Cayan, D.R. (1996). Interannual climate variability and snowpack in the Western United States. *Journal of Climate* **9**: 928 - 948.

Chen, J., S.C. Saunders, T.R. Crow, R.J. Naiman, K.D. Brosofske, G.D. Mroz, B.L. Brookshire and J.F. Franklin (1999). Microclimate in forest ecosystem and landscape ecology. *Bioscience* **49**: 288 - 297.

Cobb, K.M., C.D. Charles and D.E. Hunter (2001). A central tropical Pacific coral demonstrates Pacific, Indian, and Atlantic decadal climate connections. *Geophysical Research Letters* **28**: 2209 - 2212.

Cohen, S.J., K.A. Miller, A.F. Hamlet and W. Avis (2000). Climate change and resource management in the Columbia River basin. *Water International* **25**: 253 - 272.

Cole, J.E., J.T. Overpeck and E.R. Cook (2002). Multiyear La Niña events and persistent drought in the contiguous United States. *Geophysical Research Letters* **29**: 1647 - 1650.

Colenutt, M.E. and B.H. Luckman (1991). Dendrochronological investigation of *Larix lyallii* at Larch Valley, Alberta. *Canadian Journal of Forest Research* **21**: 1222 - 1233.

Colenutt, M.E. and B.H. Luckman (1995). The dendrochronological characteristics of alpine larch. *Canadian Journal of Forest Research* **25**: 777 - 789.

Cook, E.R. (1987). The decomposition of tree-ring series for environmental studies. *Tree-Ring Bulletin* **47**: 37 - 59.

Cook, E.R., K. Briffa, S. Shiyatov and V. Mazepa (1990). Tree-ring standardization and growth-trend estimation. *Methods of Dendrochronology: Applications in the Environmental Sciences*. Eds. E.R. Cook and L.A. Kairiukstis. Dordrecht, Netherlands, Kluwer Academic Publishers: 104 - 123.

Cook, E.R. and R.L. Holmes (1986). Program ARSTAN *(Version 1.72P)*.

Cook, E.R. and G.C. Jacoby (1983). Potomac River streamflow since 1730 as reconstructed by tree rings. *Journal of Applied Meteorology* **22**: 1659 - 1672.

Cook, E.R., D.M. Meko, D.W. Stahle and M.K. Cleaveland (1999). Drought reconstructions for the continental United States. *Journal of Climate* **12**: 1145 - 1162.

Cook, E.R. and K. Peters (1981). The smoothing spline: a new approach to standardizing forest interior tree-ring width series for dendrochronology. *Tree-Ring Bulletin* **41**: 45 - 53.

Countryman, C.M., M.H. McCutchan and B.C. Ryan (1969). Fire weather and fire behavior at the 1968 Canyon fire.U.S.D.A. Forest Service, Berkely, California, Research Paper PSW-55.

Cwynar, L.C. (1987). Fire and the forest history of the North Cascade range. *Ecology* **68**: 791 - 802.

D'Arrigo, R. and G.C. Jacoby (1991). A 1000-year record of winter precipitation from northwestern New Mexico, USA: A reconstruction from tree-rings and its relation to El Niño and the southern oscillation. *The Holocene* **1**: 95 - 101.

D'Arrigo, R., R. Villalba and G. Wiles (2001). Tree-ring estimates of Pacific decadal climate variability. *Climate Dynamics* **18**: 219 - 224.

Earle, C.J. (1991). Asynchronous droughts in California streamflow as reconstructed from tree rings. *Quaternary Research* **39**: 290 - 299.

Edmonds, R.L., T.B. Thomas and K.P. Maybury (1993). Tree population dynamics, growth, and mortality in old-growth forests in the western Olympic Mountains, Washington. *Canadian Journal of Forest Research* **23**: 512 - 519.

Enfield, D.B. (1989). El Niño, past and present. *Reviews of Geophysics* **27**: 159 - 187.

Ettl, G.J. and D.L. Peterson (1995). Growth response of subalpine fir (*Abies lasiocarpa*) to climate in the Olympic Mountains, Washington, USA. *Global Change Biology* **1**: 213 - 230.

Evans, M.N., M.A. Cane, D.P. Schrag, A. Kaplan, B.K. Linsley, R. Villalba and G.M. Wellington (2001). Support for tropically-driven Pacific decadal variability based on paleoproxy evidence. *Geophysical Research Letters* **28**: 3689 - 3692.

Evans, M.N., A. Kaplan, R. Villalba and M.A. Cane (2000). Globality and Optimality in Climate Field Reconstructions from Proxy Data. *Interhemispheric Climate Linkages*. Ed. V. Markgraf. San Diego, Academic: 53 - 72.

Everett, R.L., R. Schellhaas, D. Keenum, D. Spurbeck and P. Ohlson (2000). Fire history in the ponderosa pine/Douglas-fir forests on the east slope of the Washington Cascades. *Forest Ecology and Management* **129**: 207 - 225.

Fahnestock, G.R. and J.K. Agee (1983). Biomass consumption and smoke production by prehistoric and modern forest fires in western Washington. *Journal of Forestry* **81**: 653 - 657.

Finklin, A.I. (1973). Meteorological factors in the Sundance fire run.USDA Forest Service, Ogden, Utah, General Technical Report INT-6.

Finney, B.P., I. Gregory-Eaves, J. Sweetman, M.S.V. Douglas and J.P. Smol (2000). Impacts of climatic change and fishing on Pacific salmon abundance over the past 300 years. *Science* **290**: 795 - 799.

Flannigan, M.D. and J.B. Harrington (1988). A study of the relation of meteorological variables to monthly provincial area burned by wildfire in Canada (1953 - 1980). *Journal of Applied Meteorology* **27**: 441 - 452.

Folland, C.K., J.A. Renwick, M.J. Salinger and A.B. Mullan (2002). Relative influences of the Interdecadal Pacific Oscillation and ENSO on the South Pacific Convergence Zone. *Geophysical Research Letters* **29**: 1643 - 1646.

Franklin, J.F. and C.T. Dyrness (1973). *Natural Vegetation of Oregon and Washington*. Portland, Oregon, Forest Service, U.S. Department of Agriculture.

Fritts, H.C. (1976). *Tree Rings and Climate*. London, Adademic.

Fritts, H.C. (1991). *Reconstructing Large-scale Climatic Patterns from Tree-Ring Data*. Tucson, University of Arizona Press.

Fritts, H.C., J. Guiot, G.A. Gordon and F. Schweingruber (1990). Methods of calibration, verification, and reconstruction. *Methods of Dendrochronology: Applications in the Environmental Sciences*. Eds. E.R. Cook and L.A. Kairiukstis. Dordrecht, Netherlands, Kluwer Academic Publishers: 163 - 217.

Gara, R.I., W.R. Littke, J.K. Agee, D.R. Geiszler, J.D. Stuart and C.H. Driver (1985). Influence of fires, fungi, and mountain pine beetles on development of a lodgepole pine forest in south-central Oregon. *Lodgepole Pine: The Species and Its Management. Proceedings of a Symposium*. Ed. D.M. Baumgartner. Pullman, WA, Washington State University Cooperative Extension: 155 - 162.

Garreaud, R.D. and D.S. Battisti (1999). Interannual (ENSO) and interdecadal (ENSO-like) variability in the Southern Hemisphere tropospheric circulation. *Journal of Climate* **12**: 2113 - 2123.

Gauch, H.G. (1980). Noise reduction by eigenvector ordinations. *Ecology* **63**: 1643 - 1649.

Gavin, D.G., L.B. Brubaker and K.P. Lertzman (in press). Holocene fire history of a coastal temperate rainforest based on soil charcoal radiocarbon dates. *Ecology*.

Gedalof, Z., N.J. Mantua and D.L. Peterson (*in press*). A multi-century perspective of variability in the Pacific Decadal Oscillation: new insights from tree rings and coral. *Geophysical Research Letters*.

Gedalof, Z. and D.J. Smith (2001a). Dendroclimatic Response of Mountain Hemlock (*Tsuga mertensiana*) in Pacific North America. *Canadian Journal of Forest Research* **31**: 322 - 332.

Gedalof, Z. and D.J. Smith (2001b). Interdecadal climate variability and regime-scale shifts in Pacific North America. *Geophysical Research Letters* **28**: 1515 - 1518.

Gershunov, A. and T.P. Barnett (1998). Interdecadal modulation of ENSO teleconnections. *Bulletin of the American Meteorological Society* **79**: 2715 - 2725.

Graumlich, L.J. (1987). Precipitation variation in the Pacific Northwest (1675 - 1975) as reconstructed from tree-rings. *Annals of the Association of American Geographers* **77**: 19 - 29.

Graumlich, L.J. and L.B. Brubaker (1986). Reconstruction of annual temperature (1590 - 1979) for Longmire, Washington, derived from tree rings. *Quaternary Research* **25**: 223 - 234.

Grissino-Mayer, H.D. and H.C. Fritts (1997). The International Tree-Ring Data Bank: An enhanced global database serving the global scientific community. *The Holocene* **7**: 235 - 238.

Grissino-Mayer, H.D. and T.W. Swetnam (2000). Century-scale climate forcing of fire regimes in the American Southwest. *The Holocene* **10**: 213 - 220.

Guiot, J. (1991). The bootstrapped response function. *Tree-Ring Bulletin* **51**: 39 - 41.

Guttman, N.B. and R.G. Quayle (1996). A historical perspective of U.S. climate divisions. *Bulletin of the American Meteorological Society* **77**: 293 - 303.

Hamlet, A.F. and D.P. Lettenmaier (1999a). Columbia River streamflow forecasting based on ENSO and PDO climate signals. *Journal of Water Resources Planning and Management* **125**: 333 - 341.

Hamlet, A.F. and D.P. Lettenmaier (1999b). Effects of climate change on hydrology and water resources in the Columbia River basin. *Journal of American Water Resources Association* **35**: 1597 - 1623.

Hamlet, A.F., P.W. Mote, A.K. Snover and E.L. Miles (*in review*). Climate, water cycles, and water resources management in the Pacific Northwest. *Rhythms of Change: Climate Impacts on the Pacific Northwest*. Eds. E.L. Miles, A.K. Snover and t.C.I. Group.

Hare, S.R. (1996). *Low Frequency Climate Variability and Salmon Production*. Unpublished Ph.D. dissertation, University of Washington, Seattle. 303 pp.

Hare, S.R. and N.J. Mantua (2000). Empirical evidence for North Pacific regime shifts in 1977 and 1989. *Progress in Oceanography* **47**: 103-146.

Heikkinen, O. (1985). Relationships between tree growth and climate in the subalpine Cascade Range of Washington, U.S.A. *Annales Botanici Fennici* **22**: 1 - 14.

Hemstrom, M.A. and J.F. Franklin (1982). Fire and other disturbances of the forests in Mount Rainier National Park. *Quaternary Research* **18**: 32 - 51.

Hessburg, P.F., B.G. Smithb, R.B. Saltera, R.D. Ottmarc and E. Alvarado (2000). Recent changes (1930s - 1990s) in spatial patterns of interior northwest forests, USA. *Forest Ecology and Management* **136**.

Heyerdahl, E.K., L.B. Brubaker and J.K. Agee (2001). Spatial controls of historical fire regimes: a multiscale example from the Interior West, USA. *Ecology* **82**: 660 - 678.

Hidalgo, H.G., T.C. Piechota and J.A. Dracup (2001). Alternative principal components regression procedures for dendrohydrologic reconstructions. *Water Resources Research* **36**: 3241 - 3249.

Huff, M.H. (1995). Forest age structure and development following wildfires in the western Olympic Mountains, Washington. *Ecological Applications* **5**: 471 - 483.

IPCC (2001). Climate Change 2001: Impacts, Adaptation and Vulnerability. *Contribution of Working Group II to the Third Assessment Report of the Intergovernmental Panel on Climate Change*. Eds. J.J. McCarthy, O.F. Canziani, N.A. Leary, D.J. Dokken and K.S. White.

Jackson, P.L. and A.J. Kimerling, Eds. (1993). *Atlas of the Pacific Northwest, 8th Edition*. Corvallis, Oregon, OSU Press.

Johnson, E.A. (1992). *Fire and Vegetation Dynamics: Studies from the North American boreal forest*. Cambridge, Cambridge University Press.

Johnson, E.A. and D.R. Wowchuk (1993). Wildfires in the southern Canadian Rocky Mountains and their relationship to mid-tropospheric anomalies. *Canadian Journal of Forest Research* **23**: 1213 - 1222.

Jones, P.D., K.R. Briffa and J.R. Pilcher (1984). Riverflow reconstruction from tree rings in southern Britain. *Journal of Climatology* **4**: 461 - 472.

Kadonaga, L.K., O. Podlaha and M.J. Whiticar (1999). Time-series analyses of tree-ring chronologies from Pacific North America: Evidence for sub-century climate oscillations. *Chemical Geology* **161**: 339 - 363.

Kaiser, H.F. (1958). The Varimax criterion for analytic rotation in factor analysis. *Psychometrika* **23**: 187 - 201.

Kalnay, E., *et al.* (1996). The NCEP/NCAR 40-year reanalysis project. *Bulletin of the American Meteorological Society* **77**: 437 - 471.

Karl, T.R., A.J. Koscienly and H.F. Diaz (1982). Potential errors in the application of principal component (eigenvector) analysis to geophysical data. *Journal of Applied Meteorology* **21**: 1183 - 1186.

Knox, J.L. and R.G. Lawford (1990). The relationship between Canadian Prairie dry and wet months and circulation anomalies in the mid troposphere. *Atmosphere-Ocean* **28**: 189 - 215.

Kumar, A. and M.P. Hoerling (1998). Annual cycle of Pacific-North American seasonal predictability associated with different phases of ENSO. *Journal of Climate* **11**: 3295 - 3308.

Laroque, C.P. and D.J. Smith (1999). Tree-ring analysis of yellow cedar (*Chamaecyparis nootkatensis*) on Vancouver Island, British Columbia. *Canadian Journal of Forest Research* **21**: 115 - 123.

Latif, M. and T.P. Barnett (1994). Causes of decadal climate variability over the North Pacific and North America. *Science* **266**: 634 - 637.

Legates, D.R. (1991). The effect of domain shape on principal components analyses. *International Journal of Climatology* **11**: 135 - 146.

Lertzman, K., J. Fall and B. Dorner (1998). Three kinds of heterogeneity in fire regimes: at the crossroads of fire history and landscape ecology. *Northwest Science* **72**: 4 - 23.

Linsley, B.K., G.M. Wellington and D.P. Schrag (2000). Decadal sea surface temperature variability in the sub-tropical South Pacific from 1726 to 1997 A.D. *Science* **290**: 1145 - 1148.

Lotan, J.E. and W.B. Critchfield (1990). *Pinus contorta* Dougl. ex. Loud. Lodgepole Pine. *Silvics of North America*. Eds. R.M. Burns and B.H. Honkala. Washington, U.S. Dept. of Agriculture, Forest Service: 302 - 315.

Luckman, B.H. and M.E. Colenutt (1992). Developing tree-ring series for the last millennium in the Canadian Rocky Mountains. *Tree Rings and Environment: Proceedings of the International Symposium, Ystad, South Sweden, 3-9 September, 1990*. Eds. S. Bartholin, B.E. Berglund, D. Eckstein, F.H. Schweingruber and O. Eggertsson. Lund University, Department of Quaternary Geology, Lundqua Report 34: 207-211.

Mantua, N.J., S.R. Hare, Y. Zhang, J.M. Wallace and R.C. Francis (1997). A Pacific interdecadal climate oscillation with impacts on salmon production. *Bulletin of the American Meteorological Society* **78**: 1069 - 1079.

Matheussen, B., R.L. Kirschbaum, I.A. Goodman, G.M. O'Donnell and D.P. Lettenmaier (2000). Effects of land cover change on streamflow in the interior Columbia River Basin (USA and Canada). *Hydrological Processes* **14**: 867 - 885.

McGarigal, K., S. Cushman and S. Stafford (2000). *Multivariate Statistics for Wildlife and Ecology Research*. New York, Springer.

McKenzie, D., A.E. Hessl and D.L. Peterson (2001). Recent growth of conifer species of western North America: assessing spatial patterns of radial growth trends. *Canadian Journal of Forest Research* **31**: 526 - 538.

Meko, D.M. and D.A. Graybill (1995). Tree-ring reconstruction of Upper Gila River discharge. *Water Resources Bulletin* **31**: 605 - 616.

Meko, D.M., M.D. Therrell, C.H. Baisan and M.K. Hughes (2001). Sacramento River flow reconstructed to A.D. 869 from tree rings. *Journal of the American Water Resources Association* **37**: 1029 - 1039.

Miles, E.L., A.K. Snover, A.F. Hamlet, B. Callahan and D. Fluharty (2000). Pacific Northwest regional assessment: the impacts of climate variability and climate change on the water resources of the Columbia River basin. *Journal of the American Water Resources Association* **36**: 399 - 420.

Minobe, S. (1997). A 50 - 70 year climatic oscillation over the North Pacific and North America. *Geophysical Research Letters* **24**: 683 - 686.

Minobe, S. (1999). Resonance in bidecadal and pentadecadal climate oscillations over the North Pacific: role in climatic regime shifts. *Geophysical Research Letters* **26**: 855 - 858.

Minobe, S. (2000). Spatio-temporal structure of the pentadecadal variability over the North Pacific. *Progress in Oceanography* **47**: 381 - 408.

Moore, R.D. (1996). Snowpack and runoff responses to climatic variability, southern Coast Mountains, British Columbia. *Northwest Science* **70**: 321 - 333.

Mosteller, F. and J.W. Tukey (1977). *Data Analysis and Regression*. New York, Addison Wesley.

Muhs, D.R. and V.T. Holliday (1995). Evidence of active dune sand on the Great Plains in the 19th century from accounts of early explorers. *Quaternary Research* **43**: 198 - 208.

Nakamura, H., G. Lin and T. Yamagata (1997). Decadal climate variability in the North Pacific during recent decades. *Bulletin of the American Meteorological Society* **78**: 2215 - 2225.

Nigam, S., M. Barlow and E.H. Berbery (1999). Analysis links Pacific decadal variability to drought and streamflow in United States. *EOS* **80**: 621,622,625.

North, G.R., T.L. Bell, R.F. Cahalan and F.J. Moeng (1982). Sampling errors in the estimation of empirical orthogonal functions. *Monthly Weather Review* **110**: 699 - 706.

Peterson, D.L., D.G. Silsbee and K.T. Redmond (1999). Detecting long-term hydrological patterns at Crater Lake, Oregon. *Northwest Science* **73**: 121 - 130.

Peterson, D.W. and D.L. Peterson (1994). Effects of climate on radial growth of subalpine conifers in the North Cascade Mountains. *Canadian Journal of Forest Research* **24**: 1921 - 1932.

Peterson, D.W. and D.L. Peterson (2001). Mountain hemlock growth responds to climatic variability at annual and decadal time scales. *Ecology* **82**: 3330 - 3345.

Peterson, D.W., D.L. Peterson and G.J. Ettl (2002). Growth responses of subalpine fir to climatic variability in the Pacific Northwest. *Canadian Journal of Forest Research* **32**: 1503 - 1517.

Pitcher, D.C. (1987). Fire history and age structure in red fir forests of Sequoia National Park, California. *Canadian Journal of Forest Research* **17**: 582 - 587.

Preisendorfer, R.W. (1988). *Principal Component Analysis in Meteorology and Oceanography*. New York, Elsevier.

Quinn, W.H., V.T. Neal and S.E. Antunez de Mayolo (1987). El Niño occurrences over the past four and a half centuries. *Journal of Geophysical Research* **92**: 14449 - 14461.

Richman, M.B. (1993). Comments on: 'The effect of domain shape on principal components analyses'. *International Journal of Climatology* **13**: 203 - 218.

Ropelewski, C.F. and M.S. Halpert (1986). North American precipitation and temperature patterns associated with the El Niño / Southern Oscillation (ENSO). *Monthly Weather Review* **114**: 2352 - 2362.

Rorig, M.L. and S.A. Ferguson (1999). Characteristics of lightning and wildland fire ignition in the Pacific Northwest. *Journal of Applied Meteorology* **38**: 1565 - 1575.

Rorig, M.L. and S.A. Ferguson (2002). The 2000 fire season: lightning-caused fires. *Journal of Applied Meteorology* **41**: 786 - 791.

Sando, R.W. and D.A. Haines (1972). Fire weather and behavior of the Little Sioux fire.U.S.D.A. Forest Service, St. Paul, Minnesota, Research Paper NC-76.

Schroeder, M.J. (1969). Critical Fire Weather Patterns in the Conterminous United States.Weather Bureau, U.S. Department of Commerce, Environmental Science Services Administration, Silver Spring, Maryland, Technical Report WB 8.

Schweingruber, F.H. (1993). *Trees and Wood in Dendrochronology: Morphological, Anatomical, and Tree-Ring Analytical Characteristics of Trees Frequently Used in Dendrochronology*. Berlin, Springer-Verlag.

Skinner, W.R., B.J. Stocks, D.L. Martell, B. Bonsal and A. Shabbar (1999). The association between circulation anomalies in the mid-troposphere and area burned by wildfire in Canada. *Theoretical Applied Climatology* **63**: 89 - 105.

Stahle, D.W., *et al.* (1998). Experimental dendroclimatic reconstruction of the southern oscillation. *Bulletin of the American Meteorological Society* **79**: 2137 - 2152.

Stahle, D.W., E.R. Cook, M.K. Cleaveland, M.D. Therrell, D.M. Meko, H.D. Grission-Mayer, E. Watson and B.H. Luckman (2000). Tree-ring data document 16th century megadrought over North America. *EOS* **81**: 1 24 - 125.

Stockton, C.W. (1990). Climatic, hydrologic and water supply inferences from tree rings. *Civil Engineering Practice* **5**: 37 - 51.

Strauss, D., L. Bednar and R. Mees (1989). Do one percent of forest fires cause ninety-nine percent of the damage. *Forest Science* **35**: 319 - 328.

Street, R.B. and E.C. Birch (1986). Synoptic fire climatology of the Lake Athabasca - Great Slave Lake Area, 1977 - 1982. *Climatological Bulletin* **21**: 3 - 25.

Stuart, J.D., J.K. Agee and R.I. Gara (1989). Lodgepole pine regeneration in an old, self-perpetuating forest in south central Oregon. *Canadian Journal of Forest Research* **19**: 1096 - 1104.

Swetnam, T.W. (1990). Fire history and climate in the southwestern United States. *Proceedings of the Symposium: November 15 - 17, 1988, Tucson, AZ.* Ed. J.S. Krammes. Tucson, Arizona, USDA Forest Service General Technical Report RM-191: 6 - 17.

Swetnam, T.W. and J.L. Betancourt (1990). Fire - Southern Oscillation relations in the southwestern United States. *Science* **249**: 961 - 1076.

Swetnam, T.W. and J.L. Betancourt (1998). Mesoscale disturbance and ecological response to decadal climatic variability in the American Southwest. *Journal of Climate* **11**: 3128 - 3147.

Taylor, A.H. and C.B. Halpern (1991). The structure and dynamics of *Abies magnifica* forests in the southern Cascade Range, USA. *Journal of Vegetation Science* **2**: 189 - 200.

Taylor, A.H. and C.N. Skinner (1998). Fire history and landscape dynamics in a late-successional reserve, Klamath Mountains, California, USA. *Forest Ecology and Management* **111**: 285 - 301.

Trenberth, K.E. and J.W. Hurrell (1994). Decadal atmosphere-ocean variations in the Pacific. *Climate Dynamics* **9**: 303 - 319.

Urban, F.E., J.E. Cole and J.T. Overpeck (2000). Influence of mean climate change on climate variability from a 155-year tropical Pacific coral record. *Nature* **407**: 989 - 993.

Vautard (1992). Singular spectrum analysis: a toolkit... *Physica D* **58**: 95 - 126.

Villalba, R., R.D. D'Arrigo, E.R. Cook, G. Wiles and G.C. Jacoby (1999). *Inter-decadal climate oscillations along the extra-tropical western coasts of the Americas-evidence from tree rings over the past four centuries.* Paper presented at the 10th Symposium on Global Change Studies, 79th Annual Meeting of the American Meteorological Society, 10-15 January 1999, Dallas, Texas. 13 - 16.

Wallace, J.M. and D.S. Gutzler (1981). Teleconnections in the geopotential height field during the Northern Hemisphere winter. *Monthly Weather Review* **109**: 784 - 812.

Ware, D.M. (1995). A century and a half of change in the climate of the NE Pacific. *Fisheries Oceanography* **4**: 267 - 277.

Weaver, H. (1959). Ecological changes in the ponderosa pine forest of the Warm Springs Indian Reservation in Oregon. *Journal of Forestry* **57**: 15 - 20.

White, D., M. Richman and B. Yarnal (1991). Climate regionalization and rotation of principal components. *International Journal of Climatology* **11**: 1 - 25.

Wiles, G.C., R.D. D'Arrigo and G.C. Jacoby (1996). Temperature changes along the Gulf of Alaska and the Pacific Northwest coast modeled from coastal tree rings. *Canadian Journal of Forest Research* **26**: 474 - 481.

Woodhouse, C.A. (2001). A tree-ring reconstruction of streamflow for the Colorado Front Range. *Journal of the American Water Resources Association* **37**: 561 - 569.

Woodhouse, C.A. and J.T. Overpeck (1998). 2000 years of drought variability in the central United States. *Bulletin of the American Meteorological Society* **79**: 2693 - 2714.

Yarnal, B. (1993). *Synoptic Climatology in Environmental Analysis*. London, Belhaven.

Yarnal, B. and H.F. Diaz (1986). Relationships between extremes of the Southern Oscillation and the winter climate of the Anglo-American Pacific coast. *Journal of Climatology* **6**: 197 - 219.

Zar, J. (1999). *Biostatistical Analysis, 4th Edition*. Upper Saddle River, N.J, Prentice Hall Press.

Zhang, Q. (1996). *A 2122-Year Tree-Ring Chronology of Douglas-fir and Spring Precipitation Reconstruction at Heal Lake, Southern Vancouver Island, British Columbia*. M.Sc., School of Earth and Ocean Sciences, University of Victoria, Victoria. 88 pp.

Zhang, Y., J.M. Wallace and D. Battisti (1997). ENSO-like interdecadal variability: 1900 - 93. *Journal of Climate* **10**: 1004 - 1020.

Vita

Ze'ev Gedalof was born in London, England, but grew up in London, Ontario. At the Department of Geography, University of Victoria, Canada, he earned a Bachelor of Science in 1996 and a Master of Science in 1999. In 2002 he completed a Doctor of Philosophy in Ecosystem Analysis at the College of Forest Resources, University of Washington. He has always cheered for the Habs, and wears a lot of plaid flannel shirts.